

AD-A016 113

A SOLUTION FOR LAMINAR FLOW PAST A ROTATING  
CYLINDER IN CROSSFLOW

Kevin S. Fansler, et al

Ballistic Research Laboratories  
Aberdeen Proving Ground, Maryland

August 1975

DISTRIBUTED BY:



National Technical Information Service  
U. S. DEPARTMENT OF COMMERCE

302149

AD

BRL R 1816

# B R L

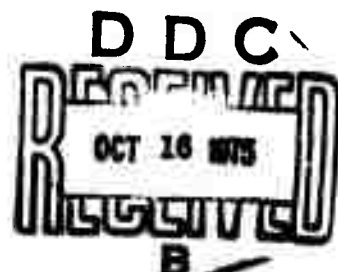
REPORT NO. 1816

ADA016113

## A SOLUTION FOR LAMINAR FLOW PAST A ROTATING CYLINDER IN CROSSFLOW

Kevin S. Fansler  
James E. Danberg

August 1975



Approved for public release; distribution unlimited.

USA BALLISTIC RESEARCH LABORATORIES  
ABERDEEN PROVING GROUND, MARYLAND

UNCLASSIFIED  
SECURITY CLASSIFICATION OF THIS PAGE (When Data Entered)

| REPORT DOCUMENTATION PAGE  |                       | READ INSTRUCTIONS BEFORE COMPLETING FORM   |
|--|-----------------------|--|
| 1. REPORT NUMBER<br><b>BRL Report No. 1816</b>   | 2. GOVT ACCESSION NO. | 3. RECIPIENT'S CATALOG NUMBER  |
| 4. TITLE (and Subtitle)<br><b>A SOLUTION FOR LAMINAR FLOW PAST A ROTATING CYLINDER IN CROSSFLOW</b>  |                       | 5. TYPE OF REPORT & PERIOD COVERED<br><b>Final</b>   |
| 7. AUTHOR(s)<br><b>Kevin S. Fansler<br/>James E. Danberg</b>   |                       | 6. PERFORMING ORG. REPORT NUMBER   |
| 9. PERFORMING ORGANIZATION NAME AND ADDRESS<br><b>U.S. Army Ballistic Research Laboratories<br/>Aberdeen Proving Ground, Maryland 21005</b>  |                       | 10. PROGRAM ELEMENT, PROJECT, TASK AREA & WORK UNIT NUMBERS<br><b>RDT&amp;E 1T161102A33H</b> |
| 11. CONTROLLING OFFICE NAME AND ADDRESS<br><b>U.S. Army Materiel Command<br/>5001 Eisenhower Avenue<br/>Alexandria, Virginia 22333</b>   |                       | 12. REPORT DATE<br><b>August 1975</b>  |
| 14. MONITORING AGENCY NAME & ADDRESS (if different from Controlling Office)  |                       | 13. NUMBER OF PAGES<br><b>87</b>   |
| 16. DISTRIBUTION STATEMENT (of this Report)<br><br><b>Approved for public release; distribution unlimited.</b>   |                       |  |
| 17. DISTRIBUTION STATEMENT (of the abstract entered in Block 20, if different from Report)   |                       |  |
| 18. SUPPLEMENTARY NOTES  |                       |  |
| 19. KEY WORDS (Continue on reverse side if necessary and identify by block number)<br><b>Fluid Dynamics                          Two-Dimensional Fluid Flow<br/>Boundary Layer Theory                 Conformal Mapping<br/>Wakes                                      Inviscid-Flow Models<br/>Moving-Wall Boundary Layers</b>  |                       |  |
| 20. ABSTRACT (Continue on reverse side if necessary and identify by block number) (ner)<br><b>Two-dimensional subcritical flow past a rotating cylinder has been theoretically treated to obtain agreement with the boundary-layer calculations. This study combined a source-wake bound-vortex flow model with a moving-wall boundary-layer calculation to force the final inviscid-flow model to be consistent with boundary-layer theory. Consistency was obtained by an iterative process whereby the separation points of the inviscid-flow model converged toward the separation points found by boundary-layer calculations. The boundary-layer is calculated using the integral-momentum and the integral-energy</b> |                       |  |

UNCLASSIFIED

SECURITY CLASSIFICATION OF THIS PAGE(When Data Entered)

equations where the family of moving-wall similarity boundary-layer solutions provide relationships between some parameters of the equations.

To obtain the inviscid flow model, flows in two planes were considered. The inviscid flow in the untransformed plane results from the superposition onto a uniform flow of a doublet, two sources located on the downstream side of a cylinder, their image sinks located along the axis of the cylinder, and a point vortex located in the center. The resulting complex-potential field was conformally mapped onto the physical plane by a Zhukovskii transformation. The free streamlines for the flow in the physical plane were used to simulate the free-shear layers in the near wake in order to approximate the velocity distribution on that part of the cylinder with attached flow. Other conditions were then imposed on the inviscid-flow model to take into account the vorticity transport into the wake and to allow for the possibility of boundary-layer theory to agree with the inviscid-flow model near separation.

Results were obtained for ratios of cylinder peripheral velocity to free-stream velocity from zero to 0.52. Lift coefficients were calculated; particularly good agreement with experiment was obtained for ratios equal to or less than 0.15. The calculated drag coefficients varied at most by 20% from those observed experimentally.

Reproduced from  
best available copy.

## TABLE OF CONTENTS

|  | Page |
|--|------|
| LIST OF ILLUSTRATIONS . . . . .  | 5    |
| LIST OF TABLES . . . . .   | 7    |
| I. INTRODUCTION . . . . .  | 9    |
| II. THE INVISCID-FLOW MODEL . . . . .  | 18   |
| A. General Description . . . . .   | 18   |
| B. Curvature and Pressure Conditions at the Separation Points . . . . .                                      | 23   |
| C. Numerical Method of Obtaining the Model . . . . .   | 25   |
| D. Method of Obtaining Agreement Between the Flow Model and the Boundary-Layer Calculation Results . . . . . | 31   |
| III. FLOW-MODEL RESULTS AND DISCUSSION . . . . .   | 32   |
| A. External-Velocity Distributions . . . . .   | 32   |
| B. Lift and Drag Coefficients . . . . .  | 50   |
| IV. SUMMARY AND CONCLUSIONS . . . . .  | 54   |
| ACKNOWLEDGMENT . . . . .   | 56   |
| LIST OF REFERENCES . . . . .   | 57   |
| APPENDIX A . . . . .   | 61   |
| LIST OF SYMBOLS . . . . .  | 87   |
| DISTRIBUTION LIST . . . . .  | 91   |

## LIST OF ILLUSTRATIONS

| <u>Figure</u>  | <u>Page</u> |
|--|-------------|
| 1. Boundary-Layer Profiles on a Rotating Cylinder . . . . .                                  | 12          |
| 2. Flow Past Cylinder in the Untransformed Planes (Source-Wake Bound-Vortex Model) . . . . . | 15          |
| 3. Flow Past Rotating Cylinder in the Physical Planes . . . . .                              | 17          |
| 4. $Q_1$ vs. $\Delta\sigma$ . . . . .  | 29          |
| 5. $\gamma$ vs. $\Delta\sigma$ . . . . .   | 30          |
| 6. Comparison between First and Converged Velocity Distributions ( $u_w = 0.2$ ) . . . . .   | 33          |
| 7. Velocity Distribution Details - Upper Side Adverse Pressure Gradient Region . . . . .     | 34          |
| 8. Velocity Distribution Details - Lower Side in Adverse Pressure Gradient Region . . . . .  | 35          |
| 9. Location of Boundary-Layer Separation vs. Trial Number ( $u_w = 0.15$ ) . . . . .         | 37          |
| 10. Lift Coefficient vs. Trial Number ( $u_w = 0.15$ ) . . . . .                             | 38          |
| 11. $u_e$ vs. $x$ - Comparison with Experiment ( $u_w = 0$ ) . . . . .                       | 39          |
| 12. $ u_e $ vs. $ x $ -- Parameter is $u_w$ . . . . .  | 42          |
| 13. Streamline Pattern Around Cylinder in Untransformed Plane -- $u_w = 0.0$ . . . . .       | 43          |
| 14. Streamline Pattern Around Cylinder in Physical Plane -- $u_w = 0.0$ . . . . .            | 44          |
| 15. Streamline Pattern Around Cylinder in Untransformed Plane -- $u_w = 0.2$ . . . . .       | 45          |
| 16. Streamline Pattern Around Cylinder in Physical Plane -- $u_w = 0.2$ . . . . .            | 46          |
| 17. $u_e$ vs. $x$ -- $u_w = 0.25$ and $u_w = 0.15$ . . . . .                                 | 48          |

LIST OF ILLUSTRATIONS (Continued)

| <u>Figure</u>  | <u>Page</u> |
|--|-------------|
| 18. Location of Separation vs. Rotation Rate . . . . .     | 49          |
| 19. $C_L$ vs. $u_w$ - Comparison with Experiment . . . . . | 51          |
| 20. $C_D$ vs. $u_w$ - Comparison with Experiment . . . . . | 53          |

## LIST OF TABLES

| <u>Table</u> |  | <u>Page</u> |
|--------------|--|-------------|
| I.           | Initial and Final Values of Separation . . . . .                       | 40          |
| II.          | Stagnation Point on Cylinder for Different Rates of Rotation . . . . . | 47          |
| III.         | Parameters Obtained for the Untransformed Plane . . .                  | 52          |

## I. INTRODUCTION

In this study, the lift and drag coefficients are calculated as a function of the ratio of the cylinder's tangential velocity to the velocity of the free stream flow. Here the boundary-layer is laminar to separation with the free shear layers near the separation points also being laminar. According to Swanson<sup>1</sup>, the nondimensionalized wall velocity (peripheral velocity of cylinder divided by freestream velocity) must always be less than 0.5 or the boundary layer will not be laminar to separation. From Wu's<sup>2</sup> review article on wakes and cavities, laminar flow for the shear layers near the separation points requires flows with Reynolds numbers less than  $5 \cdot 10^5$ . Yet the Reynolds number must be high enough for the boundary-layer approximation to be valid; that is, the boundary-layer is very thin and the pressure immediately outside the boundary-layer is impressed through the boundary layer thickness.

Rotating a body of revolution so that its axis of rotation is at an angle with its direction of relative fluid velocity not only affects the drag but also introduces a new force. This force, called the Magnus force, is directed perpendicular to the plane in which the rotational axis and direction of translation lie. G. Magnus<sup>3</sup> correctly attributed this force to the pressure field produced by the inviscid-velocity distribution about the rotating body in the airstream. He did this, and set the tone for subsequent experiments, by considering the apparently simpler two-dimensional problem of the rotating cylinder in crossflow. Using this model, he established that the force was directed toward the side of the cylinder moving with the direction of flow.

Lord Rayleigh<sup>4</sup> was the first to construct a mathematical model of the flow field by assuming an ideal fluid; a potential vortex combined with a doublet in a uniform flow induces a circulation and pro-

- 
1. W. M. Swanson, "An Experimental Investigation of the Two-Dimensional Magnus Effect," Final Report, Office of Ordnance Research Contract No. DA-33-019-ORD-1434, Dept. of Mech Eng., Case Institute of Technology, 31 December 1956.
  2. T. Y. Wu, "Cavity and Wake Flows," in Annual Review of Fluid Mechanics, Vol. IV, Van Dyke, Vincenti, and Wehausen (eds.), Annual Reviews, Inc., Palo Alto, Calif., 1972, pp. 243-284.
  3. G. Magnus, "On the Deflection of a Projectile," English translation in Taylor's Scientific Memoirs, 1853.
  4. Lord J. W. S. Rayleigh, "On the Irregular Flight of a Tennis Ball," Scientific Papers 1, 1857, pp. 344-346.

duces a side force according to Zhukovskii's theorem. However, no mathematical method could yet be used to couple the rotation of the cylinder with the fluid to produce the circulation. A missing element was found when Prandtl<sup>5</sup> introduced the concept of the boundary-layer in 1904, thus providing a better understanding of the rotating cylinder problem. Prandtl and Tietjens<sup>6</sup> also showed that separation was delayed on the upper part of the cylinder wall moving with the flow while separation was hastened on the underside of the cylinder. However, no successful theoretical solutions were found for quantifying the lift and drag forces.

Reid<sup>7</sup> measured the lift and drag coefficients of the rotating cylinder for rotational velocities up to  $u_w = 3.4$ , where  $u_w$  is the tangential velocity of the surface of the cylinder divided by the free stream velocity. A maximum lift to drag ratio of 7.8 was observed, and it was noted that the drag decreased somewhat with increasing velocity of rotation. A. Thom<sup>8,9,10,11,12,13</sup> and his associates made comprehensive studies involving the variations of the Magnus force with Reynolds number, surface condition, end conditions and other factors. Pressure field data were also obtained with the lift and

- 
5. L. Prandtl, "Über Flüssigkeitsbewegung bei sehr kleiner Reibung," *Verb. III. int. Math Kongr., Heidelberg, 1904*, pp. 484-491. English translation available as NACA TM-452.
  6. L. Prandtl and O. G. Tietjens, Applied Hydro- and Aeromechanics, New York, Dover Publications, Inc., 1957, p. 82.
  7. E. G. Reid, "Tests of Rotating Cylinders," NACA TN 209, 1924.
  8. A. Thom, "The Aerodynamics of a Rotating Cylinder," Ph.D. Dissertation, University of Glasgow, 1926.
  9. A. Thom, "Experiments on the Air Forces on Rotating Cylinders," ARC R&M 1018, 1925.
  10. A. Thom, "The Pressures Round a Cylinder Rotating in an Air Current," ARC R&M 1082, 1926.
  11. A. Thom, "Experiments on the Flow Past a Rotating Cylinder," ARC R&M 1410, 1931.
  12. A. Thom and S. R. Sengupta, "Air Torque on a Cylinder Rotating in an Air Stream," ARC R&M 1520, 1932.
  13. A. Thom, "Effects of Discs on the Air Forces on a Rotating Cylinder," ARC R&M 1623, 1934.

drag coefficients being deduced from these. More recently, Swanson<sup>1</sup> has investigated the rotating cylinder and has presented experimental results for a wider range of rotation rates and Reynolds numbers than were previously available. In his careful study, three-dimensional effects due to finite length of the cylinder were minimized and pressure probe results for the boundary-layer were obtained in addition to lift and drag.

Figure 1, obtained from Swanson's work, illustrates some features of the flow in the boundary layer for a wall velocity to free-stream velocity ratio ( $u_w$ ) of one. Caution must be used in applying some

features of this boundary-layer flow to the problem under investigation since Swanson concluded that the boundary layer on the underside of the cylinder for this rotation rate was very probably turbulent before separation. The stagnation point location corresponding to this velocity ratio is nearly the same as the location for the nonrotating cylinder. On the top of the cylinder, at an angle of about 120° from the stagnation point, the boundary layer thickens rapidly and separation appears to occur with a velocity profile satisfying the Moore-<sup>14</sup> Rott<sup>15</sup>-Sears (unpublished) criterion of  $u = \frac{\partial u}{\partial y} = 0$  at a coincident point. A boundary layer then appears and grows on the cylinder in the wake starting at the upper separation point. The profile corresponding to the apparent lower separation point does not obey the Moore-Rott-Sears criterion for separation; from the form of the profiles, it is not obvious what the correct criterion would be. But, as noted before, the boundary layer is probably turbulent in this region.

Griffiths and Ma<sup>16</sup> have investigate the Magnus force phenomena particularly with regard to the negative Magnus force and its relationship to the Reynolds number. The negative force is thought to occur because the side of the cylinder going against the flow will have a higher local relative Reynolds number for corresponding points than the other side. Here the relative Reynolds number is defined as

- 
14. F. K. Moore, "On the Separation of the Unsteady Laminar Boundary Layer," *Proceedings of Symposium on Boundary Layer Research held on August 1957, H. Görtler (ed.), Springer-Verlag Press, Berlin, 1958.*
  15. N. Rott with F. K. Moore, (ed.) *Theory of Laminar Flows*, Princeton University Press, Princeton, N.J., 1964, p. 432.
  16. R. T. Griffiths and C. Y. Ma, "Differential Boundary-Layer Separation Effects in the Flow over a Rotating Cylinder," *Aero. J. of the Roy. Aero. Soc.*, Vol. 73, 1969, pp. 521-526.

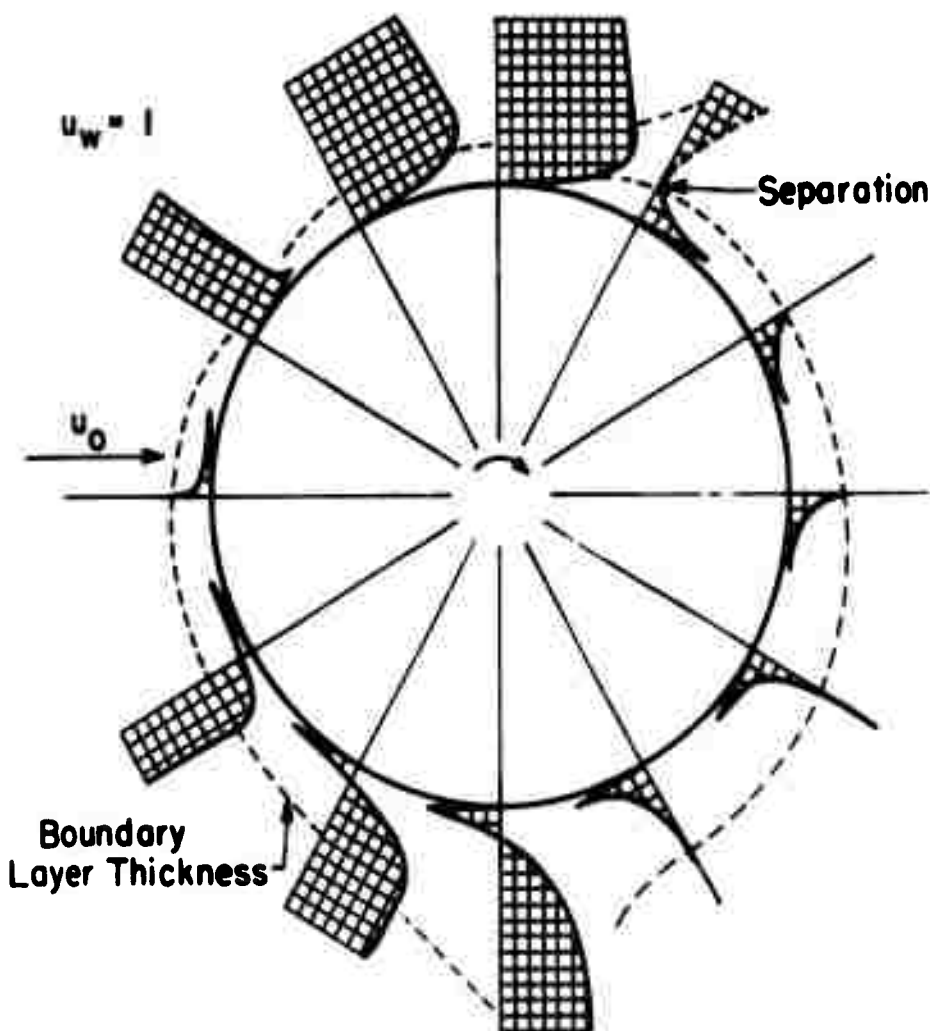


Figure 1. Boundary-Layer Profiles on a Rotating Cylinder

$u_o \times (1 + \bar{u}_w/u_o)/v$ , where the minus sign corresponds to the upper side and the plus sign refers to the lower side. If the Reynolds number for the flow is in a certain range, transition to turbulence will occur on the upstream moving wall thus delaying separation and causing the circulation strength to be of opposite sign. The present theoretical investigation, however, is not concerned with the turbulent boundary layer and this interesting aspect of Magnus forces will not be discussed further. Nevertheless, Griffiths and Ma's results would seem suspect in a quantitative sense because their lift and drag forces do not agree for common regions of the Reynolds number with those of Thom and Swanson's. In fact, their drag coefficient for the non-rotating cylinder is some 30% lower than found by other investigators. Consequently, their results will not be used for comparison purposes in this study.

The most successful attempt to theoretically treat the Magnus force (for any rotation rate) is M. B. Glauert's<sup>17</sup> treatment of a cylinder whose peripheral velocity is large enough so that the streamlines around the immediate vicinity of the cylinder are closed. He then assumes that the velocity outside the boundary layer is

$$\bar{u}_e = \bar{u}_c + 2u_o \sin x,$$

where  $u_o$  is the free stream speed,  $\bar{u}_c$  is the circulatory component of the fluid velocity and  $x$  is the angular displacement from the line through the center of the cylinder aligned with the direction of the unperturbed flow. He further assumes a parameter perturbation expansion together with an expansion in terms of  $\exp(ix)$  and substitutes the expansion into the boundary layer equations. He solves the equations and obtains

$$\frac{\Gamma}{2\pi a u_w} = 1 - 3 \left(\frac{u_o}{u_w}\right)^2 - 3.24 \left(\frac{u_o}{u_w}\right)^4 \dots$$

where  $\Gamma$  is the circulation strength and  $a$  is the radius of the cylinder. This indicates that the lift force  $F_1 = \rho u_o \Gamma$  is asymptotically a linear function of the peripheral velocity of the cylinder and has no upper limit. This result contradicts Prandtl's<sup>18</sup> assertion that the

17. M. B. Glauert, "The Flow Past a Rapidly Rotating Circular Cylinder," Royal Soc. of London Proceedings, Vol. A-242, 1957, pp. 103-115.

18. L. Prandtl, Die Naturwissenschaften, Vol. 13, 1925, pp. 93-108.

upper limit for the lift coefficient is 4. Glauert is supported by Swanson's experimental results; Prandtl's upper limit is exceeded and no other upper limit was encountered.

In contrast, some other attempts to predict the lift and drag coefficients need data from experiment to obtain meaningful results. W. G. Bickley<sup>19</sup> placed a single vortex downstream of a cylinder with circulation superimposed upon a flow around a cylinder. The location of this vortex was selected to give the experimentally obtained relationship between  $C_L$  and  $C_D$  for large values of  $C_L$ . T. Gustafson<sup>20</sup> expanded Bickley's analysis, but distributed the vorticity on the separation streamlines extending to infinity instead of using a single concentrated vortex. The vortices traveling downstream result in net drag and lift forces on the cylinder. Gustafson was also concerned with modeling the pressure distribution upstream of separation but Bickley was not concerned with such details of the flow field.

The inviscid-flow model used in the present investigation is a specialized case of Piercy, Preston and Whitehead's<sup>21</sup> model. Their model was used to consider the flow around other shapes such as ellipses and flat plates set at various angles to the direction of free stream flow. Two complex planes are considered: the physical plane and the untransformed plane. The inviscid flow in the untransformed plane, shown in Figure 2, results from the following superpositions onto a uniform flow: a doublet, two sources located on the downstream part of the cylinder and also rear the rear of the cylinder, their image sinks at the center of the cylinder, and a point vortex located in the center. With this configuration, the separation streamlines emanate from the cylinder at right angles to the surface. This complex potential field is conformally mapped onto the physical plane by a Zhukovskii transformation that doubles the angle of the streamlines emanating from the cylinder at  $S_1$  and  $S_2$ . The cylinder in the

- 
19. W. G. Bickley, "The Influence of Vortices Upon the Resistance Experienced by Solids Moving Through a Liquid," Proc. Roy. Soc. of London, Vol. A-119, 1928, pp. 146-156.
  20. T. Gustafson, "On the Magnus Effect According to the Asymptotic Hydrodynamic Theory," Hakan Ohlssons Buchdruckerei, Lund, Sweden, 1933. NACA translation N-25921, 1954.
  21. N. A. Piercy, J. H. Preston, and L. G. Whitehead, "The Approximate Prediction of Skin-Friction and Lift," Phil. Mag. Vol. 26, 1938, pp. 791-815.

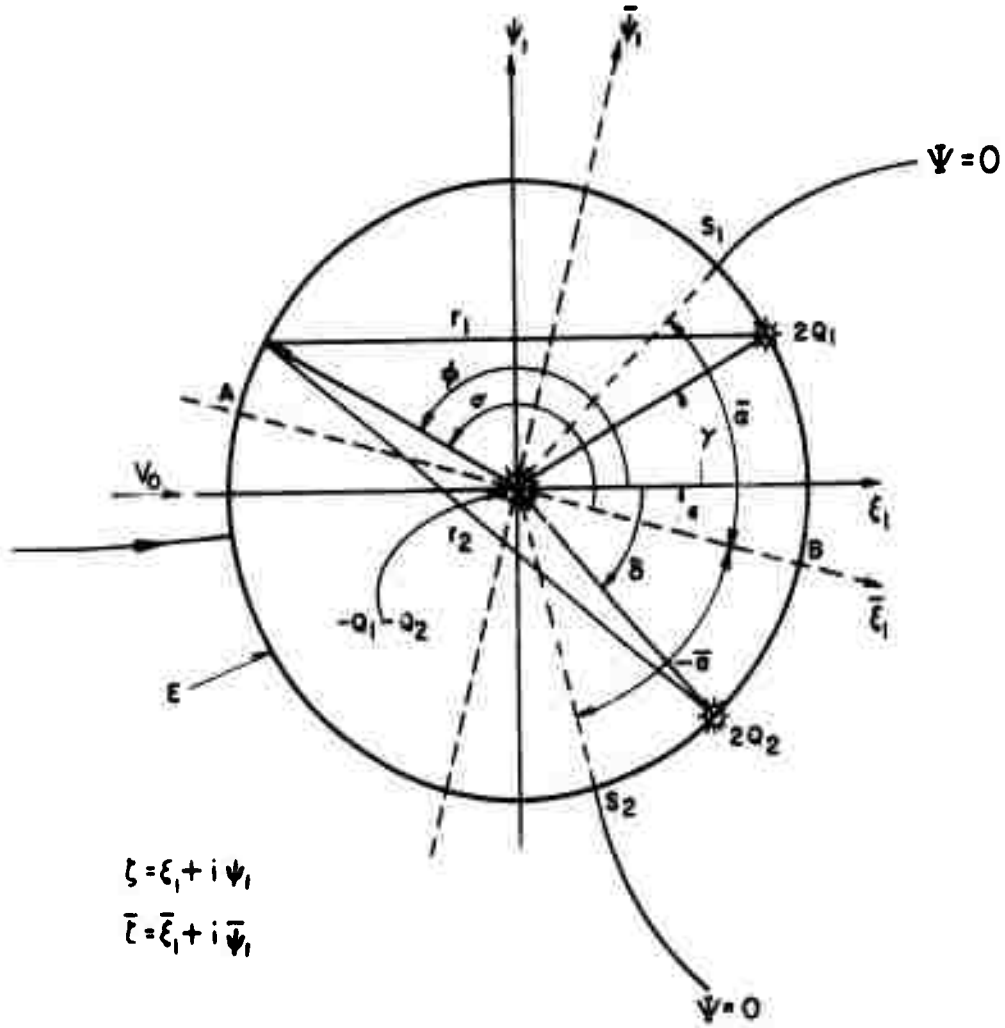


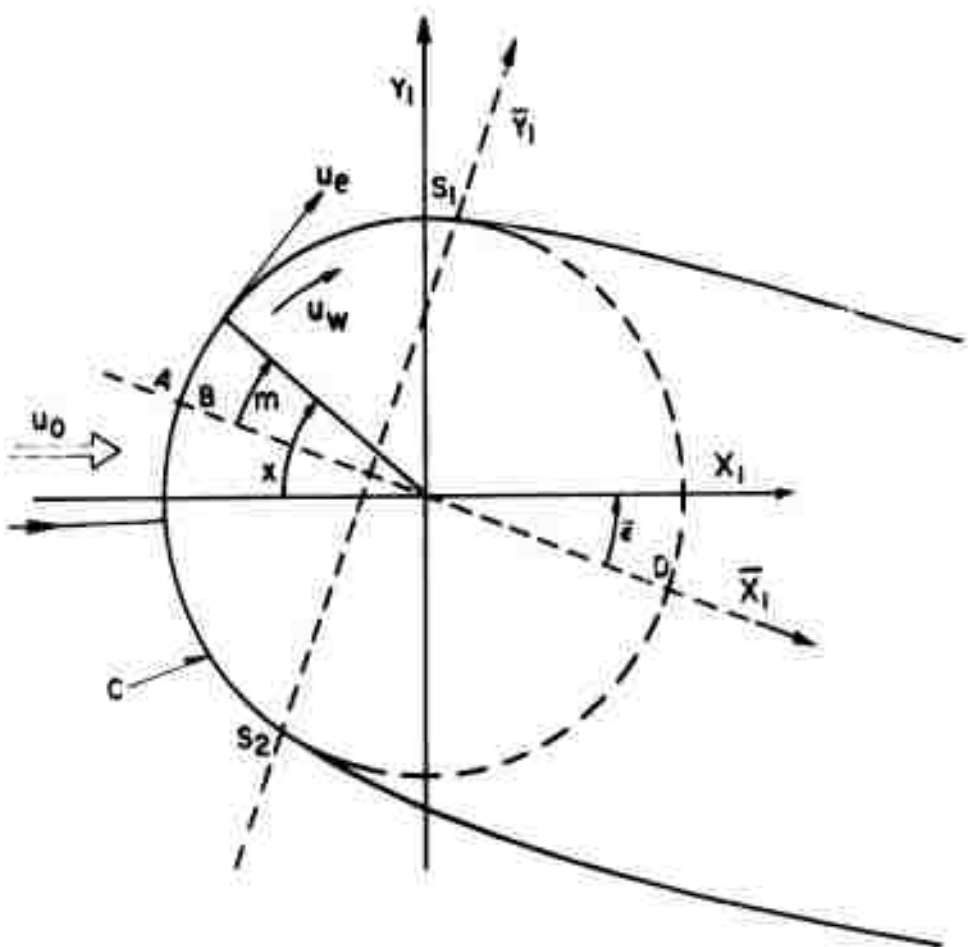
Figure 2. Flow Past Cylinder in the Untransformed Planes (Source-Wake Bound-Vortex Model)

physical plane together with the corresponding streamlines are shown in Figure 3. For purposes of calculating the drag and the lift forces, the flow inside the separation streamlines is ignored and the base pressure is assumed constant at the separation value. The pressure gradients near the separation points are required to be finite as is found experimentally. In this inviscid flow model, the pressure values on the separation streamlines increase asymptotically towards the free-stream value as actually occurs. The separation streamlines asymptotically approach a finite width apart with distance from the cylinder. It is assumed that this inviscid flow model simulates the shear-layers near the separation points and hence produces a more realistic velocity distribution on the cylinder ahead of separation.

The general approach defined above was used for the problem of the nonrotating cylinder in crossflow by Bluston and Paulson<sup>22</sup>. They employed the source-wake of Parkinson and Jandali<sup>23</sup>, a specialized model of the Piercy, Preston and Whitehead model. Their inviscid-flow model in the untransformed plane had two equal sources located symmetrically about the flow axis together with their image sinks at the center of the circle to produce symmetric separation streamlines. The resultant complex potential field was transformed to the physical plane by a Zhukovskii transformation. Parkinson and Jandali needed the velocity at separation and the location of the separation point to specify their inviscid flow model. However, Bluston and Paulson obtained their inviscid-flow model by specifying the separation point and requiring that the pressure gradient be finite at separation.

The inviscid-flow model used by Bluston and Paulson was made to agree with the results of boundary-layer theory. Using the resulting velocity distribution for a trial value of the inviscid-flow separation point, they calculated the boundary layer over the surface of the cylinder until boundary layer separation was reached. A second inviscid velocity distribution was generated with the inviscid-flow separation point determined from the first boundary-layer calculation. This procedure was repeated until the location of the separation points calculated by boundary layer theory agreed approximately with the separation points of the inviscid flow model. Separation was achieved at  $83^\circ$  compared with about  $82^\circ$  for experiment; furthermore, the pressure distribution over the cylinder ahead of separation was in good agreement with experimental measurements. These results suggested the

- 
22. H. S. Bluston and R. W. Paulson, "A Theoretical Solution for Laminar Flow Past a Bluff Body with a Separated Wake," Journal de Mecanique, Vol. 2, No. 1, 1972, pp. 161-180.
  23. G. V. Parkinson and T. Jandali, "A Wake Source Model for Bluff Body Potential Flow," J. Fluid Mech. Vol. 40, Part 3, 1970, pp. 577-594.



$$z = X_1 + iY_1$$

$$\bar{z} = \bar{X}_1 + i\bar{Y}_1$$

Figure 3. Flow Past Rotating Cylinder in the Physical Planes

possibility of extending the technique to the more difficult problem of the rotating cylinder in crossflow.

Although the approach of the present problem is similar to Bluston and Paulson's approach, the problem addressed in the present report is more difficult than their problem in at least two ways. The inviscid-flow model used is complicated by the loss of symmetry (unequal source strengths located asymmetrically with respect to the free stream flow) and the addition of a point vortex. A computer had to be used to find five unknown parameters in the untransformed plane whereas, the parameters for Bluston and Paulson's problem were found analytically. The other difficulty involved calculating the boundary layer on the rotating cylinder. For the part of the cylinder where the wall is moving against the flow, there is a region in the boundary layer near the wall which has reverse flow and calculations of boundary layers with regions of reverse flow have seldom been attempted. However, an integral technique has been used to numerically compute the boundary layer for such a situation<sup>24</sup> in which the integral-momentum equation and the integral-energy equation were simultaneously integrated. The moving-wall similarity solutions<sup>25</sup> were used to approximate the nonsimilar velocity profiles encountered on the rotating cylinder.

## II. THE INVISCID-FLOW MODEL

### A. General Description

The two-dimensional, incompressible, irrotational point vortex source-wake model for a spinning cylinder is represented in the physical plane in Figure 3 where  $u_e$  is the dimensionless inviscid velocity tangential to the surface,  $u_w$  is the peripheral dimensionless velocity of the cylinder rotating in the clockwise sense,  $u_0$  is the free stream velocity that is used to nondimensionalize  $u_e$  and  $u_w$ , and  $x$  is a nondimensionalized coordinate which defines an angular position on the cylinder. The cylinder and general flow field are described in two complex planes:

the  $z$  complex plane having its real axis aligned with the direction of unperturbed flow and the  $z$  plane having its imaginary axis going through

---

24. K. S. Fansler and J. E. Danberg, "An Integral Analysis of Boundary Layers on Moving Walls," U. S. Army Ballistics Research Laboratories Report 1792, June 1975. AD HA012205

25. J. E. Danberg and K. S. Fansler, "Similarity Solutions of the Boundary Layer Equations for Flow over a Moving Wall," U.S. Army Ballistic Research Laboratories Report 1714, April 1974, AD 781496.

the points of breakaway,  $S_1$  and  $S_2$ . The center of the cylinder is a point on the real axis of the  $\bar{z}$  plane. The  $\bar{z}$  plane is used in an intermediate step of the transformation from the untransformed plane  $\zeta$  to the description of the flow in the  $z$  plane. At the points  $S_1$  and  $S_2$ , the free streamlines leave the cylinder smoothly and are a finite distance apart at infinity. The stagnation point will not generally be at  $x = 0$ , and the flow field will normally be asymmetrical with respect to the  $X_1$  axis.

To put this source-wake model in better perspective, wake flow for nonrotating cylinders with Reynolds numbers between 1500 and  $10^5$  will be discussed briefly. This is a subcritical region within which the boundary layer on the cylinder is nowhere turbulent. According to Roshko and Fiszdon<sup>26</sup>, shear layers separate from the body and envelop a region of recirculating flow called the near wake. These free or separating shear layers are thin and well defined near the cylinder; the flow outside the free shear layers is irrotational. The near wake is unstable and oscillates periodically, particularly close to the end of the near wake region; the shear layers roll up into large vortices near the closure of the near-wake and then break away creating a Karman vortex street. Behind this near wake, the flow, being vortical and turbulent, is called the turbulent far-wake. As the Reynolds number is increased, the transition to turbulence advances along the free shear layers towards the points of separation. The time-averaged pressure is found to have an almost constant value over the part of the cylinder immersed in the wake.

The source-wake bound-vortex model used in this investigation does take into account some phenomena observed. The free streamlines of the model take the place of the time-averaged free-shear layers and form boundaries of the irrotational flow external to the wake region. Also, the fluid velocities on the free stream-lines decrease with distance from the cylinder towards the free stream velocity as observed in experiments. It is found, however, that streamlines continually enter the actual wake which widens downstream because of the diffusion of vorticity. Also the near wake is continuously shedding Karman vortex streets at the rear of the bubble and thus the free shear layers are unsteady over part of the near-wake region. A successful treatment to take into account the diffusion of vorticity and unsteadiness in the wake has not been developed. A flow model taking into account these features of the wake would require an extensive investigation of the wake region. Since the intention is

---

26. A. Roshko and W. Fiszdon, Problems of Hydrodynamics and Continuum Mechanics, Soc. Ind. Appl. Math, Philadelphia, 1967, pp. 606-616.

not to study the wake itself but rather to account for the effect of the wake on the upstream (attached flow) pressure distribution, it is expected that a reasonable model for the time-averaged near-wake free shear layers would result in an improvement over their complete neglect.

To construct the flow field just described, flow in an untransformed plane  $\zeta$  is considered as in Figure 2. The fundamental flow past the circle is the uniform flow plus a doublet. Additionally, sources of strength  $2\tilde{Q}_1$  and  $2\tilde{Q}_2$  are located at angles  $\gamma$  and  $\delta$  respectively from the direction of unperturbed flow. Image sinks  $-\tilde{Q}_1$  and  $-\tilde{Q}_2$  are placed at the origin to satisfy the boundary conditions on the circle. A point vortex of strength,  $\Gamma$ , is also placed at the origin and does not affect the boundary conditions on the circle but does affect the positions of  $S_1$  and  $S_2$  and the complex potential field. Here  $R$  is the radius of the cylinder. Now half the distance between the two sources will be assigned the value unity. Therefore,  $R$  is equal to  $\csc \bar{\alpha}$ .

The complex potential of the resulting flow referred to the  $\zeta$  plane is:

$$\begin{aligned} \chi(\zeta) = V_0 (\zeta + R^2/\zeta) + \{ & 2\tilde{Q}_1 [\ln(\zeta - Re^{i\gamma}) - \frac{1}{2}\ln(\zeta)] / 2\pi \} + \\ & \{ 2\tilde{Q}_2 [\ln(\zeta - Re^{i\delta}) - \frac{1}{2}\ln(\zeta)] / 2\pi \} + (\frac{1}{2}i\Gamma/\pi) \ln \zeta \quad (1) \end{aligned}$$

For the  $\zeta$  plane, only the fluid dynamical properties on the circle  $C$  will be of primary interest. The velocity on the circle  $C$  can be obtained as shown below. From Figure 2, the directed vectors from the sources  $2\tilde{Q}_1$  and  $2\tilde{Q}_2$  to the point  $\zeta$  can be seen to be respectively,

$$\begin{aligned} \zeta - Re^{i\gamma} &= r_1 e^{is}, \\ \zeta - Re^{i\delta} &= r_2 e^{it}, \quad (2) \end{aligned}$$

where  $s$  and  $t$  are angles between the lines drawn from the sources to a point  $\zeta$  on the circle and the lines drawn through the sources parallel to the real axis. Here,  $r_1$  and  $r_2$  are the lengths from the point  $\zeta$  to the sources  $2\tilde{Q}_1$  and  $2\tilde{Q}_2$  respectively. Thus, using equation (2) to rewrite the expression for the complex potential in equation (1), the velocity potential can then be expressed as

$$\begin{aligned} \psi = 2V_0 \csc \bar{\alpha} \cos \phi + \frac{\tilde{Q}_1}{2\pi} \ln(r_1^2/\csc \bar{\alpha}) + \frac{\tilde{Q}_2}{2\pi} \ln(r_2^2/\csc \bar{\alpha}) - \\ \frac{\phi \Gamma}{2\pi} \quad (3) \end{aligned}$$

Now  $r_1^2$  and  $r_2^2$  can be seen to be the following in terms of  $\csc \bar{\alpha}$ ,  $\gamma$ ,  $\delta$ , and  $\phi$ :

$$r_1^2 = 2 (\csc^2 \bar{\alpha}) [1 - \cos(\phi - \gamma)] ,$$

$$r_2^2 = 2 (\csc^2 \bar{\alpha}) [1 - \cos(\phi - \delta)] . \quad (4)$$

The tangential velocity at the surface of the cylinder is just

$$q = - \frac{d\phi}{d\theta} \sin \bar{\alpha} \quad (5)$$

Thus, substituting equation (4) into equation (3), differentiating according to equation (5), and using trigonometric identities, the following equation can be obtained:

$$q = 2 V_0 \sin \phi - \frac{1}{2\pi \csc \bar{\alpha}} [\tilde{Q}_1 \cot(\frac{\phi - \gamma}{2}) + \tilde{Q}_2 \cot(\frac{\phi - \delta}{2})] + \Gamma / 2\pi \csc \bar{\alpha}. \quad (6)$$

By using the following definitions

$$q \equiv q/V_0 ,$$

$$Q_{1,2} \equiv \tilde{Q}_{1,2} / 2\pi V_0 \csc \bar{\alpha} , \quad (7)$$

$$u_c \equiv \Gamma / 2\pi V_0 \csc \bar{\alpha} ,$$

the following equation can be obtained from equation (6):

$$q = 2 \sin \phi - [Q_1 \cot(\frac{\phi - \gamma}{2}) + Q_2 \cot(\frac{\phi - \delta}{2})] + u_c . \quad (8)$$

Equation (8) is the expression for the dimensionless tangential velocity at a point on the surface of the cylinder in the untransformed plane  $\zeta$ .

The resulting complex potential and the complete circle  $E$  in the  $\zeta$  plane can be mapped to the physical plane  $z$  by first transforming to the  $\bar{\zeta}$  plane. The complex plane  $\zeta$  has its real axis aligned with the direction of the freestream flow. The complex plane  $\bar{\zeta}$  has its real axis at an angle  $-\epsilon$  from the real axis of the  $\zeta$  plane and is located such that  $S_1$  and  $S_2$  are symmetric about the real axis. An angle  $\phi$

describing the position on the circle in the  $\zeta$  plane can be described in the  $\bar{\zeta}$  plane by the relationship

$$\sigma = \phi + \epsilon$$

The  $\zeta$  and  $\bar{\zeta}$  planes will be termed the untransformed planes. Points on the  $\zeta$  plane can be mapped conformally into points on the  $\bar{z}$  plane by an analytic function:

$$\bar{z} = M(\zeta) . \quad (9)$$

The particular mapping function is a Zhukovskii transformation:

$$M(\zeta) = \bar{\zeta} - \cot \bar{\alpha} - \frac{1}{\bar{\zeta} - \cot \bar{\alpha}} . \quad (10)$$

Here  $\cot \bar{\alpha}$  is just the distance from the origin along  $\bar{\xi}_1$  to the straight line drawn from  $S_1$  to  $S_2$  in Figure 2. The points  $S_1$ ,  $S_2$ , are critical points and  $M'(\zeta)$  the derivative of  $M$  is zero at the points. Angles of intersection in the  $\zeta$  plane are doubled in the  $\bar{z}$  plane by the mapping function at  $S_1$  and  $S_2$ . Thus, the angle of intersections of the separation streamlines with the circle E in the  $\zeta$  plane increase from  $90^\circ$  to a tangential intersection with the arc C. Also, the circle E is mapped onto the slit  $S_1AS_2BS_1$ . The points  $S_1$  and  $S_2$  lie on the  $\bar{\gamma}_1$  axis of the  $\bar{z}$  plane.

The relationship between the two complex velocities in the two planes  $\bar{z}$  and  $\zeta$  is given by

$$W(\bar{z}) = w(\zeta) / M'(\zeta) , \quad (11)$$

where

$$M'(\zeta) = 1 + 1/(\bar{\zeta} - \cot \bar{\alpha})^2 . \quad (12)$$

From equation (11) and equation (12), it is apparent that at large distances from the flow, the complex velocities in the two planes asymptotically approach each other; and this implies that  $u_o = v_o$  and  $\varepsilon = \bar{\varepsilon}$ .

The transformation from the  $\bar{z}$  plane to the  $z$  plane is accomplished by a translation and then a rotation through an angle  $\epsilon$ . The  $z$  and  $\bar{z}$  planes will be termed the physical planes. As mentioned before, only the dynamical quantities on the cylinder are of primary interest; hence, only the circle E of Figure 2 will be mapped into the arc C of Figure 3.

In the sections that follow, it will be necessary to know the tangential velocity  $u_e$  on the arc C of the cylinder in the  $z$  plane in terms of the position  $\phi$  on the circle E. The tangential velocity on the cylinder in the physical plane  $z$ , given the corresponding velocity in the plane  $\zeta$ , can be obtained if equation (11) is used specialized to the circle:

$$u_e(x) = q(\phi)/N(\phi) \quad , \quad (13)$$

when  $N(\phi)$  is defined as

$$N(\phi) \equiv |M'(\bar{\zeta})|_E \quad (14)$$

The subscript E means that  $M'(\bar{\zeta})$  is evaluated on the cylinder E. The value  $N(\phi)$  is obtained by multiplying  $M'(\bar{\zeta})$  on the circle E by its complex conjugate and using trigonometric identities to obtain squared quantities in both numerator and denominator. Then taking the square root and putting  $\sigma$  in terms of  $\phi$  and  $\epsilon$ , the expression for  $N(\phi)$  becomes

$$N(\phi) = \frac{2 [\cos \bar{\alpha} - \cos (\phi + \epsilon)]}{1 - 2 \cos \bar{\alpha} \cos (\phi + \epsilon) + \cos^2 \bar{\alpha}} \quad (15)$$

The inviscid flow velocity can then be found by using equation (13). The function for  $N(\phi)$ , equation (15), is known (since  $\bar{\alpha}$  and  $\epsilon$  can be obtained from equation (33)).

### B. Curvature and Pressure Conditions at the Separation Points

Parkinson and Jandali<sup>23</sup>, with their symmetric flow model, related the location and strength of the source in the untransformed plane to two parameters in the physical plane: the position of separation and the local external velocity at separation. By using the finite curvature condition at the separation point originally suggested and used by Woods<sup>27</sup>, Bluston and Paulson<sup>22</sup> could characterize the inviscid flow in the physical plane with one parameter: the position of separation. The number of parameters of the physical plane needed to describe the present flow model will also be reduced by imposing similar conditions. The streamline curvature condition imposed by Bluston and Paulson is applied to both separation points in the present case and thus reduces the number of descriptive parameters by two. After applying a second condition of equal pressures at the separation points, only two parameters of the physical plane will be needed to determine the five parameters in the untransformed plane. These two parameters are specified by the locations of the separation points on the rotating cylinder.

The first conditions imposed are designed to insure that streamline curvatures and pressures at the separation points are physically

27. L. C. Woods, "Two-Dimensional Flow of a Compressible Fluid past given Curved Obstacles with Infinite Wakes," Proc. Roy. Soc. Lond., Vol. A227, 1955, pp. 367-387.

meaningful and are consistent with boundary-layer theory. The curvatures of the free streamlines at the separation points are required to be finite. If the curvature of the separation streamline is negative infinite, the separation streamline will be concave downwards and will cut into the rear of the cylinder. The negative infinite curvature of the separation streamline should, therefore, be forbidden since this is physically impossible. If the separation streamline has positive infinite curvature at  $S_1$ , a very large adverse pressure gradient will occur upstream of separation becoming infinite at  $S_1$ . Clearly this is not consistent with the results of boundary layer theory since boundary-layer separation would then occur before the assumed separation point. Thus, only the case of finite streamline curvature will be considered.

The other condition of equal pressures at the separation points results from vorticity transport considerations. In wing-airfoil theory, no net vorticity is shed from the wing in steady flow; that is, the average flux of vorticity out of any fixed circuit around the airfoil is zero. For the rotating cylinder, the average flux of vorticity out of any fixed circuit around the cylinder should also be zero. Now, if no vorticity were transported into the wake from the rear part of the rotating cylinder immersed in the wake, then equal amounts of vorticity (but with opposite signs) should be transported into the wake at the separation points from the upper and lower parts of the cylinder. The rate of vorticity transport downstream at a separation point is

$$\int_c^\infty u \frac{\partial u}{\partial y} dy = (u_{es}^2 - u_w^2) / 2 , \quad (16)$$

where the subscript s denotes conditions at separation. This is the result obtained considering either the lower or upper side of the cylinder. Since vorticity transport must then be the same at both separation points, this implies that the magnitudes of  $u_e$  at both separation points will be equal. From Bernoulli's equation, the pressure at both separation points will be the same.

The original assumption of equal pressures at the separation points was attributed to Howarth<sup>28</sup> by Piercy, Preston, and Whitehead. Although this assumption is also used in the present work, Piercy, Preston, and Whitehead<sup>21</sup> took into account the possibility that vorticity is gener-

28. L. Howarth, "The Theoretical Determination of the Lift Coefficient for a Thin Elliptic Cylinder," Proceedings of the Royal Society, Vol. A-149, 1935, pp. 558-586.

ated by the part of the cylinder that is immersed in the wake. He obtained good results for an ellipse at a nonzero angle of attack. To take this castoff vorticity into account would complicate the problem to be addressed here although it would be a suitable refinement to be considered in subsequent investigations.

### C. Numerical Method of Obtaining the Model

To obtain the values of the five basic parameters appearing in equation (8) in the  $\zeta$  plane - given the two separation points in the physical plane - a system of five nonlinear equations must be solved. One might attempt to solve these equations analytically as was done for Bluston and Paulson's relatively simple model. For their model,  $u_e$  finally reduced to a trigonometric expression that involved only the untransformed-plane angles  $\phi$  and  $\bar{\alpha}$ . An unsuccessful attempt was made to solve the present more complicated set of equations analytically; therefore, it was decided to solve for the five parameters systematically using numerical techniques.

The system of five equations is obtained from requirements imposed by separation and the previously discussed curvature and pressure conditions at separation. The first requirement is derived from the nature of the critical points,  $S_1$  and  $S_2$ ; these are the stagnation points in the untransformed plane caused by the upstream flow from the sources placed on the circle. Thus, the untransformed velocity  $q$  at the critical points is zero.

From the expression for  $q$ , equation (8), the following two equations are then obtained at the critical points,  $\phi = \pm \bar{\alpha} - \varepsilon$ , respectively:

$$2 \sin(\bar{\alpha} - \varepsilon) - \left[ Q_1 \cot\left(\frac{\bar{\alpha} - \gamma - \varepsilon}{2}\right) + Q_2 \cot\left(\frac{\bar{\alpha} - \delta - \varepsilon}{2}\right) \right] + u_c = 0. \quad (17)$$

$$2 \sin(\bar{\alpha} + \varepsilon) - \left[ Q_1 \cot\left(\frac{\bar{\alpha} + \gamma + \varepsilon}{2}\right) + Q_2 \cot\left(\frac{\bar{\alpha} + \delta + \varepsilon}{2}\right) \right] - u_c = 0. \quad (18)$$

The next requirement imposed was that the magnitude of the velocities should be equal at separation in the physical plane as required by Howarth's assumption; i.e.:

$$u_e(x_{s1}) = -u_e(x_{s2}) \quad (19)$$

where the subscript symbols  $s1$  and  $s2$  indicate the upper and lower separation points respectively. The negative sign occurs in this equation because  $x$  increases on the upper side of the cylinder and decreases on the lower side of the cylinder. Now from the expression for  $u_e$  in equation (13),  $u_e$  is indeterminate at the separation points since  $q$  and  $N$  are both zero there. This indeterminacy could have

been removed if the problem had been solved analytically. Since the computer was available, an approximation to the requirement of equation (19) was obtained using numerical computation techniques. For angular positions very near to the critical points, the absolute values of the velocities in the physical plane were set equal to each other at the following two points:

$$\pm \alpha_1 = (\bar{\alpha} + \Delta\sigma) , \quad (20)$$

where  $\pm \alpha_1$  are the values of  $\sigma$  very near to  $\pm \bar{\alpha}$  and  $\Delta\sigma$  is a small incremental angle. Now from equation (15) it is seen that

$$N(\alpha_1 - \varepsilon) = N(-\alpha_1 - \varepsilon) \quad (21)$$

where  $\varepsilon$  is a parameter for  $N$ . Hence, a condition almost equivalent to equation (19) can be imposed:

$$q(\alpha_1 - \varepsilon) = -q(-\alpha_1 - \varepsilon) . \quad (22)$$

Thus, from equation (8), the following equation will result:

$$2 [\sin(\alpha_1 - \varepsilon) - \sin(\alpha_1 + \varepsilon)] - Q_1 \left[ \cot\left(\frac{\alpha_1 - \gamma - \varepsilon}{2}\right) - \cot\left(\frac{\alpha_1 + \gamma + \varepsilon}{2}\right) \right] \\ - Q_2 \left[ \csc\left(\frac{\alpha_1 - \delta - \varepsilon}{2}\right) - \csc\left(\frac{\alpha_1 + \delta + \varepsilon}{2}\right) \right] + 2 u_c = 0 . \quad (23)$$

The smoothness or finite curvature requirement is used to obtain two more equations. A result of the smoothness requirement is that the value of  $du_e/dx$  is finite at the separation point. Now from the chain rule:

$$\frac{du_e}{dx} = \frac{du_e}{d\phi} / \frac{dx}{d\phi} . \quad (24)$$

But  $x$  as a function of  $\phi$  at the separation points ( $S_1, S_2$ ) are extrema since the circle  $E$  in the untransformed plane (Figure 2) is mapped onto the curved slit  $S_1 AS_2 BS$ , in the physical plane (Figure 3). Therefore

$$\frac{dx}{d\phi} \Big|_{S_1, S_2} = 0 ,$$

and thus

$$\frac{du_e}{d\phi} \Big|_{S_1, S_2} = 0 \quad (25)$$

is a necessary condition that  $du_e/dx$  be finite at the critical points.

But  $N(\phi)$ , which is zero at the critical points, occurs in the denominator in the expression for  $du_e/d\phi$  as a squared term. So then in a similar manner as was done for the equal pressure condition, use points at angle  $\Delta\phi$  away from the points  $S_1, S_2$ :

$$\frac{du_e(\alpha_1 - \epsilon)}{d\phi} = \frac{du_e(-\alpha_1 - \epsilon)}{d\phi} = 0 \quad . \quad (26)$$

The smoothness condition at  $\phi = \alpha_1 - \epsilon$  becomes

$$\begin{aligned} & \frac{(1-2 \cos \bar{\alpha} \cos \alpha_1 + \cos^2 \bar{\alpha})}{2 (\cos \bar{\alpha} - \cos \alpha_1)} \left\{ 2 \cos (\alpha_1 - \epsilon) \right. \\ & + \frac{1}{2} \left[ Q_1 \csc^2 \left( \frac{\alpha_1 - \epsilon - \gamma}{2} \right) + Q_2 \csc^2 \left( \frac{\alpha_1 - \epsilon - \delta}{2} \right) \right] \left. \right\} \\ & + \frac{\sin \alpha_1 (\cos^2 \bar{\alpha} - 1)}{2 (\cos \bar{\alpha} - \cos \alpha_1)^2} \left\{ 2 \sin (\alpha_1 - \epsilon) - \left[ Q_1 \cot \left( \frac{\alpha_1 - \epsilon - \gamma}{2} \right) \right. \right. \\ & \left. \left. + Q_2 \cot \left( \frac{\alpha_1 - \epsilon - \delta}{2} \right) \right] + u_c \right\} = 0 \quad . \end{aligned} \quad (27)$$

The smoothness condition at  $\phi = -\alpha_1 - \epsilon$  is given as

$$\begin{aligned} & \frac{(1-2 \cos \alpha_1 + \cos^2 \bar{\alpha})}{2 (\cos \bar{\alpha} - \cos \alpha_1)} \left\{ 2 \cos (\alpha_1 + \epsilon) + \frac{1}{2} \left[ Q_1 \csc^2 \left( \frac{\alpha_1 + \epsilon + \gamma}{2} \right) \right. \right. \\ & \left. \left. + Q_2 \csc^2 \left( \frac{\alpha_1 + \epsilon + \delta}{2} \right) \right] \right\} - \frac{\sin \alpha_1 (\cos^2 \bar{\alpha} - 1)}{2 (\cos \bar{\alpha} - \cos \alpha_1)^2} \left\{ -2 \sin (\alpha_1 + \epsilon) \right. \\ & \left. + Q_1 \cot \left( \frac{\alpha_1 + \epsilon + \gamma}{2} \right) + Q_2 \cot \left( \frac{\alpha_1 + \epsilon + \delta}{2} \right) + u_c \right\} = 0 \quad . \end{aligned} \quad (28)$$

Equations (17), (18), (23), (27), and (28) constitute a nonlinear system of equations to be solved for  $Q_1, Q_2, \gamma, \delta$ , and  $u_c$ . These values are determined by only two parameters in the untransformed plane,  $\bar{\alpha}$  and  $\epsilon$ . These two parameters are in turn determined by  $x_{s1}$  and  $x_{s2}$  as given by equation (33).

Equations (17), (18), (23), (27), and (28) are solved using the iterative Newton-Raphson method and the parameters are said to be found when the biggest change in any of the parameters is less than  $2 \cdot 10^{-5}$  from one iteration to the next.

To approximate the values of the parameters that would be obtained if the pressure and curvature conditions could be applied at the separation points, the following procedure is followed. The value of  $\Delta\sigma = -0.08^\circ$  is first used and the corresponding parameters are computed. The parameters for  $\Delta\sigma = 0.08^\circ$  are next found and these two sets of parameters are used to find the estimated parameters for  $\Delta\sigma = 0$  by linear interpolation. A question might occur as to how accurate this approximation might be, especially if the parameters changed in a nonlinear manner and rapidly with  $\Delta\sigma$ . Figures 4 and 5 show the variation of  $Q_1$  and  $\gamma$  versus  $\Delta\sigma$  and both are approximately linear with  $\Delta\sigma$  which is very encouraging in light of the linear interpolation used in the program. The circulation was also found to have similar linear behavior.

To numerically calculate the solution, some relationships and quantities need to be found, such as the radius of the cylinder in the  $z$  plane. Using the mapping function  $M(\bar{z})$  described by equation (10), it is found that the position of  $S_1$  in the  $\bar{z}$  plane is given by  $2i$ . Drawing a line from the center of the circular arc  $C$  in the  $\bar{z}$  plane to  $S_1$ , the radius is seen to be

$$a = 2 \csc m_{s1} \quad (29)$$

where --as mentioned before--the subscript  $s1$  denotes evaluation at the upper separation point  $S_1$ . The length from the origin in the  $\bar{z}$  plane along the real line to the arc  $C$  is given by

$$M(-\csc \bar{\alpha}) = -2 \cot \bar{\alpha} \quad . \quad (30)$$

Thus, drawing a straight line from point  $A$  to  $S_1$ , it is seen from equation (30) that

$$\bar{\alpha} = (\pi - m_{s1}) / 2 \quad . \quad (31)$$

Using equation (31),  $a$  is then found to be, from equation (29):

$$a = 2 \csc 2 \bar{\alpha} \quad . \quad (32)$$

Knowing  $x_{s1}$  and  $x_{s2}$ , the values  $\bar{\alpha}$  and  $\epsilon$ , which determine the five parameters in the plane  $\zeta$ , can be found using Figure 3 and equation (31):

$$\epsilon = (x_{s1} + x_{s2}) / 2 \quad , \quad (33)$$

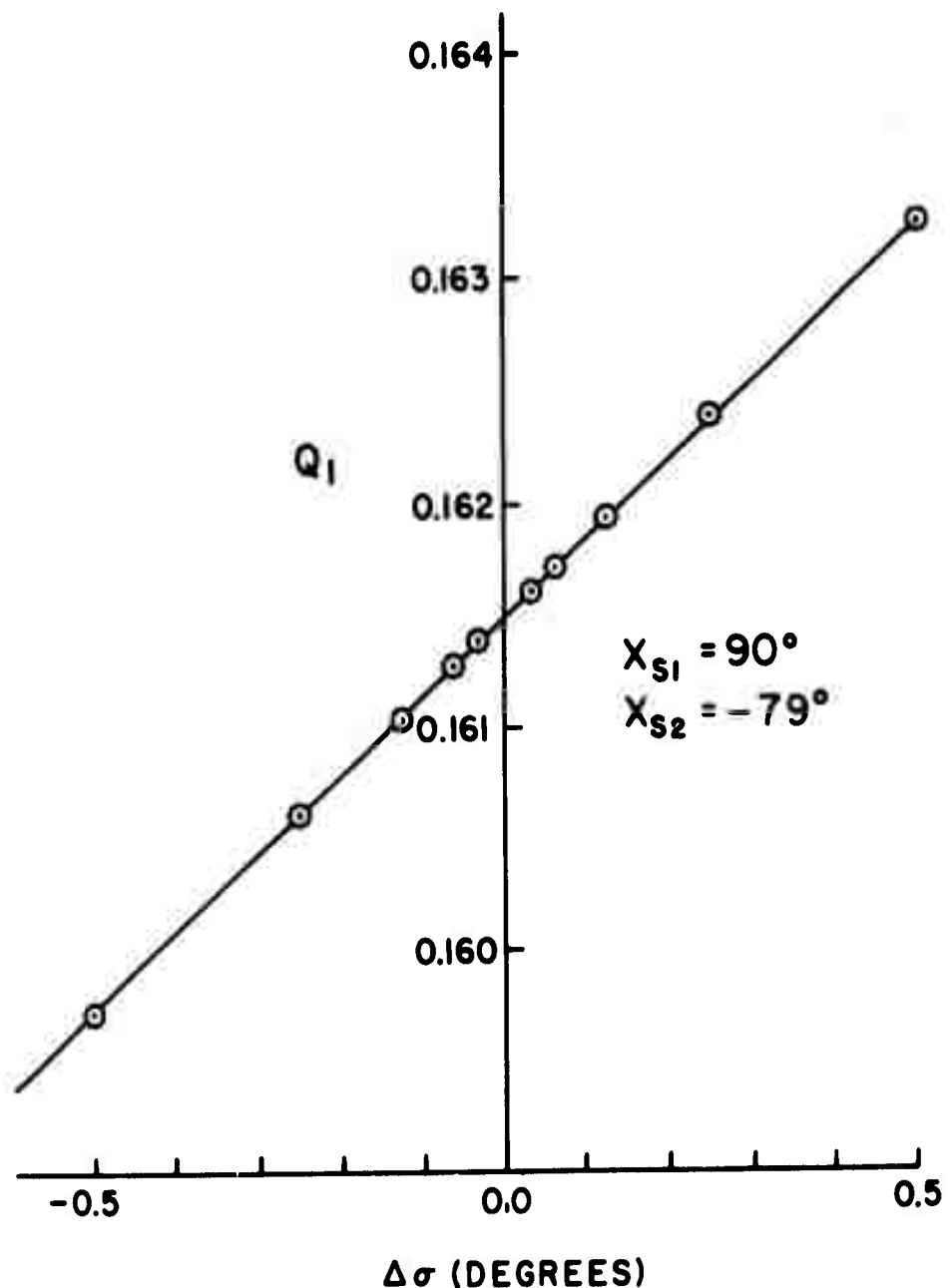


Figure 4.  $Q_1$  vs.  $\Delta\sigma$

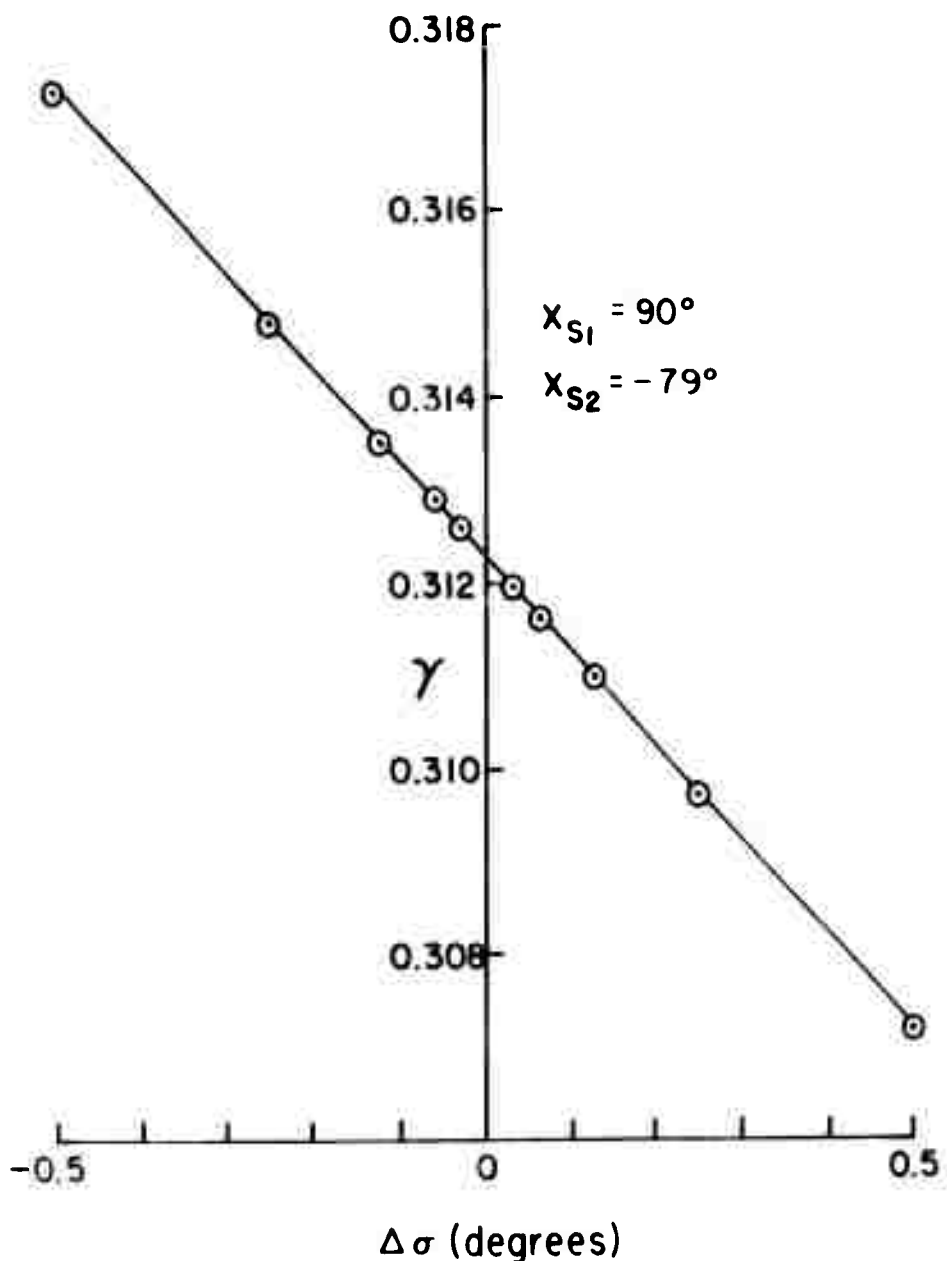


Figure 5.  $\gamma$  vs.  $\Delta\sigma$

$$\bar{\alpha} = (\pi - x_{s1} + \epsilon) / 2 . \quad (33)$$

Since the quantities in the plane  $z$  will be calculated in terms of the angular position  $\phi$  in the  $\zeta$  plane, it is necessary to determine a relationship between  $\phi$  and  $x$ . To do this, consider the directed vector  $\vec{a}$  from the center of the circular arc  $C$  in the physical planes to a point on the arc  $C$  in the physical planes. Using the mapping function given by equation (10), the expression for  $\vec{a}$  is given by the following:

$$\vec{a} = M [ \csc \bar{\alpha} \exp (i\sigma) ] - M(0) . \quad (34)$$

This expression can be manipulated to a form such that the imaginary part of  $\vec{a}$  can be taken. The imaginary part of  $\vec{a}$  is just  $a \sin m$ . Using the imaginary part of the expression for  $\vec{a}$  from equation (34) and applying trigonometric identities, the following relationship is obtained:

$$\sin m = \frac{\sin \sigma (1 - \cos \bar{\alpha} \cos \sigma)}{(\sec \bar{\alpha} + 1/\sec \bar{\alpha}) - \cos \sigma} . \quad (35)$$

Expressing equation (35) in terms of  $\phi$  and  $x$ , the following equation is obtained:

$$\sin(x - \epsilon) = \frac{\sin(\phi + \epsilon) [1 - \cos \bar{\alpha} \cos(\phi + \epsilon)]}{[(\sec \bar{\alpha} + 1/\sec \bar{\alpha})/2] - \cos(\phi + \epsilon)} \quad (36)$$

The velocity and derivative of the velocity with respect to angle in the physical plane are calculated as these quantities appear in the integral boundary-layer equations. A subprogram was constructed to obtain these quantities found in terms of the untransformed variable ( $\phi$ ) and parameters in the plane  $\zeta$ . This subprogram is called at each step of the integration of the boundary-layer equations. First the relationship between  $x$  and  $\phi$  is found using equation (36). The value of  $\phi$  is found using the iterative method of Newton. Successive values of  $\phi$  found during iteration must be within  $10^{-6}$  before the method is declared to have converged. The values of  $u_e$  and  $du_e/dx$  can then be found from equation (8), its derivative with respect to  $\phi$ , equation (15), its derivative with respect to  $\phi$ , and substituting the results into equations (13) and its derivative with respect to  $\phi$ . For more details, the listing of the computer program is given in Appendix A.

#### D. Method of Obtaining Agreement Between the Flow Model and the Boundary-Layer Calculation Results

For bodies with fixed surfaces, boundary-layer calculations can approximately predict the point of separation given the external velocity distribution. In this investigation of the rotating cylinder,

the final inviscid-flow model's separation points are made to agree with the location of the separation points found by numerical calculation of the boundary layer. This flow-model can thus be made consistent with boundary-layer theory using the integral boundary-layer technique developed here.

The procedure for obtaining consistency between the flow-model and boundary layer theory is quite simple in principle. The boundary layer equations for flow over the rotating circular cylinder are solved with assumed separation points for the inviscid-flow model further back on the cylinder than they would be anticipated to actually occur. Separation points are then obtained from the results of the boundary-layer calculation and a revised inviscid flow model is then constructed using these new separation points. Again new boundary-layer separation points are found and the flow model is again modified using these new separation points. This process is repeated until the largest absolute value of the difference in separation location for the last two particular flow models is less than a value called  $E_c$ . The value of  $E_c$  used in this work was  $E_c = 0.46$  degrees.

### III. FLOW-MODEL RESULTS AND DISCUSSION

The external velocity distributions consistent with the boundary-layer calculations and the corresponding lift and drag coefficients are of chief interest for comparison with experiment. The range of  $u_w$  considered here ( $0 \leq u_w \leq 0.32$ ) is chiefly limited by stability of the boundary-layer calculation method used although Swanson<sup>1</sup> indicates that turbulence always appears before separation on the lower side of the cylinder when  $u_w > 0.5$  for the range of Reynolds numbers investigated. He investigated the Magnus effect for  $3.58 \cdot 10^4 \leq Re_d \leq 5.01 \cdot 10^5$ .

#### A. External-Velocity Distributions

Figure 6 illustrates the first trial external-velocity distribution up to the point of separation and compares it with the converged or final velocity distribution when  $u_w = 0.2$ . Figures 7 and 8 present, in the adverse pressure gradient region, details of these distributions with additional distributions found in the iteration process to obtain convergence. The graphs are representative of the convergence behavior using this iterative method for all corresponding values of  $u_w$  considered with one exception. For  $u_w = 0.3$ , various initial values of separation points were tried, but after a few iterations the boundary layer calculations would not separate up to and including the breakaway point of the inviscid-flow model. It is felt that the boundary layer needs to

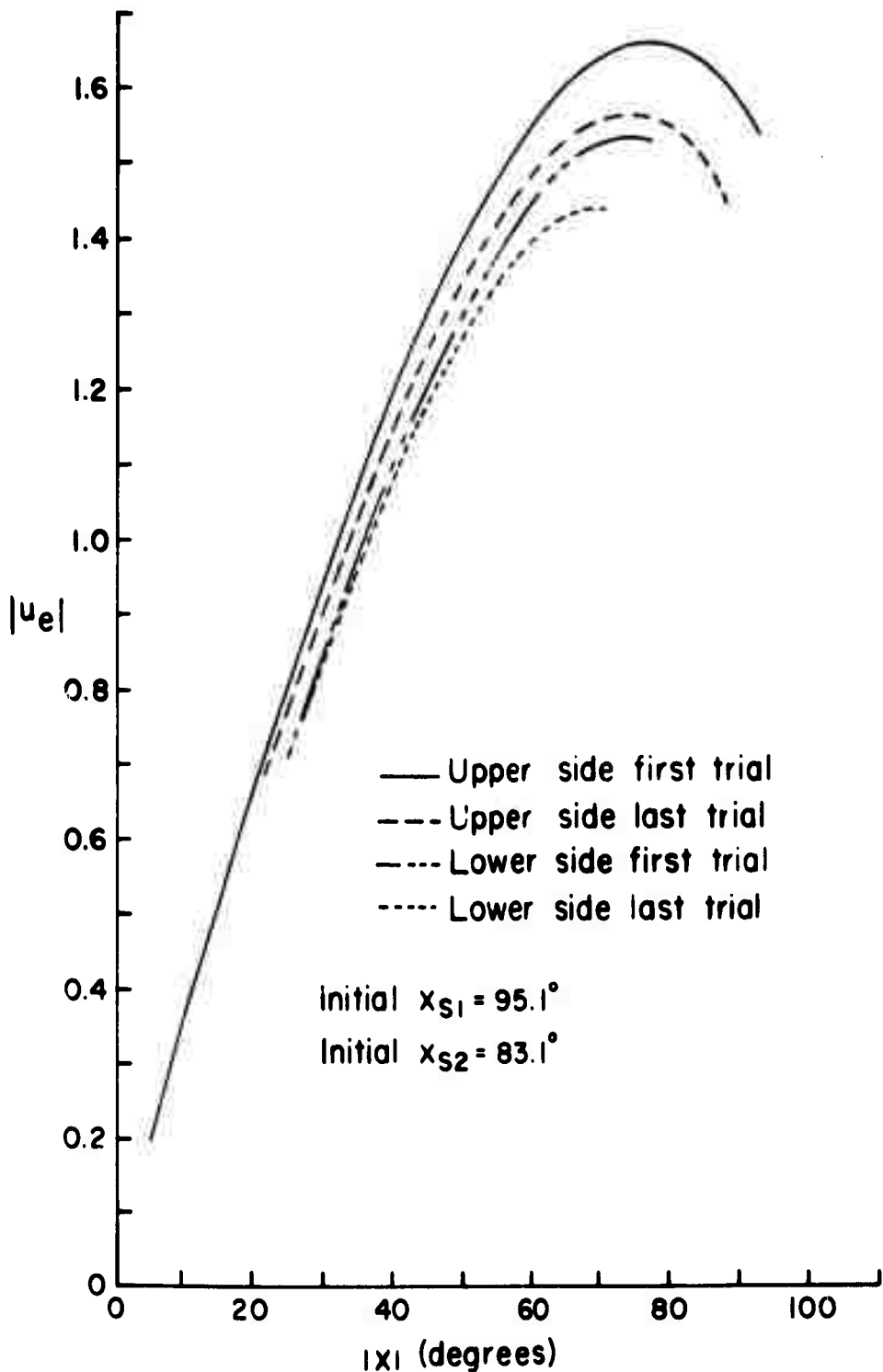


Figure 6. Comparison Between First and Converged Velocity Distributions ( $u_w = 0.2$ )

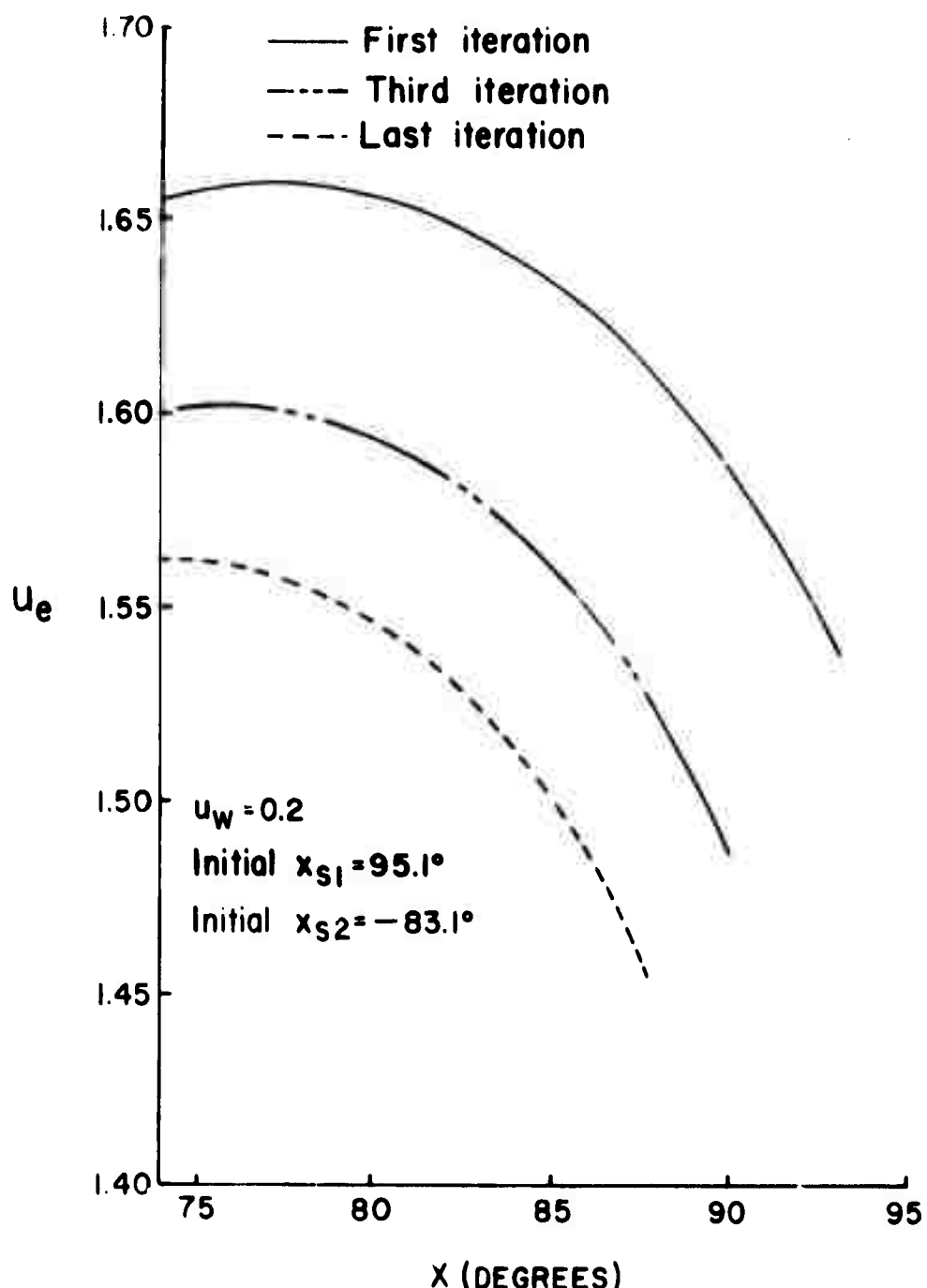


Figure 7. Velocity Distribution Details - Upper Side Adverse Pressure Gradient Region

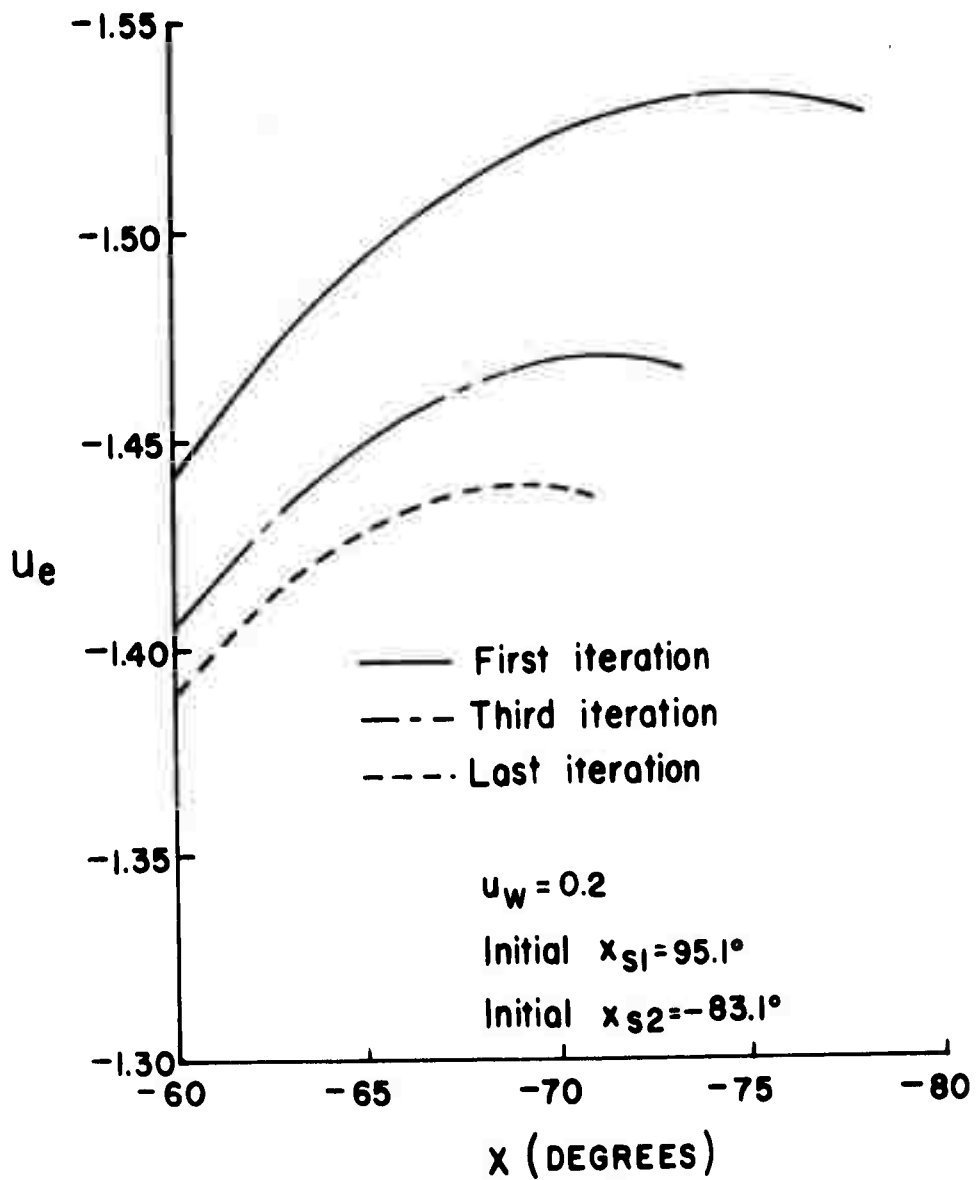


Figure 8. Velocity Distribution Details - Lower Side  
in Adverse Pressure Gradient Region

be calculated more accurately near separation for larger negative values of  $u_w/u_e$ . Granted adequate time, it is thought that consistent and more meaningful results could be achieved by improving the integral boundary-layer technique.

For a cylinder rotation rate of 0.15, the locations of separation versus the trial number in the iteration process to find a converged solution is shown in Figure 9. As mentioned before, when the absolute value  $E_c$  of the differences between the positions of succeeding values of separation points on both sides of the cylinders become less than 0.46 degrees, convergence was considered to be achieved. Bluston and Paulson's value of  $E_c$  was  $0.5^\circ$ . For  $u_w = 0.15$ , the value of  $E_c$  was decreased to 0.16 degrees to observe the convergence behavior more closely. In Figure 9, it is seen that three more iterations were required to satisfy the tighter convergence criterion.

The convergence of the lift coefficient can also be studied in Figure 10. Here it is seen that the value of  $C_L$  from circulation considerations is quite sensitive to separation location. The value of  $C_L$  for  $E_c = 0.16$  was about 80% of  $C_L$  for  $E_c = 0.46$  degrees. However, by integrating the vertical component of the pressure coefficient over the cylinder up to the point of separation, the values of  $C_L$  were found to be within 10% of each other for the two values of  $E_c$ .

In choosing a precision criterion, one must accept a compromise between computing time and accuracy of the boundary layer calculation method. In retrospect, it appears that by using an accelerated convergence technique, a more rigorous standard for the convergence criterion could have been adopted. However, it might be better to improve the inviscid flow model in some other way; for instance, one could change the flow model to take into account the cast-off vorticity from that part of the cylinder immersed in the wake region.

Figure 11 compares some experimental velocity distributions with the results of the current analysis for the nonrotating cylinder. The curve of Fage and Falkner<sup>29</sup> was obtained from Bluston and Paulson's paper while the curve of Petrie and Simpson<sup>30</sup> was taken directly from

- 
29. A. Fage and V. M. Falkner, "The Flow Around a Circular Cylinder," ARC E&M No. 1369, 1931.
  30. A. M. Petrie and H. C. Simpson, "An Experimental Study of the Sensitivity to Freestream Turbulence of Heat Transfer in Wakes of Cylinders in Crossflow," Int. J. of Heat and Mass Transfer, Vol. 15, 1972, pp. 1497-1513.

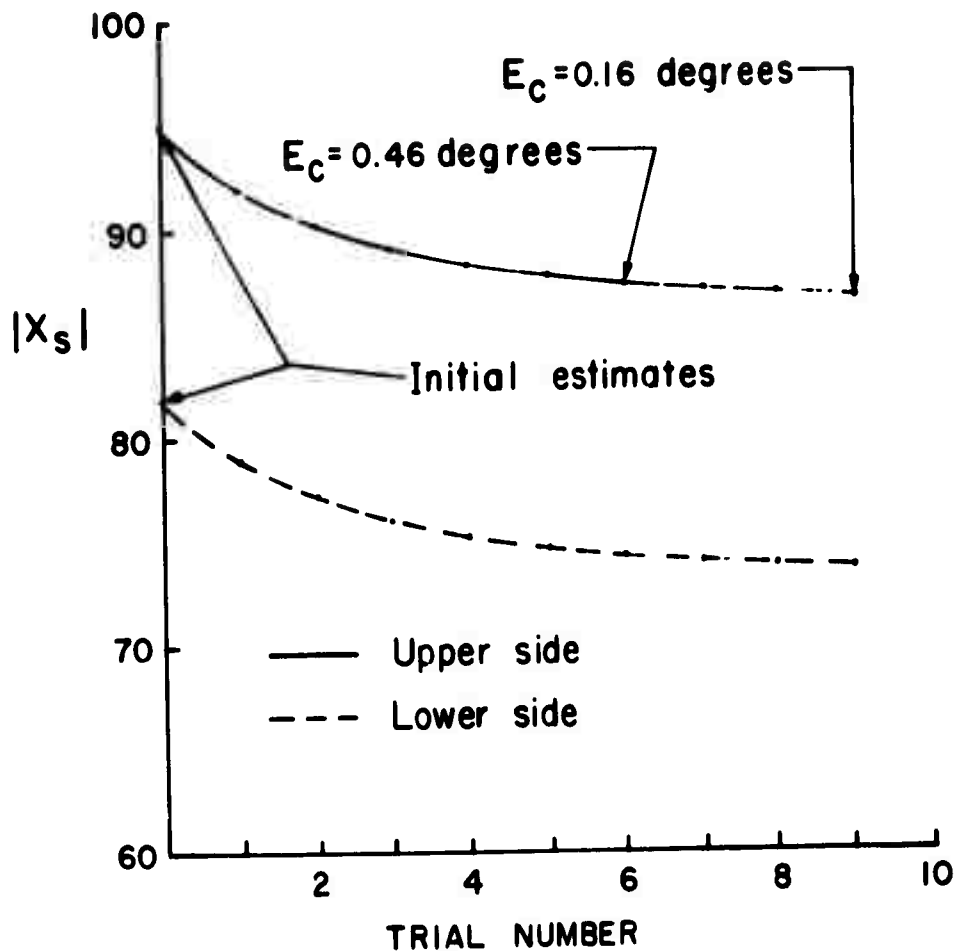


Figure 9. Location of Boundary-Layer Separation vs. Trial Number  
 $(u_w = 0.15)$

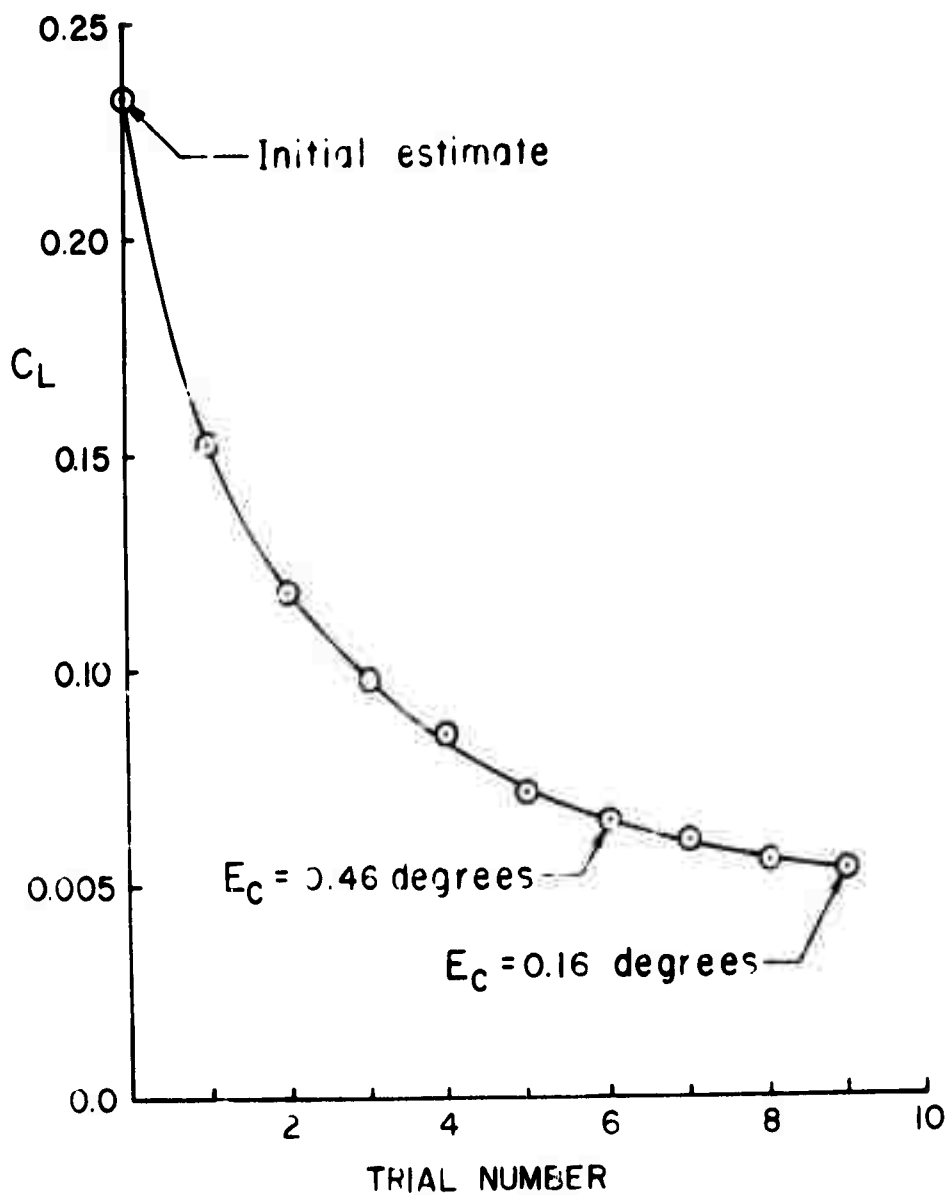


Figure 10. Lift Coefficient vs. Trial Number ( $u_w = 0.15$ )

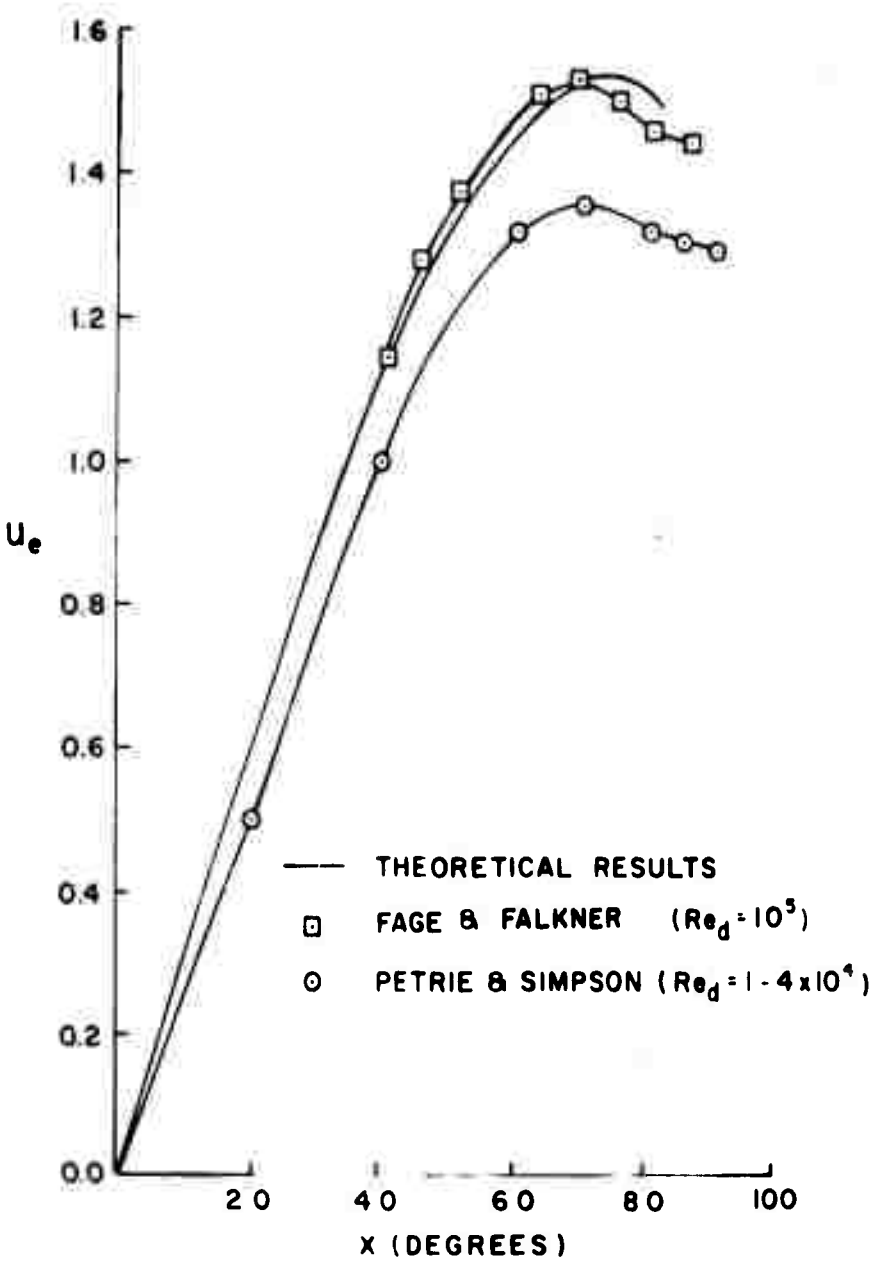


Figure 11.  $u_e$  vs.  $x$  - Comparison with Experiment ( $u_w = 0$ )

their paper. Fage and Falkner's curve gives the better agreement with the theoretical curve, but is for a higher Reynolds number than for the other curves with the amount of turbulence in the freestream unknown. The curve of Petrie and Simpson was obtained with very little mainstream turbulence; by introducing a large amount of turbulence into the mainstream, they obtained data similar to the Fage and Faulkner's results. The theoretical curve approximates the experimental curves better than the simple sine curves or series curves. Nevertheless, some sort of refinement of the inviscid-flow model might better represent the observed pressure distributions in the adverse pressure gradient region.

A check of Bluston and Paulson's velocity distribution reveals it to be nearly identical to the theoretical distribution found in the present investigation. This agreement with Bluston and Paulson further increases confidence in the procedure of finding the five parameters ( $Q_1$ ,  $Q_2$ ,  $\gamma$ ,  $\delta$ ,  $u_c$ ) in the untransformed plane by computer.

It has been seen that converged separation points can be found by this iterative process given certain initial trial separation points. The question naturally arises as to how the final separation points are affected by the particular choice of initial separation points. To answer this question, different sets of initial separation point values were used in the computer program. The results are tabulated as follow:

TABLE I. INITIAL AND FINAL VALUES OF SEPARATION

| $u_w$ | Initial Values         |                        | Final Values           |                        |
|-------|------------------------|------------------------|------------------------|------------------------|
|       | Upper Side<br>$x_{s1}$ | Lower Side<br>$x_{s2}$ | Upper Side<br>$x_{s1}$ | Lower Side<br>$x_{s2}$ |
| 0.2   | $95.1^{\circ}$         | $-81.9^{\circ}$        | $87.50^{\circ}$        | $-70.61^{\circ}$       |
| 0.2   | $92.8^{\circ}$         | $-83.1^{\circ}$        | $87.57^{\circ}$        | $-70.82^{\circ}$       |
| 0.1   | $94.5^{\circ}$         | $-87.6^{\circ}$        | $85.77^{\circ}$        | $-77.30^{\circ}$       |
| 0.1   | $95.0^{\circ}$         | $-81.9^{\circ}$        | $85.86^{\circ}$        | $-77.28^{\circ}$       |

The final values for the separation points vary at most  $0.2^{\circ}$  with these initial choices. As will be seen later, the variation in the lift and drag coefficients will also vary a small amount with initial choice of the breakaway points. This dependence of the final values on the initial values could probably be decreased further by using a more rigorous standard for convergence.

Figure 12 shows absolute values of  $u_e$  plotted against the absolute value of  $x$  for some different values of  $u_w$ . The separation points can be seen to be delayed on the upper side and advanced on the lower side in agreement with observation.

The inviscid flow fields external to the cylinder were also investigated. Figure 13 shows the streamlines in the untransformed plane for the nonrotating cylinder and Figure 14 exhibits the streamlines in the corresponding physical plane. Figure 15 and 16 gives the pattern of streamlines in the untransformed and physical plane respectively for  $u_w = 0.2$ . The zero stream function lines in the untransformed plane are seen to leave perpendicular to the cylinder whereas in the transformed plane these lines leave the circle tangentially as required by the transformation. It may be observed that the streamlines that form the boundary of the wake in the physical plane are very nearly parallel; the main effect of the low rotation rate is to produce a slight asymmetry in the streamlines near the separation points. The streamline pattern in the untransformed plane show greater departures from a symmetrical pattern than for the physical plane case.

The stagnation points shift to negative  $x$  values as  $u_w$  is increased. Below is a table giving these stagnation points for different values of  $u_w$ .

---

\*The curves do not extend to  $x = 0$  since values of  $u_e$  and  $du_e/dx$  are printed out only for that region being numerically calculated with the integral boundary-layer equations. The limitations of the computer code restrict integration of the boundary-layer equations on the lower side to the region where  $u_w/u_e \geq -0.3$ . Thus, the value of  $|x|$  at which integration can start becomes larger with increasing  $u_w$ .

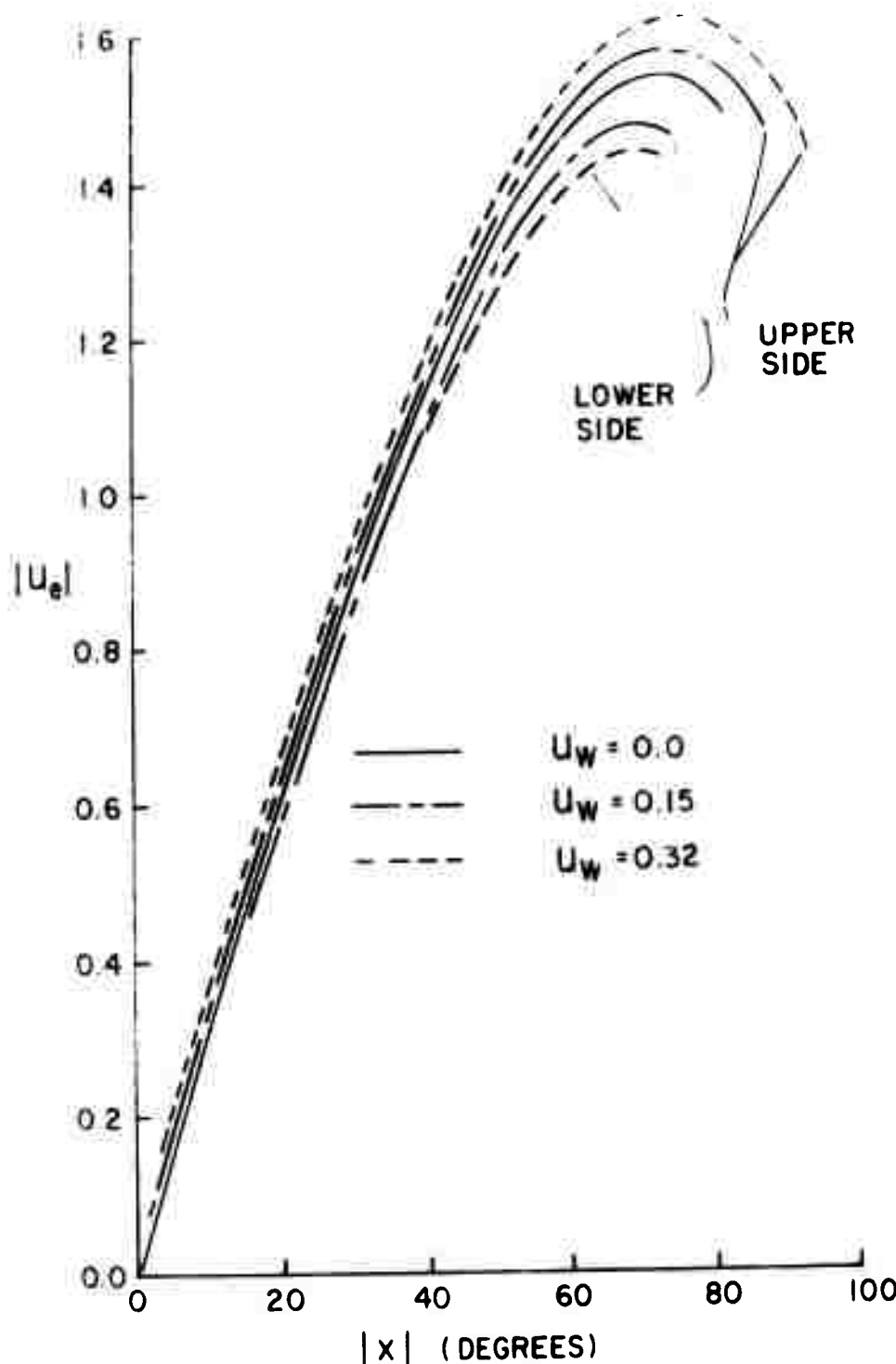
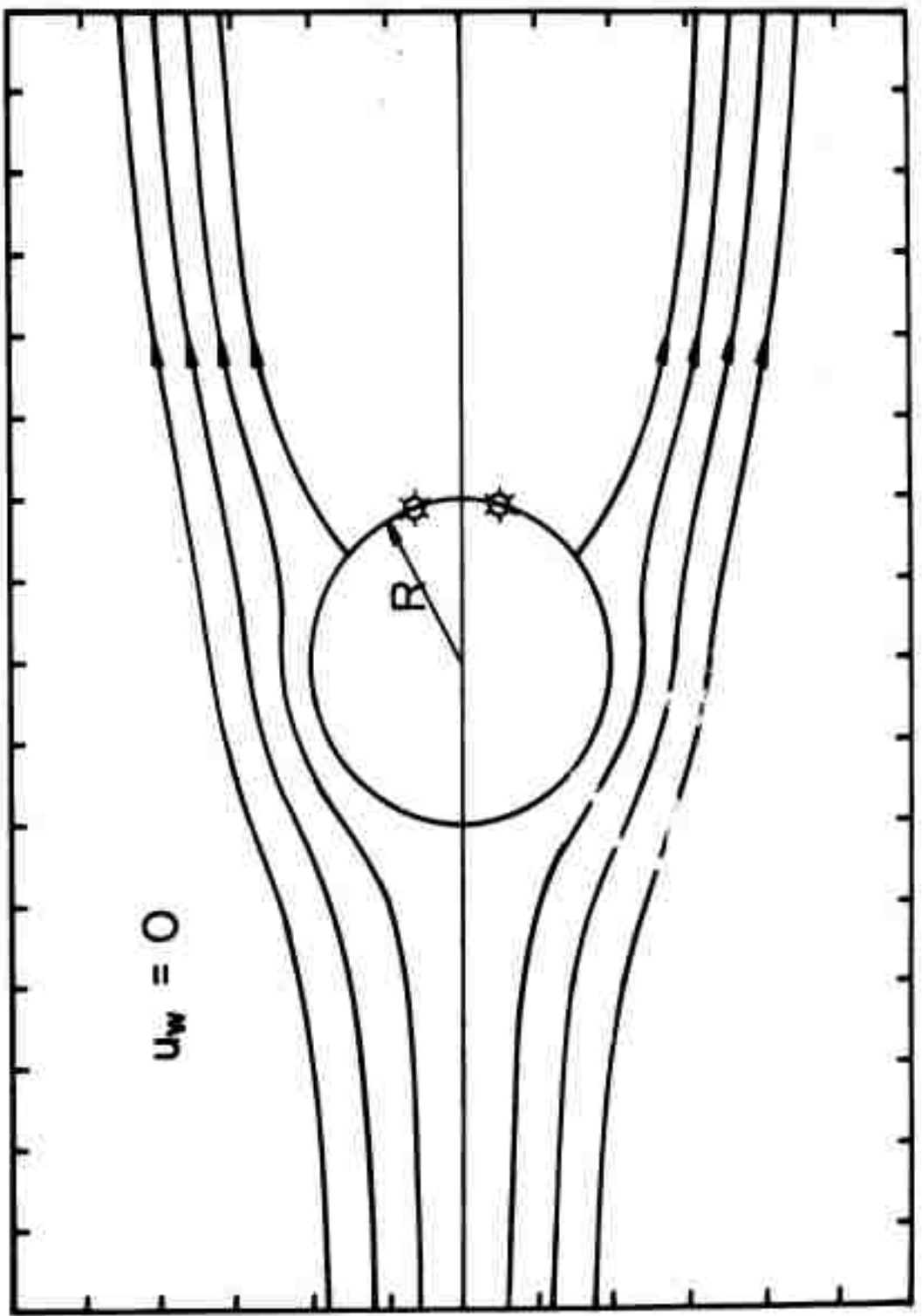


Figure 12.  $|u_e|$  vs.  $|x|$  -- Parameter is  $u_w$

Figure 13. Streamline Pattern Around Cylinder in Untransformed Plane --  $u_w = 0.0$



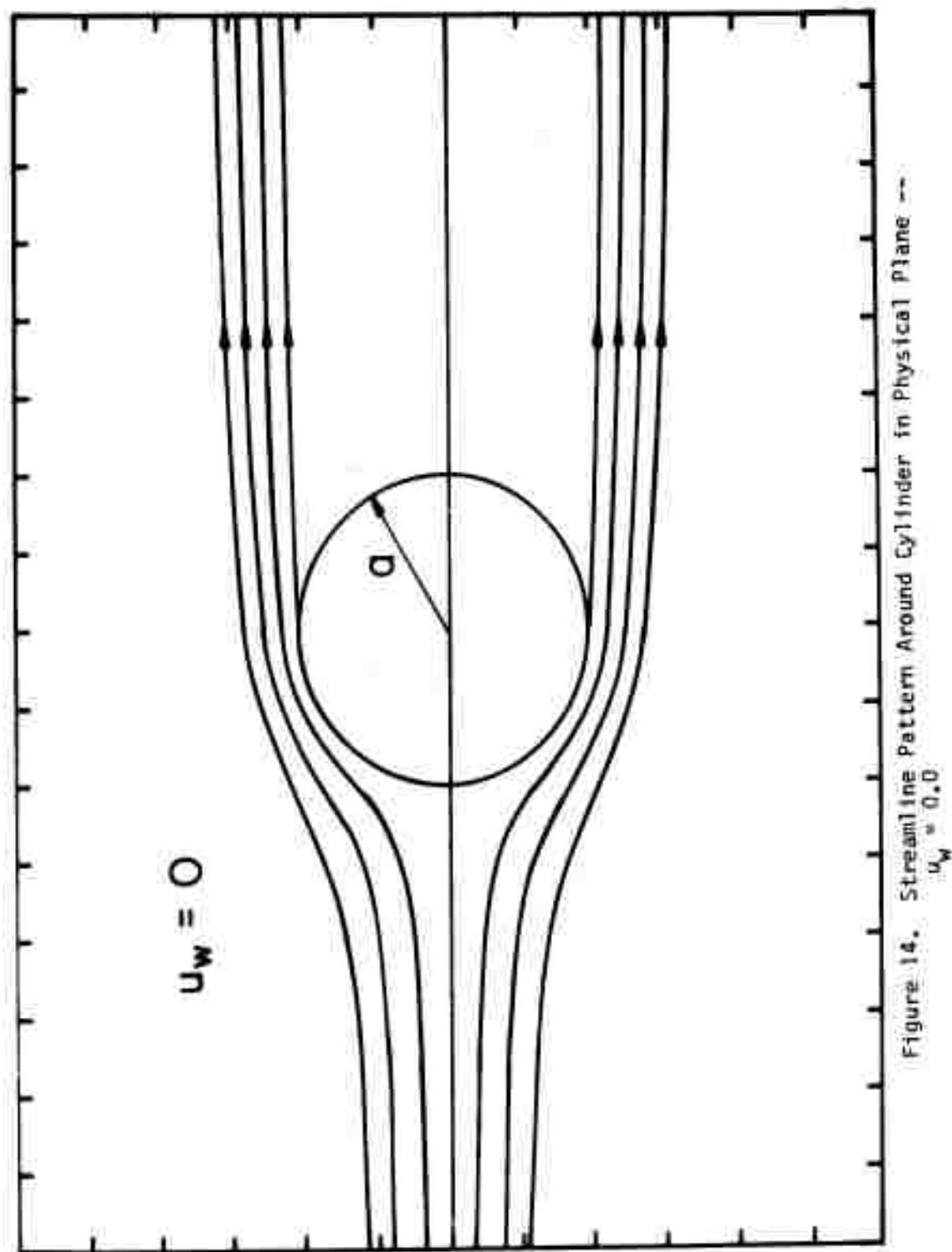


Figure 14. Streamline Pattern Around Cylinder in Physical plane  
 $U_w = 0.0$

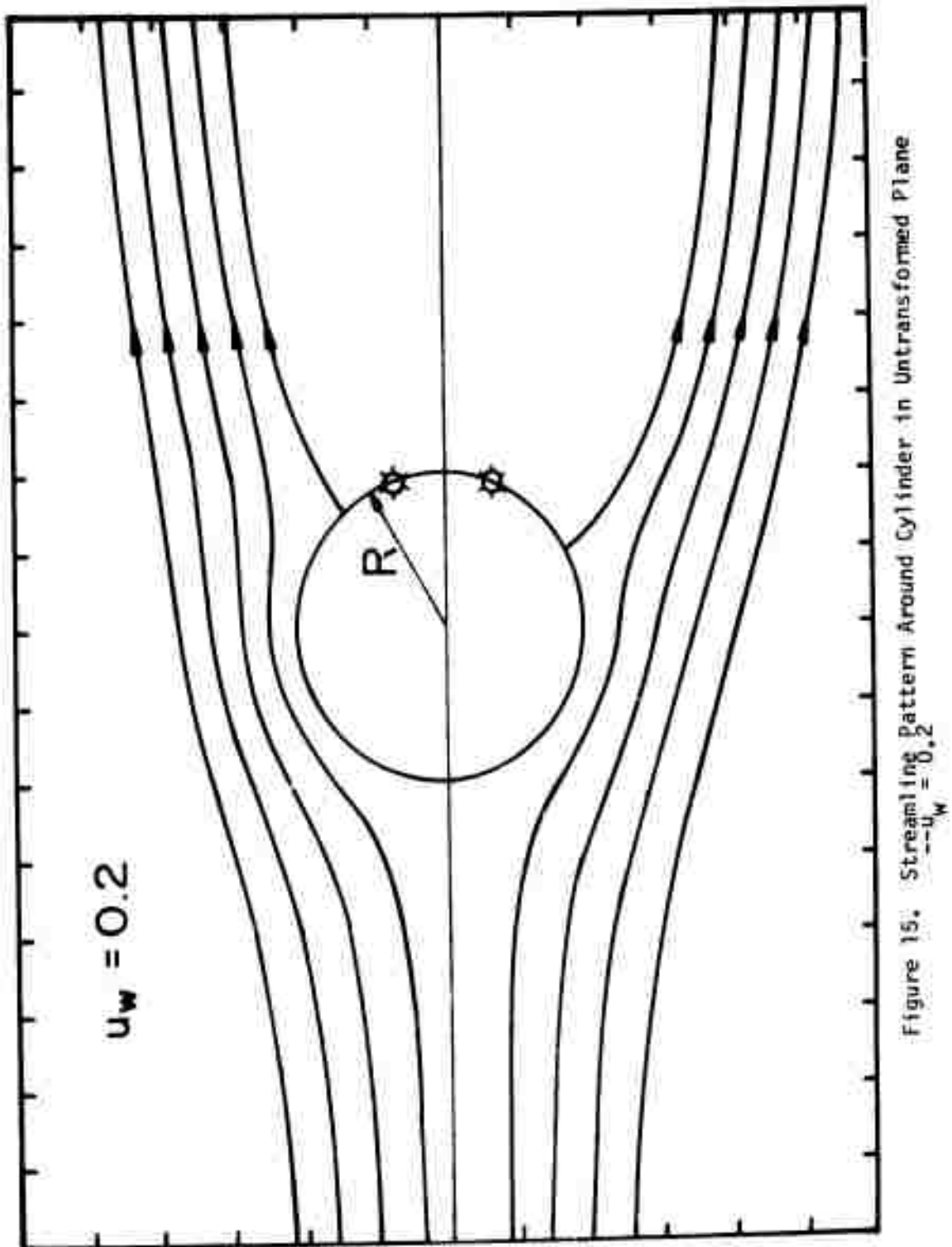


Figure 15. Streamline Pattern Around Cylinder in Untransformed Plane  
 $u_w = 0.2$

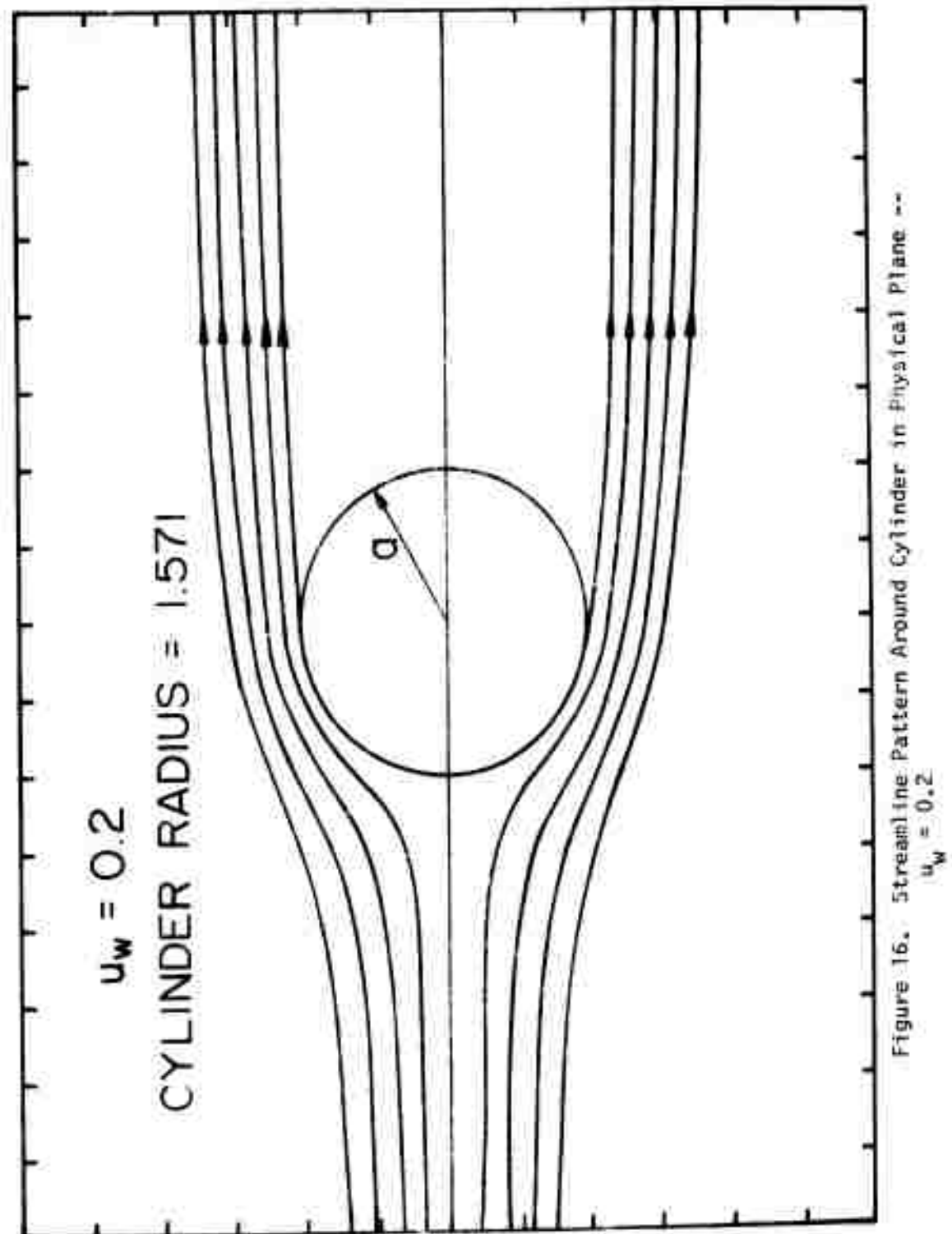


Figure 16. Streamline Pattern Around Cylinder in Physical Plane --  $U_\infty = 0.2$

TABLE II. STAGNATION POINT ON CYLINDER FOR DIFFERENT RATES OF ROTATION

| <u><math>u_w</math></u> | <u>Stagnation Point Location (Degrees)</u> |
|-------------------------|--|
| 0.0                     | 0.0  |
| 0.1                     | -0.53                                      |
| 0.2                     | -0.91                                      |
| 0.25                    | -1.19                                      |
| 0.32                    | -1.76                                      |

This displacement direction of the stagnation point also occurs in experiments. However, no detailed comparison with experiment can be made for these small rotation rates partly because of the difficulty in measuring small changes in the stagnation point location. Below  $u_w = 0.25$ , the stagnation point is displaced linearly with  $u_w$  but the displacement for  $u_w = 0.32$  is larger than the linear relationship would predict. The velocity distribution curves  $u_w = 0.2$  and  $u_w = 0.25$  do not follow the trends expected and noted in Figure 12. Comparing the upper-side velocity distributions in Figure 17 reveals that the maximum value of velocity for  $u_w = 0.15$  is actually higher than it is for  $u_w = 0.25$ . The upper side displacement of separation increases only a minimal amount with the increase in  $u_w$ . However, the lower side curve follows the trend noted for the lower values of wall velocity. The reasons for this behavior are not known.

For laminar boundary layers, the positions of separation should be a monotonic function of  $u_w$  according to experimental indications and also as expected from boundary layer theory. Figure 18 shows the computer results for the absolute values of the separation points versus  $u_w$ . It appears that for values of  $u_w \leq 0.15$ , the displacements of the separation points from the nonrotating case are almost linear. However, the absolute value of the slope for the line approximating the computer results is greater for the lower side than it is for the upper side of the cylinder. In prior work,<sup>24</sup> where sine-function external-velocity distributions were used with this integral method, a linear variation with  $u_w$  was also observed but extending up to values of  $u_w = 0.4$ . The slope of this line is somewhat less than for the present bound-vortex source-wake model.

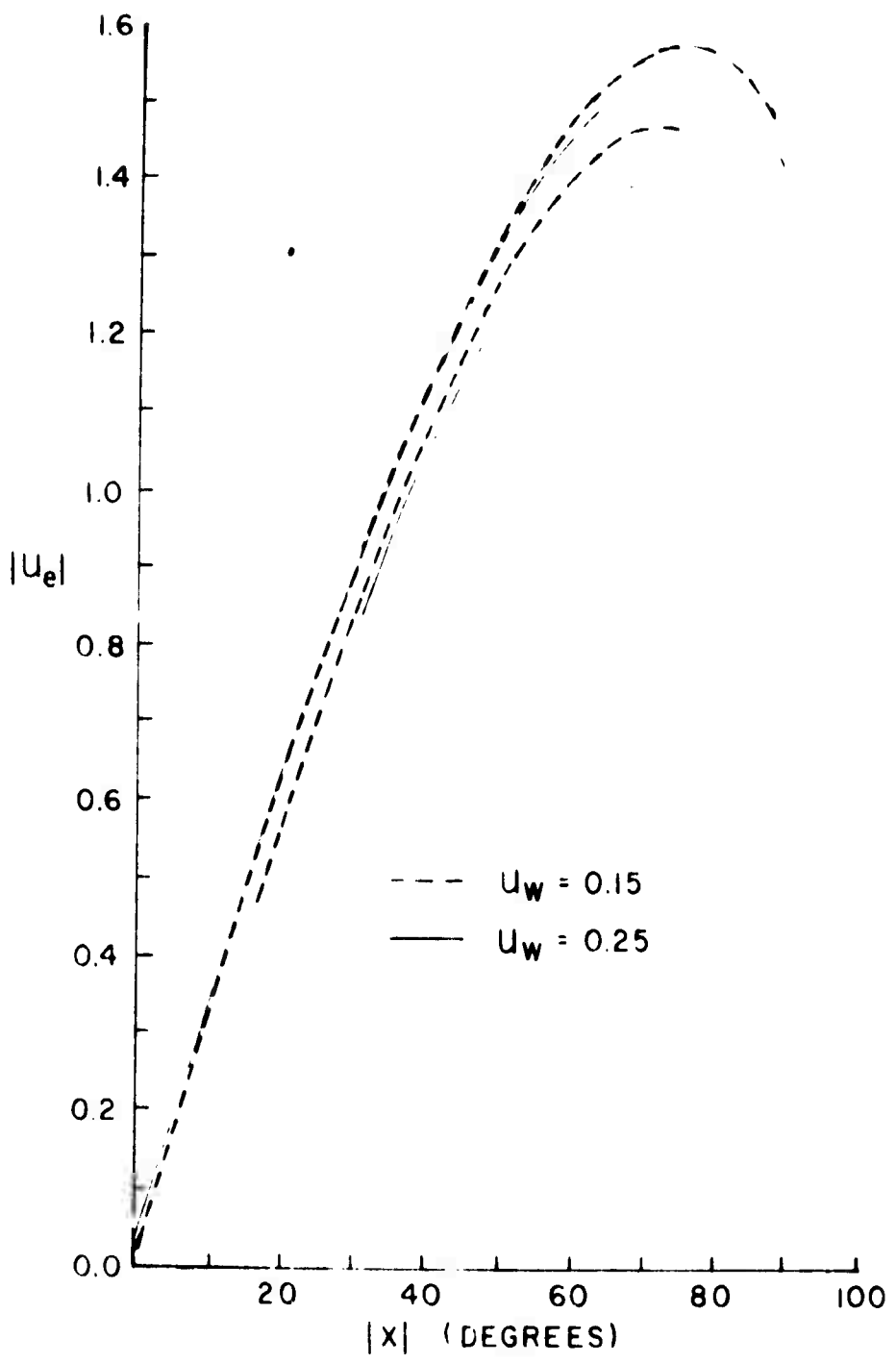


Figure 17.  $|u_e|$  vs.  $|x|$ --  $u_w = 0.25$  and  $u_w = 0.15$

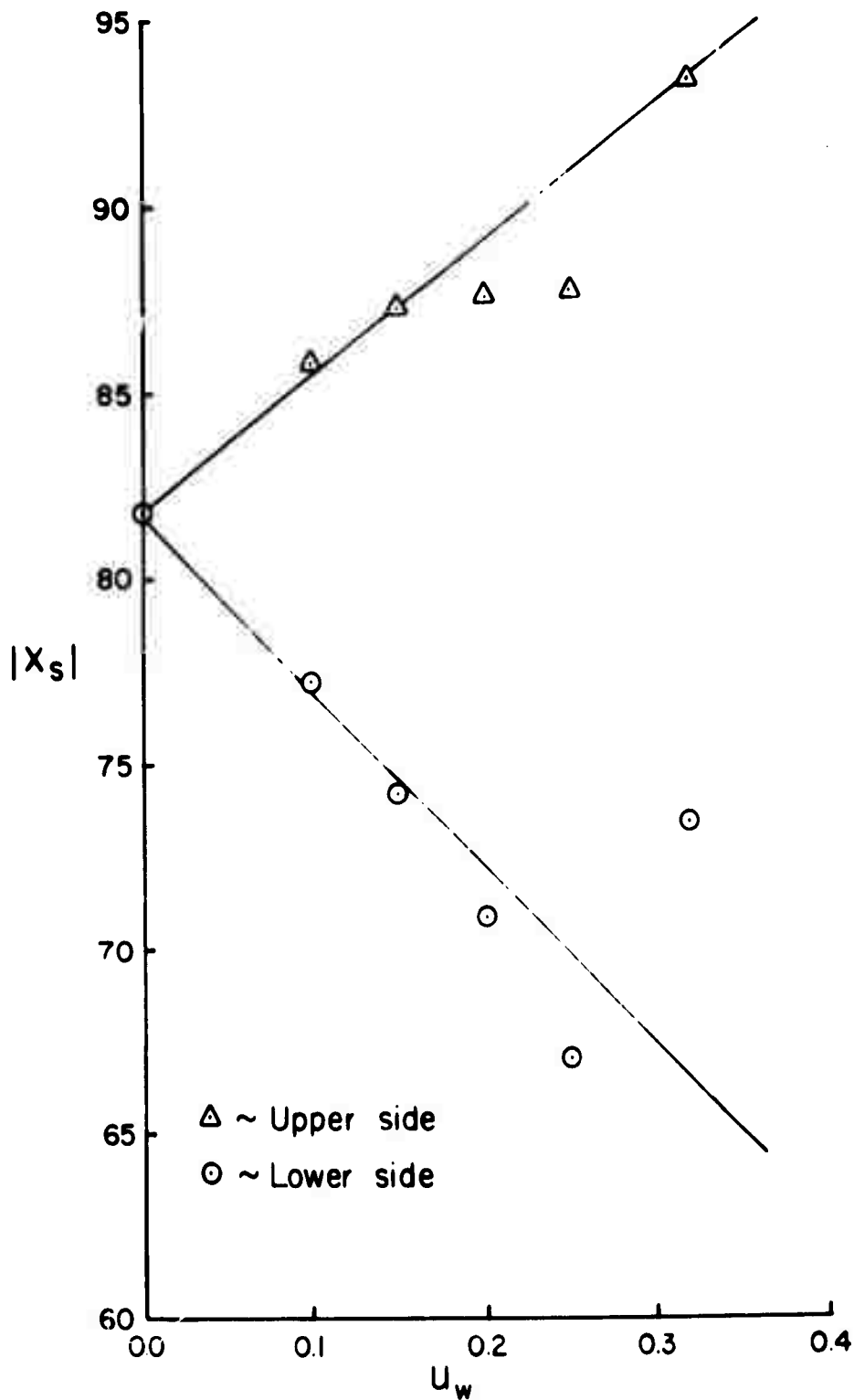


Figure 18. Location of Separation vs. Rotation Rate

## B. Lift and Drag Coefficients

Approaches representing two different views can be utilized to obtain the lift coefficient. The first approach stems from the consideration that the rotating cylinder, through the action of the boundary layer, has induced in the inviscid flow a certain circulation strength around the cylinder. This inviscid flow model takes this induced circulation into account by introducing a bound vortex in the physical plane or more precisely, a point vortex of strength  $\Gamma$  at the center of the circle in the untransformed plane. This bound vortex gives a lift force according to the Zhukovskii theorem. In the other approach, one is concerned with providing a flow model with velocity distributions approximating the experimental distributions. The assumption of Howarth<sup>26</sup> is then made in which constant pressure is assumed over that part of the cylinder immersed in the wake. The lift coefficient can thus be calculated knowing the velocity distribution. No attempt will be made here to reconcile these two approaches or choose between them. Nevertheless, it might be pointed out that the latter approach is the same approach used in obtaining the drag coefficients. Calculations were made for both approaches: the bound-vortex approach and the integrated-pressure approach.

The lift coefficient for the bound-vortex approach can be found by first considering that the circulation strength and hence the lifting force of the point vortex can be shown to be invariant under the transformation between the two complex planes. The lift coefficient can then be found to be

$$C_L = 2\pi u_c \cos \bar{\alpha}$$

In the second approach, the lift coefficient is obtained by first integrating the vertical component of the local force coefficient on the cylinder as calculation of the boundary-layer on the cylinder proceeds. The vertical component of the force coefficient on the cylinder surface in the wake is then calculated assuming the pressure constant in the region. Finally, these contributions are used to obtain the total lift force coefficient on the cylinder.

Using these two approaches, the lift coefficient as a function of rotation rate ( $u_w/u_0$ ) is shown in Figure 19. These lift coefficient values are compared with the experimental results obtained by Swanson for Reynolds numbers from  $3.58 \times 10^4$  to  $9.9 \times 10^4$ . The integrated pressure approach gives the better agreement for most of the range of  $u_w$  and the lift coefficient is linear with  $u_w$  up to and including  $u_w = 0.15$ . For  $u_w = 0.2$ , two computer runs were made with different initial values of separation points; the variation in the final results are also shown in Figure 19. The variation of the lift coefficient with variation of initial values could probably be lessened by making

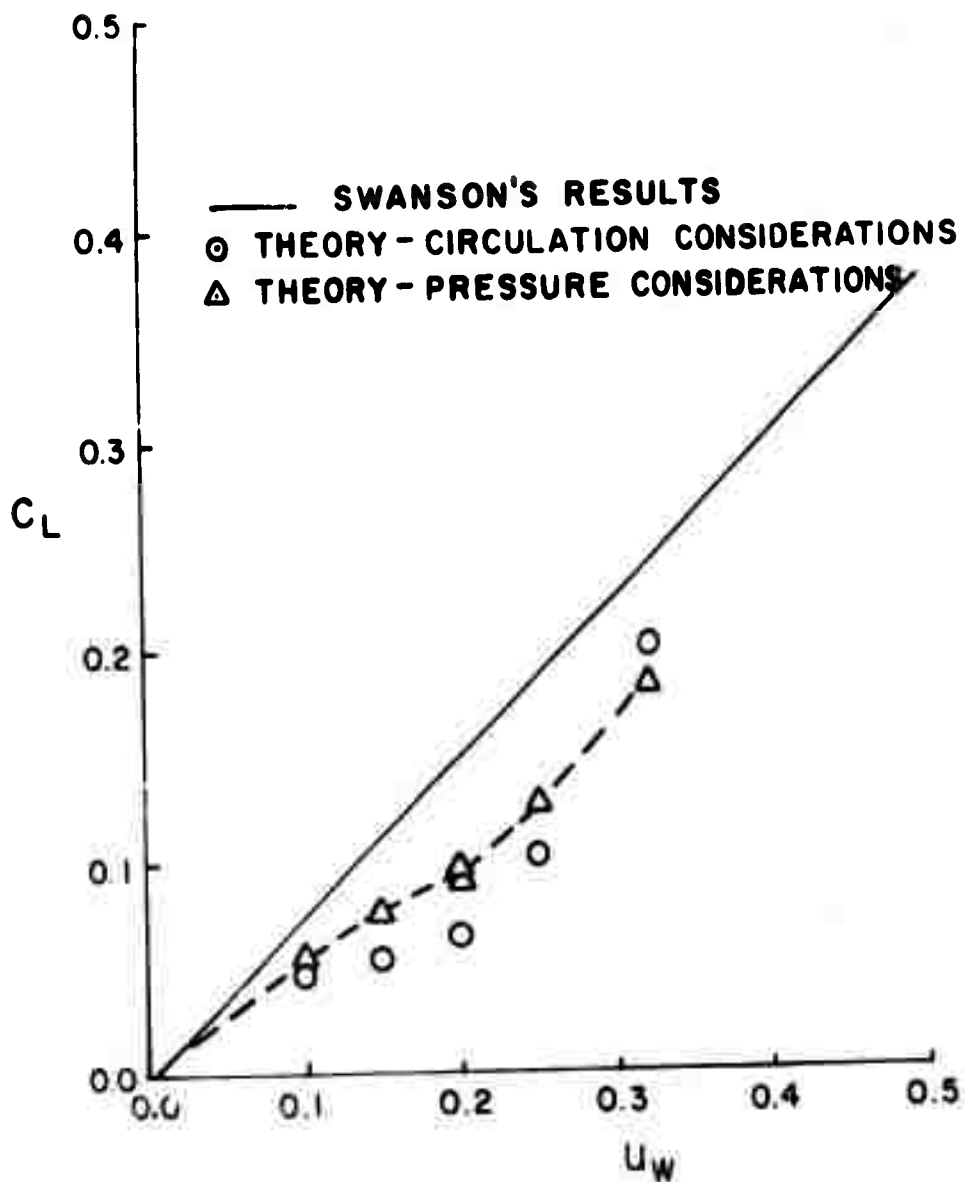


Figure 19.  $C_L$  vs.  $u_w$  - Comparison with Experiment

the convergence criterion for this iteration procedure more severe.

To obtain the drag coefficient, the horizontal component of the local force coefficient on the cylinder is integrated as the boundary layer quantities are calculated; the contribution to the drag coefficient in the wake region is found assuming that it is a region of constant pressure. The drag coefficient obtained by computer is shown together with experimental results in Figure 20. The values obtained from the model are comparable to values found experimentally, although the general trends do not agree very well. Similarly, as for the lift coefficient comparison, the value at  $u_w = 0.25$  is in the worst agreement with the experimental value.

The values of the obtained untransformed-plane parameters corresponding to the lift and drag force results are summarized in the following table.

TABLE III. PARAMETERS OBTAINED FOR THE UNTRANSFORMED PLANE  
(Angles are in radians except that values in parentheses are expressed in degrees)

| $u_w$ | $Q_1$   | $Q_2$  | $\gamma$ | $\delta$ | $u_c$              | $\bar{\alpha}$     | $\epsilon$   |
|-------|---------|--------|----------|----------|--------------------|--------------------|--------------|
| 0.0   | .28918  | .28918 | .3322    | -.3322   | 0.0                | .8551<br>(48.994)  | 0.0<br>(0.0) |
| 0.1   | .18564  | .40316 | .32267   | -.34984  | .01125<br>(49.216) | .85898<br>(4.2926) | .07492       |
| 0.15  | .13037  | .48559 | .3324    | -.35289  | .0132<br>(49.916)  | .87119<br>(6.5208) | .11381       |
| 0.2   | .082203 | .55964 | .3552    | -.3545   | .016<br>(50.471)   | .88089<br>(8.45)   | .14748       |
| 0.25  | .035223 | .64684 | .41081   | -.34946  | .02198<br>(51.281) | .89503<br>(10.397) | .18146       |
| 0.32  | .08099  | .49354 | .3164    | -.4011   | .0484<br>(48.296)  | .84293<br>(9.9924) | .1744        |

Here it is seen that the angles  $\gamma$  and  $\delta$  are relatively insensitive to separation point locations. The reasons for the insensitivity are not known..

This flow model could probably be improved by taking into account the vorticity shed from that part of the cylinder immersed in the wake. This is deduced from Swanson's observation that for  $u_w = 0.2$  and

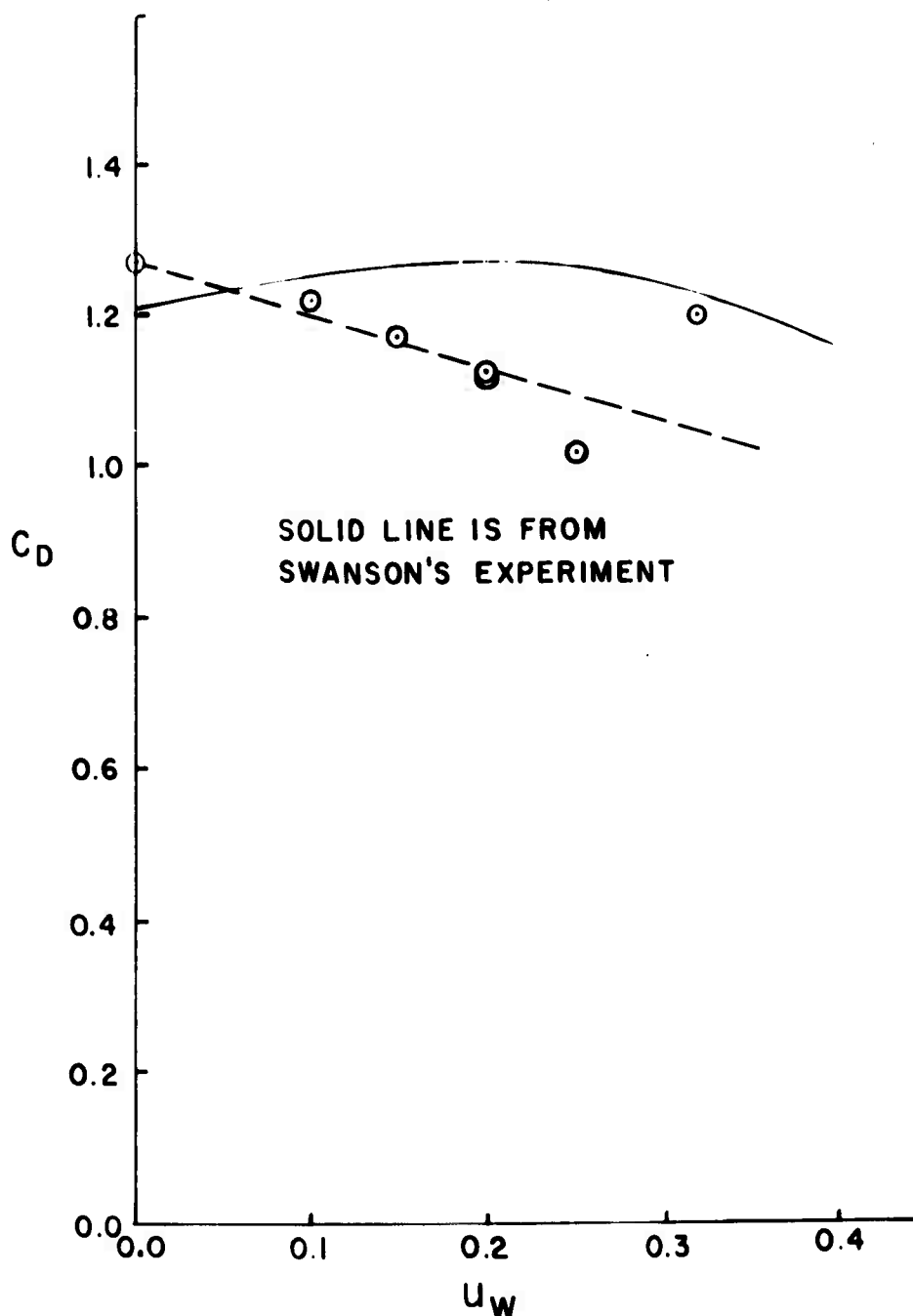


Figure 20.  $C_D$  vs.  $u_w$  - Comparison with Experiment

$Re_d = 4 \times 10^4$ , the pressure at the upper separation point is lower than it is for the separation point where the wall is moving upstream. According to equation (16) and Bernoulli's equation, this implies that the transport of vorticity into the wake at the upper separation point is greater than for the vorticity of opposite sign transported into the wake at the lower separation point. Thus, vorticity of the same sign as for the lower cylinder surface must be cast off from the cylinder surface immersed in the wake. This feature might be taken into account by setting the velocity magnitudes of the two free stream-lines equal to each other where they intersect a vertical line perhaps three or four diameters downstream of the cylinder. For an ellipse at angle of attack, Piercy, Preston and Whitehead took the cast-off vorticity in the wake region into account by imposing the equal velocity condition along two vertical lines cutting the wake a distance  $c$  and  $2c$  from the ellipse. Here  $c$  is the length of the long axis of the cylinder. Differences in lift between calculation and observation were at most 15%, with angle of "stall" for the ellipse being predicted with good accuracy.

#### IV. SUMMARY AND CONCLUSIONS

An inviscid flow-with-wake model for a spinning cylinder in cross-flow was developed that is consistent with boundary-layer theory. This was accomplished by first considering flow around a cylinder in an untransformed plane with two sources on the cylinder, their image sinks at the center and a point vortex in the center of the circle. This resultant flow was transformed to the physical plane by a Zhukovskii transformation; this results in the separation streamlines at the separation points being tangent to the cylinder at the critical points of the transformation.

The condition that the pressure gradients are finite at the separation points was imposed on this elementary inviscid flow-model. The imposed pressure-gradient condition produces a more realistic inviscid flow near separation. This condition also makes possible the development of a self-consistent model; that is, the inviscid flow model takes the boundary-layer into account and is consistent with boundary-layer theory. With finite pressure gradients at separation, the number of parameters needed to describe the flow was reduced from five to three.

Another condition imposed upon the inviscid flow model, equal pressures at the separation points, results from vorticity transport considerations. The vorticity transport into the wake at the separation points was assumed to be equal with no vorticity cast off from the rear of the cylinder. After applying this condition, only two parameters of the flow in the physical plane were needed for the description of this flow. The two parameters used were the location of the separation points on the cylinder. Using these parameters, a

system of five equations, which describes these imposed conditions, was solved for the five basic parameters in the untransformed plane. These equations were solved numerically by computer.

An iteration procedure was used to obtain separation points located in agreement with boundary-layer theory. The boundary-layer was calculated using the integral technique and new separation points were obtained using a particular inviscid-flow model with assumed separation points. These new separation points found by the integral method then become the separation points for a new assumed inviscid-flow field and again the boundary layer is calculated to find a new separation point. The iteration procedure was stopped when the difference between two successive separation points was less than 0.46 degrees for both sides.

Comparison of the converged velocity distribution for the non-rotating case with that of the observed velocity distributions shows fair agreement. Comparison between the calculated velocity distributions for different values of  $u_w$  showed that separation is delayed and the maximum value of  $u_e$  increases with  $u_w$  for the upper or downstream-moving wall side of the cylinder with the exception of the velocity distributions for  $u_w = 0.2$  and  $u_w = 0.25$ . For the lower side of the cylinder, or in other words, the side with the upstream moving wall, separation advances toward the front of the cylinder with increasing  $u_w$  without exception. The stagnation point moves downward on the cylinder with increasing  $u_w$  as is observed in experiment.

The calculated lift coefficient was compared with the observed lift coefficient. When the lift coefficient was calculated using the integrated value of the pressure over the cylinder, a linear (also obtained by experiment) relationship was obtained up to and including  $u_w = 0.15$ , and the lift coefficient increased almost linearly after  $u_w = 0.15$ . Using the circulation or bound-vortex approach, the calculated lift coefficients were somewhat lower than the preceding approach but still in good agreement with experiment up to and including  $u_w = 0.15$ . The drag coefficients for different  $u_w$  were also calculated and are at most 20% lower than the observed value.

Although the approach does have some success in predicting the Magnus force on a rotating cylinder, refinements and modifications of the present method could possibly improve the computed results significantly. Some refinements and modifications that could be applied to the present model are the following:

- (1) tighter convergence criterion and use of an accelerated convergence technique,

(2) modification of model to take into account the vorticity shed into the wake from that part of the cylinder which is immersed in the wake, and

(3) use of a more complicated distribution of sources.

#### ACKNOWLEDGMENT

We wish to thank Dr. Raymond Sedney for making us aware of the work of Bluston and Paulson.

## REFERENCES

1. W. M. Swanson, "An Experimental Investigation of the Two-Dimensional Magnus Effect," Final Report, Office of Ordnance Research Contract No. DA-33-019-ORD-1434, Dept. of Mech Eng., Case Institute of Technology, 31 Dec 56.
2. T. Y. Wu, "Cavity and Wake Flows," in Annual Review of Fluid Mechanics, Vol. IV, Van Dyke, Vincenti, and Wehausen (eds.), Annual Reviews, Inc., Palo Alto, Calif., 1972, pp. 243-284.
3. G. Magnus, "On the Deflection of a Projectile," English translation in Taylor's Scientific Memoirs, 1853.
4. Lord J. W. S. Rayleigh, "On the Irregular Flight of a Tennis Ball," Scientific Papers 1, 1857, pp. 344-346.
5. L. Prandtl, "Über Flüssigkeitsbewegung bei sehr kleiner Reibung," Verb. III. int. Math Kongr., Heidelberg, 1904, pp. 484-491. English translation available as NACA TM-452.
6. L. Prandtl and O. G. Tietjens, Applied Hydro- and Aeromechanics, New York, Dover Publications, Inc., 1957, p. 82.
7. E. G. Reid, "Tests of Rotating Cylinders," NACA TN 209, 1924.
8. A. Thom, "The Aerodynamics of a Rotating Cylinder," Ph.D. Dissertation, University of Glasgow, 1926.
9. A. Thom, "Experiments on the Air Forces on Rotating Cylinders," ARC R&M 1018, 1925.
10. A. Thom, "The Pressures Round a Cylinder Rotating in an Air Current," ARC R&M 1082, 1926.
11. A. Thom, "Experiments on the Flow Past a Rotating Cylinder," ARC R&M 1410, 1931.
12. A. Thom and S. R. Sengupta, "Air Torque on a Cylinder Rotating in an Air Stream," ARC R&M 1520, 1932.
13. A. Thom, "Effects of Discs on the Air Forces on a Rotating Cylinder," ARC R&M 1623, 1934.
14. F. K. Moore, "On the Separation of the Unsteady Laminar Boundary Layer," Proceedings of Symposium on Boundary Layer Research held in August 1957, H. Görtler (ed.), Springer-Verlag Press, Berlin, 1958.
15. N. Rott with F. K. Moore (ed.), Theory of Laminar Flows, Princeton University Press, Princeton, N.J., 1964, p. 432.

## REFERENCES (Continued)

16. R. T. Griffiths and C. Y. Ma, "Differential Boundary-Layer Separation Effects in the Flow over a Rotating Cylinder," Aero. J. of the Roy. Aero. Soc., Vol. 73, 1969, pp. 524-526.
17. M. B. Glauert, "The Flow Past a Rapidly Rotating Circular Cylinder," Proc. Roy. Soc. of London, Vol. A-242, 1957, pp. 108-115.
18. L. Prandtl, Die Naturwissenschaften, Vol. 13, 1925, pp. 93-108.
19. W. G. Bickley, "The Influence of Vortices upon the Resistance Experienced by Solids Moving Through a Liquid," Proc. Roy. Soc. of London, Vol. A-119, 1928, pp. 146-156.
20. T. Gustafson, "On the Magnus Effect According to the Asymptotic Hydrodynamic Theory," Hakan Ohlssons Buchdruckerei, Lund, Sweden, 1933. NACA translation N-25921, 1954.
21. N. A. Piercy, J. H. Preston, and L. G. Whitehead, "The Approximate Prediction of Skin-Friction and Lift," Phil. Mag. Vol 26, 1938, pp. 791-815.
22. H. S. Bluston and R. W. Paulson, "A Theoretical Solution for Laminar Flow Past a Bluff Body with a Separated Wake," Journal de Mecanique, Vol. 2, No. 1, 1972, pp. 161-180.
23. G. V. Parkinson, and T. Jandali, "A Wake Source Model for Bluff Body Potential Flow," J. Fluid Mech., Vol. 40, Part 3, 1970, pp. 577-594.
24. K. S. Fansler and J. E. Danberg, "An Integral Analysis of Boundary Layers on Moving Walls," U. S. Army Ballistic Research Laboratories Report 1792, June 1975. AD #A012205
25. J. E. Danberg and K. S. Fansler, "Similarity Solutions of the Boundary Layer Equations for Flow over a Moving Wall," U. S. Army Ballistic Research Laboratories Report 1714, April 1974. (AD781496).
26. A. Roshko and W. Fiszdon, Problems of Hydrodynamics and Continuum Mechanics, Soc. Ind. Appl. Math., Philadelphia, 1967, pp. 606-616.
27. I. C. Woods, "Two-Dimensional Flow of a Compressible Fluid past given Curved Obstacles with Infinite Wakes," Proc. Roy. Soc. of London, Vol. A227, 1955, pp. 367-387.

REFERENCES (Continued)

28. L. Howarth, "The Theoretical Determination of the Lift Coefficient for a Thin Elliptic Cylinder," Proc. Roy. Soc. of London, Vol. A-149, 1935, pp. 558-586.
29. A. Fage, and V. M. Falkner, "The Flow Around a Circular Cylinder," ARC E&M No. 1369, 1931.
30. A. M. Petrie and H. C. Simpson, "An Experimental Study of the Sensitivity to Freestream Turbulence of Heat Transfer in Wakes of Cylinders in Crossflow," Int. J. of Heat and Mass Transfer, Vol. 15, 1972, pp. 1497-1513.

## APPENDIX A

### LISTING OF COMPUTER PROGRAM TO CALCULATE FORCE COEFFICIENTS

The listing of the entire program is given here except for the data used to form the integral quantity arrays. The computer program is written in Fortran IV. The available shape factors are given in tabulated form in Reference 24. The list of principal variables for the program is given below for the main program.

#### Fortran Implementation

#### List of Principal Variables

| PROGRAM SYMBOL    | DEFINITION  |
|-------------------|---|
| A                 | similarity solution type, A   |
| AB, ABP, ABM      | two-dimensional arrays of the pressure-gradient parameter $\beta$ ,   |
| ADELT             | angular location of lower source in the $\zeta$ plane   |
| AGAM              | angular location of upper source in $\zeta$ plane   |
| AH, AHP, AHM      | two-dimensional arrays of the shape factors H   |
| AK, AKP, AKM      | ordered one-dimensional arrays of the shape factors K   |
| AL, ALP, ALM      | two-dimensional arrays of the shape factors L   |
| AKL               | one-dimensional array of highest values of K corresponding to values $u_w/u_e$ represented by the one-dimensional array AUS         |
| AKS               | one-dimensional array of separation values of K corresponding to the values $u_w/u_e$ represented by the one dimensional array AUS. |
| AT, ATP, ATM, AUS | two-dimensional array of $u_w/u_e$ values used for interpolation purposes.  |

| PROGRAM SYMBOL | DEFINITION  |
|----------------|---|
| AU             | one-dimensional array of values of $u_w/u_e$ corresponding to the columns of the two-dimensional arrays AH, AT, AL.                           |
| AUM            | one-dimensional array of values of $u_w/u_e$ corresponding to the columns of the two-dimensional arrays AHM, ATM, ALM                         |
| AUPP           | one-dimensional array of values of $u_w/u_e$ corresponding to the columns of the two-dimensional arrays ATP, AHP, and ALP.                    |
| B              | velocity parameter defined by $B=u_e/(u_w-u_e)$   |
| BB             | two-dimensional array of values of $\beta$  |
| BETA           | pressure gradient parameter, $\beta$  |
| BH             | two-dimensional array of values of the shape factors H.   |
| BK             | two-dimensional arrays of values of the shape factors K.  |
| BT             | two-dimensional array of values of the shape factors T.   |
| BET1, BET2     | initial guessed value of the separation point on upper side and lower side respectively. Also used to store the last found separation values. |
| BETN1, BETN2   | most recent values of the separation points on the upper and lower sides respectively.  |
| CIRC           | nondimensionalized vortex strength.   |
| CKF            | initial value of K to start the integration of the boundary-layer equations.  |
| COEFD          | drag coefficient.   |
| COEFL          | lift coefficient calculated from circulation considerations.  |

| PROGRAM SYMBOL | DEFINITION  |
|----------------|---|
| COEFLF         | lift coefficient calculated from pressure considerations.   |
| CPC0EF         | local pressure coefficient.   |
| CUI            | starting value of velocity ratio, this determines the starting value of x along the cylinder.               |
| DELTA          | the non-dimensionalized displacement thickness.   |
| DERIVX         | subroutine which computes the derivatives and stores them in DX.  |
| DMAX           | absolute value of the maximum step-size to be used.   |
| DNXT           | step size to be used for next step.   |
| DPST           | actual step size used with the step just completed  |
| DUX            | derivative of boundary-layer edge velocity with respect to position.  |
| DX             | one dimensional array for storing the derivative obtained by the subroutine for evaluating the derivative . |
| DERIVX         | a subroutine which computes the derivatives and stores them in DX.  |
| EPCON          | value used as a test to see if convergence has been achieved.   |
| ER             | amount of maximum error for each step.<br>If the error is larger than ER, the step size is reduced.         |
| F11            | variable characterizing the skin friction.  |
| KUTMER         | variable step Runge-Kutta integration subroutine.   |
| N              | number of equations to be evaluated in DERIV subroutine.  |

| PROGRAM SYMBOL | DEFINITION  |
|----------------|---|
| NBP            | number of elements in the arrays AUS,<br>AKS, and AKL.  |
| NEQ            | number of equations to be solved simultaneously for the basic parameters in the plane. An input to the subroutine VELPAR. |
| NFIRST         | values which denotes whether the upper or lower half of the cylinder is being considered.                                 |
| NIT            | number of iterations required to obtain UI and DUX.   |
| NPAR           | a number value equal to NEQ plus one.   |
| PRINX          | print subroutine.   |
| PS             | print step value. PS determines the frequency of reference to subroutine PRINX.   |
| Q1             | value that is one-half of the upper dimensionless source strength.  |
| Q2             | value that is one-half of the lower dimensionless source strength.  |
| THATA          | the non-dimensionalized momentum loss thickness.  |
| THETA1         | initial value of the non-dimensional momentum thickness.  |
| TERMX          | termination subroutine.   |
| UI             | local external velocity on cylinder.  |
| UW             | tangential velocity of rotating cylinder non-dimensionalized by the free-stream velocity.                                 |
| VELOC          | subroutine to calculate the edge velocity and its derivative given a position on the cylinder.                            |

| PROGRAM SYMBOL | DEFINITION   |
|----------------|--|
| VELPAR         | subroutine used to find the basic parameters of the $\zeta$ plane. It calls other subroutines in order to effect this mission. |
| W              | one-dimensional array of length $2N$ . Not used here but is dimensioned in main program.                                       |
| X              | one-dimensional array of length $N$ , which contains the variables found by numerical integration.                             |
| XINTC          | integrated value of $G^3$ . Needed to compute the energy loss thickness and used to obtain the shape factor values.            |
| XINTSQ         | integrated value of $G^2$ . Used in obtaining some shape factor values.  |
| XNEW           | an array containing the most recently found values of the basic parameters of the $\zeta$ plane.                               |
| XOLD           | initial guessed values of the basic parameters of the $\zeta$ plane.   |
| XPV            | print variable   |
| XTC            | one-dimensional array of length NTS. KUTMER will return to main program if any element of XTC changes sign.                    |
| XZ             | position on circle in $\zeta$ plane.   |
| X1             | position on cylinder in z plane.   |
| X1D            | the value of X1 in degrees.  |
| X11NC          | integration step size used to find force coefficients before KUTMER subprogram is used.  |

PROGRAM TO CALCULATE THE 2-D BOUNDARY LAYER ON A ROTATING CYLINDER WITH A SOURCE-WAKE AND A POINT VORTEX SO THAT THE SEPARATION POINTS OF THE FLOW MODEL AGREES APPROXIMATELY WITH THE RESULTS OF THE BOUNDARY LAYER CALCULATIONS. THE INTEGRAL MOMENTUM AND INTEGRAL ENERGY EQUATIONS ARE USED TOGETHER WITH THE MOVING WALL SIMILARITY FAMILY OF VELOCITY PROFILES TO CALCULATE THE BOUNDARY LAYER.

```

CIMENSION X(5),DX(5),AKS(20),AK1(20),
CIMENSION AU(17),BK(20,25),BH(20,25),BL(20,25),
CAKP(160),AHP(17,160),ATP(17,160),ALP(17,160),AUP(17,160),
CAK(135),AM(17,135),AT(17,135),AL(17,135),M(20),W(10),
CBB(20,25),AB(17,135),ABM(14,75),XNEW(5),XOLD(5),
CAKM(75),AM(14,75),ATM(14,75),ALM(14,75),AUM(14),AU(25)
EXTERNAL CERIVX,PRINX,TERMX
COMMON UW,CU,CK,CU,CT,CH,CL,N1,N2,NBP,DEGRF,CB,TAU,THETA,NIP,
CN2P,N1M,N2M,NA,ALPH,ALPINC,EPS,Q1,Q2,AGAM,ADELT,CIRC,CBET,AU,AK,AT,
CAT,AL,AKS,AK1,AUP,AKP,AHP,ATP,ALP,ABP,AUM,AKP,AHM,ATP,ALM,
CAB,ABM,AUS,XZLAST,DUXCN,UICGM,NFRST,NINTY,NITCOM,PI

```

#### CONSTANT INPUT DATA

```

CATA(AUS(I),I=1,20)/-.3,-.25,-.2195,-.17647,-.111,-.0526,0.0,
C.0476,-.1,-.2,-.333,-.5,-.6,-.667,-.714,-.75,-.8,-.857,-.889,-.9,
CATA(AKS(I),I=1,20)/1.7534,1.7,1.67,1.631,1.581,1.543,
C1.51511,
C1.493,1.474,1.450,1.438,1.44,1.449,1.455,1.459,1.463,
C1.468,1.473,1.473,1.000/
CATA(AK1(I),I=1,20)/9.000,12.000,7.000,7.000,7.000,7.000,
C10.000,1.3410,/
CATA(CU1/3,C/CU2/-0.30/THETA1/3.93/THETA2/0.29/CK1/3.348/CK2/1.75
C8/NBP/20/

```

101 FORMAT(/,23H INTEGRATION STARTED AT ,F9.4,4H RAD,F10.3,8H DEGREES)

```

PI = DACOS(-1.0)
DEGRF = 180.0/PI
ASSIGN 601 TC NN
5 K = 0
J=1
I=0

```

READ DATA OBTAINED FROM THE SIMILARITY SOLUTIONS.

```

6 READ(5,700)B,A,BETA,F11,THATA,DELTA,XINTSQ,XINTC
I=I+1
IF(K.EQ.0) GO TO 8
7 IF(B.EQ.BX) GO TC 10

```

THE M ARRAYS COUNT THE NUMBER OF DATA ENTERED FOR A CERTAIN VELOCITY

```

M(J)=I-1

```

IF A EQUALS 0, THE SET OF DATA OBTAINED GOES TO THE ARRAY SUBROUTINE  
TO BE FORMED INTO ARRAYS

```

IF(A.EQ.0.0) GO TO 20
J=J+1
I=1
8 BX=P
9 AU(PP(J)) = 1. + 1./B
10 K=K+1

```

INTEGRAL VALUES ARE CALCULATED FROM DATA

```

THESTR = XINTC + 3.*B*THATA-B*B*DELTA
BH(J,I) = B*DELTA/THATA
ET(J,I) = -THATA*F11/B/B/B
BL(J,I) = -THATA*XINTSQ/B/B/B/B
BK(J,I) = THESTR/B/THATA
BB(J,I) = BETA

```

19 GO TO 6

20 L = 20

N=25

LJ = J

WRITE(6,705) M, K

GO TO NN,(601,602,603)

601 KPP = 150

CO 620 I = 1,LJ

620 AUP(I) = AU(PP(I))

N1P = LJ

N2P = KPP

NC = -10

```

C -----  

C      ARRAY OF INTEGRAL VALUES WHERE WALL VELOCITY IS GREATER THAN  

C      EXTERNAL VELOCITY  

C -----  

      CALL ARRAY(BB, BK, BH, BT, BL, L, N, M, AKP, AHP, ATP, ALP, K, KPP, LJ, ABP, NC)  

      GO TO 500  

      WRITE(6,707) AUP  

      WRITE(6,704)(AKP(I),(AHP(J,I),J=1,LJ),I=1,KPP)  

      WRITE(6,707) AUP  

      WRITE(6,704)(AKP(I),(ATP(J,I),J=1,LJ),I=1,KPP)  

      WRITE(6,707) AUP  

      WRITE(6,704)(AKP(I),(ALP(J,I),J=1,LJ),I=1,KPP)  

      WRITE(6,707) AUP  

      WRITE(6,704)(AKP(I),(ABP(J,I),J=1,LJ),I=1,KPP)  

500  CONTINUE  

      ASSIGN 602 TC NN  

      GO TO 5  

6C2  KP = 135  

CO 605 I = 1 LJ  

605  AU(I) = AUPP(I)  

N1 = LJ  

N2 = KP  

NC = -10  

C -----  

C      INTEGRAL VALUES ARRAY FORMED WHERE EXT.VEL.IS GREATER THAN WALL  

C -----  

      CALL ARRAY(BB, BK, BH, BT, BL, L, N, M, AK, AH, AT, AL, K, KP, LJ, AB, NC)  

      GO TO 501  

      WRITE(6,707) AU  

      WRITE(6,704)(AK(I),(AH(J,I),J=1,LJ),I=1,KP)  

      WRITE(6,707) AU  

      WRITE(6,704)(AK(I),(AT(J,I),J=1,LJ),I=1,KP)  

      WRITE(6,707) AU  

      WRITE(6,704)(AK(I),(AL(J,I),J=1,LJ),I=1,KP)  

      WRITE(6,707) AU  

      WRITE(6,704)(AK(I),(AB(J,I),J=1,LJ),I=1,KP)  

5C1  CONTINUE  

      ASSIGN 603 TC NN  

      GO TO 5  

603  KPM = 75  

CO 610 I = 1 LJ  

610  AUM(I) = AUPP(I)  

N1M = LJ  

N2M = KPM  

NC = -10  

C -----  

C      INTEGRAL VALUES ARRAY FOR REVERSE FLOW  

C -----  

      CALL ARRAY(BB, BK, BH, BT, BL, L, N, M, AKM, AHM, ATM, ALM, K, KPP, LJ, ABM, NC)  

      GO TO 502  

      WRITE(6,709) AUM  

      WRITE(6,708)(AKM(I),(AHM(J,I),J=1,LJ),I=1,KPM)  

      WRITE(6,709) AUM  

      WRITE(6,708)(AKM(I),(ATM(J,I),J=1,LJ),I=1,KPM)  

      WRITE(6,709) AUM  

      WRITE(6,708)(AKM(I),(ALM(J,I),J=1,LJ),I=1,KPM)  

      WRITE(6,709) AUM  

      WRITE(6,708)(AKM(I),(ABM(J,I),J=1,LJ),I=1,KPM)  

502  CONTINUE  

C -----  

C      UW IS THE ROTATION RATE. BET1 AND BET2 ARE THE INITIAL GUESSES FOR  

C      THE UPPER AND LOWER SEPARATION PCINTS RESPECTIVELY. XOLD ARE THE  

C      INITIAL GUESSES FOR THE STRENGTH OF THE SOURCES AND POINT VORTEX  

C      AND THE LOCATION OF THE SOURCES ON THE CYLINDER.  

C -----  

30  READ(5,700) UW,BET1,BET2,XOLD  

      WRITE(6,52) UW,BET1,BET2,XOLD  

      IF(UW.GT.10.0) GO TO 300  

      LCRIT = 0  

      NEC=5  

      NPAR=6  

      EPCCN = 8.0E-3  

CO 32 I = 1,5  

32  XNEW(I) = XOLD(I)  

      GO TO 34  

C -----  

C      CONVERGENCE IS ACHIEVED IF CONDITION IS MET.  

C -----  

35  LCRIT = 0  

      IF(ABS(BET1-BETN1).LT.EPCCN.AND.ABS(BET2-BETN2).LT. EPCCN)  

      1LCRIT = 1

```

```

C-----THE NEW SEPARATION POINTS OF THE FLOW MODEL ARE GIVEN BY THE VALUES
C-----OBTAINED FROM THE BOUNDARY-LAYER CALCULATIONS.
C-----BET1=BETN1
C-----INCREASE ANGLE OF THE LOWER SEPARATION POINT IF CONDITION IS MET.
C-----IF(ABS(BET2-BETN2).LT.1.E-3) GO TO 33
C-----BET2=BETN2
C-----GO TO 34
C-----33 BET2 = BETN2 - EPCON
C-----CONDITIONS FOR INTEGRATION OF BOUNDARY LAYER FOR THE UPPER PART
C-----OF THE CYLINDER.
C-----34 NFRST = 1
C-----CNXT = 1.0E-6
C-----CPST = 5.0E-6
C-----USE PREVIOUS VALUES OF FLOW MODEL PARAMETERS AS GUESSES FOR THE FLOW
C-----MODEL PARAMETERS TO BE FOUND.
C-----DO 36 I=1,5
C-----36 XOLD(I)=XNEW(I)
C-----CALL SUBROUTINE TO FIND THE FLOW MODEL PARAMETER VALUES GIVEN THE
C-----SEPARATION POINTS IN THE PHYSICAL PLANE AS INITIALLY GUessed OR
C-----CALCULATED FROM THE INTEGRAL BOUNDARY-LAYER EQUATIONS.
C-----CALL VELPAR(BET1,BET2,XOLD,XNEW,NEQ,NPAR)
C1 = XNEW(1)
C2 = XNEW(2)
AGAM = XNEW(3)
ADELT = XNEW(4)
CIRC = XNEW(5)
X1C = 0.0
X1 = X1D/DEGRF
XZ = PI -0.01-EPS
IF(LCRIT.EQ.1) GO TO 95
C-----CALL SUBROUTINE TO CALCULATE THE EDGE VELOCITY AND ITS DERIVATIVE
C-----WITH RESPECT TO ANGLE GIVEN A POSITION ON THE CYLINDER.
C-----CALL VELOC(UI,DUX,X1,XZ,NIT)
C-----CCINT IS THE INTEGRAL (STARTING FROM X=0) OF THE PART OF THE LOCAL
C-----PRESSURE COEFICIENT CORRESPONDING TO THE LOCAL HORIZONTAL FORCE.
C-----COINT =CSIN(X1)-UI*UI*X1/3.0+UI*UI*X1*X1*X1/10.0
C-----CLINT IS THE INTEGRAL (STARTING FROM X=0) OF THE PART OF THE LOCAL
C-----PRESSURE COEFICIENT CORRESPONDING TO THE LOCAL VERTICAL FORCE.
C-----CL INT =DCOS(X1)+UI*UI*X1*X1/4.C-1.0
40 X1IND = 0.1
X1C = X1C + X1IND
CPCOEF = 1.0-UI*UI
X1INC = X1INC/DEGRF
CL INT =CL INT+X1INC*(-CPCOEF)*SIN(X1)
CDINT = CCINT + X1INC*CPCOEF*CCS(X1)
X1=X1C/DEGRF
CALL VELOC(UI,DUX,X1,XZ,NIT)
XZLAST=XZ
CU=UW/UI
CB = UI/(UW-UI)
C-----IF THE CYLINDER IS NOT ROTATING, A DIFFERENT SET OF INITIAL
C-----CONDITIONS ARE REQUIRED FOR THE INTEGRAL B-L EQUATIONS.
C-----IF(UW*UW.LT.1.E-8) GOTO 50
C-----CONDITION USED IN ORDER TO STEP AWAY FROM THE STAGNATION POINT TO
C-----A POSITION WHERE THE B-L EQUATIONS CAN BE INTEGRATED.
C-----IF(CU.GT.CU1)GOTO 40
CK=CK1
THETA=THETA1
NA=2
GO TO 55
50 CK=1.62574
THETA=0.29234

```

```

      NA=3
      CB=-1.0
C     INPUT TO KUTMER
      55 CONTINUE
C -----
C     CONDITIONS USED DURING INTEGRATION OF THE BOUNDARY LAYER FOR BOTH
C     THE UPPER AND LOWER PART OF THE CYLINDER.
C -----
      60 X(1) =X1
      X(2)=THETA*THETA
      X(3)=CK*CK*X(2)
      X(4) = CLINT
      X(5) = CCINT
      70 CMAX = 2.0E-3
      ER= 5.0E-6
      NINTY = 1
      PS=1.0
      WRITE(6,150)
C -----
C     CALL SUBROUTINE TO INTEGRATE BOUNDARY-LAYER EQUATIONS
C -----
      CALL KUTMER(CNXT,CPST,DMAX,5,X,DX,DERIVX,ER,I,W,O,PS,XPV,PRINX,
      CXT, 4 ,NTS,TERMX)
      GO TO(75,76,77,78),NTS
      75 WRITE(6,110) NITCOM
      IF(NFRST.EQ.1) GO TO 73
      BETN2 = X(1)-0.005
      GO TO 35
      73 BETN1 = X(1) +0.01
      GO TO 85
      77 WRITE(6,111)
      GO TO 35
      78 WRITE(6,112)
      GO TO 30
      76 WRITE(6,123) X(1),X(4),X(5)
      IF(NFRST.EQ.1)GO TO 85
      IF(NFRST.EQ.2) BETN2 = X(1)
      GO TO 35
C -----
C     COMPUTE INPUT FOR LOWER PART OF CYLINDER. SEE COMMENTS FOR INPUT
C     TO UPPER PART OF THE CYLINDER.
C -----
      85 NFRST=2
      BETN1 = X(1)
      CLUPPR = X(4)
      CDUPPR = X(5)
      X1C = +1.0E-2
      X1 = X10/DEGRF
      XZ = -PI+0.01 +EPS
      CALL VELOC(UI,DUX,X1,XZ,NIT)
      CLINT = DCOS(X1)+UI*UI*X1*X1/4.0-1.0
      CDINT = CSIN(X1)-UI*UI*X1/3.0+UI*UI*X1*X1*X1/10.0
      88 X1C = X1C-X1INC
      CPCOEF = 1.0-UI*UI
      X1INC = -X1IND/CEGRF
      CLINT = CLINT+X1INC*(-CPCOEF)*SIN(X1)
      CDINT = CCINT + X1INC*CPCCEF*CCS(X1)
      X1=X1C/DEGRF
      CALL VELOC(UI,DUX,X1,XZ,NIT)
      XZLAST = XZ
      CU=UW/UI
      CB = UI/(UW-UI)
      CNXT = -1.0E-6
      CPST = -5.0E-6
      IF(UW*UW.LT.1.E-6) GO TO 50
      IF(CU.LT.CU2.OR.CU.GT.1.E-7) GO TO 88
      CK=CK2
      THETA=THETA2
      NA=1
      GO TO 55
C -----
C     THE CONVERGENCE CRITERION FOR THE SEPARATION POINTS IS SATISFIED.
C     THE COEFFICIENTS OF LIFT AND DRAG ARE CALCULATED AND WRITTEN OUT.
C -----
      95 COEFL = 2.0*PI*CIRC*COS(ALPH)
      WRITE(6,710) EPCCN
      COEFL=(CLUPPR-X(4)-(1.0-UICOM*LICOM)*(COS(BETN1)-COS(BETN2))
      C))/2.0
      COEFLF=(CDUPPR-X(5)+(1.0-UICOM*LICOM)*(SIN(BETN2)-SIN(BETN1)))/2.0
      WRITE(6,715) COEFL
      WRITE(6,720) COEFLF
      WRITE(6,725) COEFLF

```

```

GO TO 30
52 FORMAT(1H1,30H SPIN RATE AND INITIAL GUESSES /11X,2HUU,6X,
C11HSEP. ANGLE1,5X,10HSEP. ANGLE2,8X,7HSOURCE1,8X,7HSOURCE2,
C5X,10HSORC ANGL1,5X,10HSORC ANGL2,3X,12HCIRC. VELOC./8F15.4)
110 FORMAT(59H ERRCR RETURN...ITERATIONS IN VELOC SUBROUTINE HAS EXCEE
CCED , 110)
111 FORMAT(23H K EXCEEDED UPPER LIMIT)
112 FORMAT(23H K EXCEEDED LOWER LIMIT)
123 FORMAT(12F SEPARATED AT ,F12.4,8H RADIANS ,/31H LIFT COEFFICIENT C
CONTRIBUTION. ,F12.5,/31H DRAG COEFFICIENT CONTRIBLITION. ,
CF12.5)
150 FORMAT(1H0,6X,1HX,8X,5HTHETA,7X,1HK,6X,5HUL/UE,5X,5HDELTA,6X,
C3HTAU,8X,1HL,7X,4H UI ,6X,5HOU/DX,8X,2HCL,8X,2HCD,8X,2HCP))
700 FORMAT(8F10.2)
701 FORMAT(1F1,(7X,16F7.3))
702 FORMAT(1H0,(17F7.3))
703 FORMAT(1H0,(15F8.4))
704 FORMAT(1H0,(F8.4,17F7.3))
705 FORMAT(1H0,(1C10))
706 FORMAT(1H1,(8X,14F8.4))
707 FORMAT(1H1,( 8X,17F7.3))
708 FORMAT(1H0,(15F8.4))
709 FORMAT(1H1,(8X,15F8.4))
710 FORMAT(/26H ANGLE INCREMENT LESS THAN , E10.4,10H SATISFIED )
711 FORMAT(24H SEPARATION VALUE OF H.,,F10.5)
715 FORMAT(/21H LIFT COEFFICIENT IS. ,E12.5)
720 FORMAT(/32H LIFT COEFFICIENT BY INTEGRATION/ E12.5)
725 FORMAT(/32H DRAG COEFFICIENT BY INTEGRATION/ E12.5)
300 STOP
ENC

```

```

C ****
C SUBROUTINE TO CALCULATE THE DERIVATIVES FOR DIFF. EQUATIONS.
C -----

```

```

SUBROUTINE DERIVX(X,DX)
CIMENSION X(5),DX(5)
CIMENSION AU(17),AKS(20),AK1(2G),AUS(20), AK(135),AH(17,135),
CAKP(160),AHP(17,16G),ATP(17,16G),ALP(17,160),AUP(17),ABP(17,160),
CAT(17,135),AL(17,135),AB(17,135),ABM(14,75),
CAKM(75),AHM(14,75),ATM(14,75),ALM(14,75),AHM(14)
COMMON(USE MAIN)
XZ = XZLAST
X1=X(1)
CALL VELOC(UI,DUX,X1,XZ,NIT)
CU = UW/UI
CB = UI/(UW-UI)
CKSQ=X(3)/X(2)
CKSQA = ABS(CKSQ)
CK = SQRT(CKSQA)

```

```

C -----
C SELECT SET OF ARRAYS FOR PARTICULAR VELOCITY RATIO AND OBTAIN
C H,T,L,BETA FOR VALUE OF K KNOWN.
C -----

```

```

1 GO TO (1,2,3),NA
CH = TDINT(CU,CK,AUM,N1M,AKM,N2M,AHM,N1P,2,2)
CT = TCINT(CU,CK,AUM,N1M,AKM,N2M,ATM,N1P,2,2)
CL = TCINT(CU,CK,AUM,N1M,AKM,N2M,ALM,N1P,2,2)
GO TO 4
2 CH = TCINT(CU,CK,AUP,N1P,AKP,N2P,AHP,N1P,2,2)
CT = TCINT(CU,CK,AUP,N1P,AKP,N2P,ATP,N1P,2,2)
CL = TCINT(CU,CK,AUP,N1P,AKP,N2P,ALP,N1P,2,2)
GO TO 4
3 CH = TCINT(CU,CK,AU,N1,AK,N2,AH,N1,2,2)
CL = TCINT(CU,CK,AU,N1,AK,N2,AL,N1,2,2)
CT = TCINT(CU,CK,AU,N1,AK,N2,AT,N1,2,2)
GO TO 4
4 CX(1) = 1.0

```

```

C -----
C INTEGRAL MOMENTUM EQUATION
C -----

```

```

CX(2) = (4.*CT-DUX*X(2)*(CH+2.C)*2.0)/UI

```

```

C -----
C INTEGRAL ENERGY EQUATION
C -----

```

```

CX(3) = (8.*CK*(CL+CU*CT)-6.*X(3)*DUX)/UI
CPCOEF = 1.0- UI*UI
CX(4) = -CPCOEF*SIN(X1)
CX(5) = CPCOEF*COS(X1)
X2A = ABS(X(2))
THETA = SQRT(X2A)*ABS(CL)/CL
TAU = UI*CT/THETA
CUXCN = CUX
UICOMM = UI

```

```

GO TO (5,6,7),NINTY
5 XZLAST = XZ
RETURN
6 XZLAST = XZ-0.02
RETURN
7 XZLAST = XZ+ 0.01
RETURN
ENC
C **** SUBROUTINE TERMX(X,DX,XTC,XPV)
C----- SUBROUTINE FOR TERMINATING THE INTEGRATION
C----- DIMENSION X(5),DX(5),XTC(4)
C----- DIMENSION AU(17),AKS(20),AK1(20),AUS(20),AK(135),AH(17,135),
C----- CAKP(160),AHP(17,160),ATP(17,160),ALP(17,160),AUP(17),ABP(17,160),
C----- CAT(17,135),AL(17,135),AB(17,135),ABM(14,75),
C----- CAKM(75),AHM(14,75),ATH(14,75),ALM(14,75),ALH(14)
COMMON(USE MAIN)
C----- VALUE OF NA IS SET TO SELECT RIGHT ARRAYS OF INTEGRAL VALUES.
C----- NA = 1
IF(CB.GT.0.0) NA = 2
IF(CB.LE.-.999999) NA = 3
C----- OBTAIN SEPARATION VALUE(CKS) OF K FOR VELOCITY RATIO KNOWN.
C----- CALL DVCINT(CU,CKS,AUS,AKS,NBP,3)
C----- IF ANY ELEMENT OF XTC CHANGES SIGN, INTEGRATION IS STOPPED.
C----- XTC(1) = 29.0 - FLOAT(NITCOM)
1 XTC(2)=CK-CKS
XTC(3) = BET22 - X(1) +0.001
BET22 = EPS-PI + 2.*ALPH
XTC(4) = 1.0
XPV = X(1) * DEGRF
RETURN
ENC
C **** SUBROUTINE PRINX(X,DX)
C----- PRINTING SUBROUTINE ****
C----- DIMENSION X(5),DX(5)
C----- DIMENSION AU(17),AKS(20),AK1(20),AUS(20),AK(135),AH(17,135),
C----- CAKP(160),AHP(17,160),ATP(17,160),ALP(17,160),AUP(17),ABP(17,160),
C----- CAT(17,135),AL(17,135),AB(17,135),ABM(14,75),
C----- CAKM(75),AHM(14,75),ATH(14,75),ALM(14,75),ALH(14)
COMMON(USE MAIN)
FBCOM = CHLAST
XBCOM = XCLAST
X1C=X(1)*CEGRF
CPCOEF =CX(4)/SIN(X(1))
DELTA = CF*TETA
WRITE(6,1) X1D,THETA,CK,CU,DELTA,TAU,CL,UICOM,DUXCN, X(4), X(5) ,
CPCOEF
IF(ABS(X1C).GE.89.0.AND.NFRST.EQ.1) NINTY = 2
IF(ABS(X1C).GE.89.0.AND.NFRST.EQ.2) NINTY =3
XDLAST = X(1)
CHLAST = CH
1 FORMAT(12F10.5)
RETURN
ENC
C **** SUBROUTINE VELOC(U,I,DUX,X,XZ ,NIT)
C----- SUBROUTINE TO COMPUTE THE INVISCID VELOCITY AT A POINT ON THE CYLINDER IN THE PHYSICAL PLANE.
C----- DIMENSION AU(17),AKS(20),AK1(20),AUS(20),AK(135),AH(17,135),
C----- CAKP(160),AHP(17,160),ATP(17,160),ALP(17,160),AUP(17),ABP(17,160),
C----- CAT(17,135),AL(17,135),AB(17,135),ABM(14,75),
C----- CAKM(75),AHM(14,75),ATH(14,75),ALM(14,75),AUM(14)
COMMON(USE MAIN)
NIT=0
PREC=1.0E-6
CALP = DCOS(ALPH)
A1=0.5*(CALP+1.0/CALP)
SINX = DSIN(X-EPS)

```

```

C ITERATIVE METHOD OF NEWTON TO DETERMINE CORRESPONDING ANGLE IN
C UNTRANSFORMED PLANE.
C -----
1 XZ0=XZ
COSX = DCOS(XZ0+EPS)
C -----
C THE CORRECT RELATION IS GIVEN BETWEEN CORRESPONDING POINTS IN THE
C TWO PLANES WHEN FX IS ZERO.
C -----
FX = (1.0-CALP*COSX)*DSIN(XZ0+EPS)/(A1-COSX)-SINX
FPX=(A1*(COSX-CALP*(2.0*COSX*COSX-1.0))-1.0+CALP*COSX**3)/
(A1-COSX)**2
XZ=XZ0-FX/FPX
NIT=NIT+1
IF(NIT.EQ.30) GO TO 2
IF(ABS(XZ-XZ0).GT.PREC) GOTC 1
2 SINXZ = DSIN(XZ+EPS)
COSX = DCOS(XZ+EPS)
CF=2.0*SIN(XZ)-Q1*COTAN(0.5*(XZ-AGAM))-Q2*COTAN(0.5*(XZ-ADELT))
C+CIRC
CS=1.0-2.C*CALP*CCSX+CALP*CALP
C=CF+GS
F=2.0*(CALP-COSX)
C -----
C THE EDGE VELOCITY FOR THE GIVEN POINT ON THE CYLINDER.
C -----
U1 = C/H
GP=(2.*DCOS(XZ)+.5*Q1/(DSIN(.5*(XZ-AGAM))**2)+.5*Q2/(DSIN(.5*
C(XZ-ADELT))**2))*GS+GF*(2.0*CALP*SINXZ)
FP = 2.0*SINXZ
XNUME=(A1-COSX)*(COSX+CALP*((SINXZ**2)-(COSX**2)))-SINXZ*
(SINXZ-CALP*COSX*SINXZ)
XDENO = (A1-COSX)**2
YDEN = XNUME/XCENC
C -----
C THE SPATIAL DERIVATIVE OF THE VELOCITY AT THE EDGE OF THE B-L.
C -----
CUX=(H*GP-G*FP)*DCOS(X-EPS)/H/H/YDEN
NITCOM = NIT
RETURN
ENC
C **** SUBROUTINE VELPAR(BET1,BET2,XCLD,XNEW,NEQ,NPAR)
C -----
C SUBROUTINE TO CALCULATE THE PARAMETERS FOR THE FLOW MODEL GIVEN THE
C SEPARATION POINTS IN THE PHYSICAL PLANE. THIS SUBROUTINE USES
C OTHER SUBROUTINES TO OBTAIN THESE PARAMETERS BY A NEWTON-RAPHSON
C SCHEME FOR SOLVING A SYSTEM OF NONLINEAR EQUATIONS.
C -----
CIMENSION A(5,6),P(5,6),QD(5,6),IR(5),JC(5),C(5,6),X(5)
CIMENSION XOLD(NEQ),XNEW(NEQ)
CIMENSION AU(17),AKS(20),AK1(20),AUS(20),AK(135),AH(17,135),
CAKP(160),AHP(17,160),ATP(17,160),ALP(17,160),AUP(17),ABP(17,160),
CAT(17,135),AL(17,135),AB(17,135),ABM(14,75),
CAKM(75),AHM(14,75),ATH(14,75),ALM(14,75),ALM(14)
CIMENSION XNEWB(5)
COMMON/USE MAIN/
EXTERNAL JACOB
PI = DACOS(-1.0)
EPS = (BET1 + BET2)*0.5
NMAX = NEQ
N = NEQ
M = NPAR
L = 0
ITMAX = 1000
EPS1 = 1.0E-7
EPS2 = 1.0E-5
SI=1.0
CS=1.0
SF=5.0
EPS2=1.0E-2
DO 10 I=i,N
DO 5 J=1,M
P(I,J)=0.0
QD(I,J)=0.0
5 C(I,J)=0.0
10 CONTINUE
C -----
C ALPH IS HALF THE ANGLE BETWEEN THE TWO SEPARATION POINTS IN THE
C UNTRANSFORMED PLANE.
C -----
ALPH=0.5*(PI-BET1+EPS)

```

```

20 YN = 0.1
20 YN=0.5*YN
YNN = YN
25 AINC = PI*YNN/180.0
ALPINC = ALPH -AINC
C -----
C CALL SUBROUTINE THAT SOLVES A SYSTEM OF NONLINEAR EQUATIONS.
C -----
CALL NSIMEQ(JACOB,P,QQ,A,NMAX,I,J,C,N,M,L,ITMAX,SI,DS,SF,EPS1,
CEPS2,EPS3,Q,XOLC,XNEW,X,IERR1,IERR2)
IF(IERR1.LT.-01) WRITE(6,103)
IF(L.EQ.0.AND.IERR2.LT.0) WRITE(6,108) ITMAX
IF(L.EQ.1.AND.IERR2.LT.0) WRITE(6,105) EPS2
IF(IERR1.LE.C.OR.IERR2.LE.0) IJK =1
WRITE(6,107)((XNEW(I),I=1,N),YNN)
IF(YN.LT.6.0E-2.AND.YNN.LT.C.0) GO TO 50
CO 30 I=1,5
30 XNEWB(I)=XNEW(I)
IF(YNN.LT.0.C) GO TO 20
YNA = -YNN
GO TO 25
50 CO 60 I=1,5
60 XNEW(I)=0.5*(XNEW(I)+XNEWB(I))
YNA = 0.0
COEFL = 2.0*PI*XNEW(5)*COS(ALPH)
WRITE(6,109) BET1,BET2,ALPH,EPS ,CGEFL
WRITE(6,110)
WRITE(6,107)((XNEW(I),I=1,N),YNN)
200 RETURN
WRITE(6,106)((Q(I,J),J=1,M),I=1,N)
102 FORMAT(8H IERR1 =,I4//)
103 FORMAT(62H ERROR RETURN---JACCBIAN MATRIX IS SINGULAR OR ILLCONDI-
CTIONED //)
104 FORMAT(8H IERR2 =,I4//)
105 FORMAT(38H ERROR RETURN...STEP SIZE IS LESS THAN ,D16.8///)
106 FORMAT(//20H FINAL Q PARAMETERS. //,(5D16.8))
107 FORMAT(//29H FINAL SOLUTION FOR THE ROOT./ 8X,2HQ1,14X,2HC2,12X,
C5H GAMMA,1IX,5H CELTA,8X,11H CIRCULATION,5X,11H ANGLE INCR./(6F16.8))
108 FORMAT(//58H ERROR RETURN...MAXIMUM NUMBER OF ITERATIONS HAS EXCEE-
CDED.,I6//)
109 FORMAT(//56H PHYSICAL PLANE AND PRIMARY TRANSFORMED PLANE PARAMETER
CS,//8X,6H BETA1,10X,5HBETA2,10X,5HALPHA,9X,7HEPSILON,7X,9HLIFT CO
IEF,,/5F15.5// )
110 FORMAT(//24H BY LINEAR INTERPOLATION)
RETURN
ENC
C ****
FUNCTION COTAN(X)
COTAN = COT(X)
RETURN
ENC
FUNCTION CCOTAN(X)
CCOTAN = COT(X)
RETURN
ENC
FUNCTION CACCS(X)
CACCS = ACOS(X)
RETURN
ENC
C ****
SUBROUTINE JACCB(Q,NMAX,XNEW,N,M,A)
C -----
C SUBROUTINE TO COMPUTE THE JACOBIAN OF A NONLINEAR SYSTEM OF EQUATIONS
GIVEN THE TRIAL PARAMETERS ASSOCIATED WITH THE FLOW MODEL.
C -----
CIMENSION AU(17),AKS(20),AK1(20),AUS(20),AK(135),AH(17,135),
CAK(160),AHP(17,160),ATP(17,160),ALP(17,160),AUP(17),ABP(17,160),
CAT(17,135),AL(17,135),AB(17,135),ABM(14,75),
CAKM(75),AHM(14,75),ATM(14,75),ALM(14,75),AUM(14)
CIMENSION Q(NMAX,M),XNEW(N),A(NMAX,M)
COMMON/USE MAIN/
CALP = DCOS(ALPH)
CALPIN = DCOS(ALPINC)
SALPIN = DSIN(ALPINC)
CAMEM3 = DCOTAN(0.5*(ALPH-EPS-XNEW(3)))
A(1,1) = CAMEM3
CAMEM4 = DCOTAN(0.5*(ALPH-EPS-XNEW(4)))
A(1,2) = CAMEM4
SAMEM3 = DSIN(0.5*(ALPH-EPS-XNEW(3)))
A(1,3) = 0.5*XNEW(1)/SAMEM3/SAMEM3
SAMEM4 = DSIN(0.5*(ALPH-EPS-XNEW(4)))
A(1,4) = 0.5*XNEW(2)/SAMEM4/SAMEM4

```

```

A(1,5) = -1.0
SAME = DSIN(ALPH-EPS)
A(1,6) = -(XNEW(1)*CAMEM3+XNEW(2)*DAMEM4-2.0*SAME-XNEW(5))
CAPEP3 = CCOTAN(0.5*(ALPH+EPS+XNEW(3)))
A(2,1) = CAPEP3
CAPEP4 = CCOTAN(0.5*(ALPH+EPS+XNEW(4)))
A(2,2) = CAPEP4
SAPEP3 = DSIN(0.5*(ALPH+EPS+XNEW(3)))
A(2,3) = -0.5*XNEW(1)/SAPEP3/SAPEP3
SAPEP4 = DSIN(0.5*(ALPH+EPS+XNEW(4)))
A(2,4) = -0.5*XNEW(2)/SAPEP4/SAPEP4
A(2,5) = 1.0
SAPE = DSIN(ALPH+EPS)
A(2,6) = -(XNEW(1)*CAPEP3+XNEW(2)*CAPEP4-2.0*SAPE+XNEW(5))
ACMEM3 = CCOTAN(0.5*(ALPINC-EPS-XNEW(3)))
ACPEP3 = CCOTAN(0.5*(ALPINC+EPS+XNEW(3)))
A(3,1) = -ACMEM3+ACPEP3
ACPEP4 = CCOTAN(0.5*(ALPINC+EPS+XNEW(4)))
ACMEM4 = CCOTAN(0.5*(ALPINC-EPS-XNEW(4)))
A(3,2) = ACPEP4-ACMEM4
SCPEP3 = CSIN(0.5*(ALPINC+EPS+XNEW(3)))
SCMEM3 = CSIN(0.5*(ALPINC-EPS-XNEW(3)))
A(3,3) = -0.5*XNEW(1)*(1.0/SCMEM3**2+1.0/SCPEP3**2)
SCPEP4 = CSIN(0.5*(ALPINC+EPS+XNEW(4)))
SCMEM4 = CSIN(0.5*(ALPINC-EPS-XNEW(4)))
A(3,4) = -0.5*XNEW(2)*(1.0/SCMEM4**2+1.0/SCPEP4**2)
A(3,5) = 2.0
SACPE = CSIN(ALPINC+EPS)
SACME = CSIN(ALPINC-EPS)
A(3,6) = -(2.0*(SACME-SACPE)-XNEW(1)*(ACMEM3-ACPEP3)-XNEW(2)*(ACMEM4
C-ACPEP4)) + 2.0*XNEW(5))
CCMEM3 = CCOS(0.5*(ALPINC-EPS-XNEW(3)))
C = 0.5*(1.0-2.0*C*CALP*CALP+CALP**2)
C = SALPIN*(CALP**2-1.0)/(CALP-CALPIN)
A(4,1) = C/SCMEM3**2 - D*ACMEM3
A(4,2) = C/SCMEM4**2 - D*ACMEM4
A(4,3) = C*XNEW(1)*CCMEM3/SCMEM3**3 - D*XNEW(1)/SCMEM3**2/2.0
CCMEM4 = CCOS(0.5*(ALPINC-EPS-XNEW(4)))
A(4,4) = C*XNEW(2)*CCMEM4/SCMEM4**3 - D*XNEW(2)/SCMEM4**2/2.0
A(4,5) = +D
CACME = DCOS(ALPINC-EPS)
A(4,6) = -2.0*C*(2.0*CACME+0.5*(XNEW(1)/SCMEM3**2+XNEW(2)/SCMEM4**2
C))-D*(2.0*SACME-(XNEW(1)*ACMEM3+XNEW(2)*ACMEM4-XNEW(5)))
A(5,1) = C/SCPEP3**2 - D*ACPEP3
A(5,2) = C/SCPEP4**2 - D*ACPEP4
CCPEP3 = CCOS(0.5*(ALPINC+EPS+XNEW(3)))
A(5,3) = -C*XNEW(1)*CCPEP3/SCPEP3**3+0.5*D*XNEW(1)/SCPEP3**2
CCPEP4 = CCOS(0.5*(ALPINC+EPS+XNEW(4)))
A(5,4) = -C*XNEW(2)*CCPEP4/SCPEP4**3+0.5*D*XNEW(2)/SCPEP4**2
A(5,5) = -D
CACPE = DCOS(ALPINC+EPS)
A(5,6) = -(2.0*C*(2.0*CACPE+0.5*(XNEW(1)/SCPEP3**2+XNEW(2)/SCPEP4**2
C))-D*(-2.0*SACPE+XNEW(1)*ACPEP3+XNEW(2)*ACPEP4+XNEW(5)))
RETURN
ENC
LIST(STOP)
C **** SUBROUTINE ARRAY(BB,CK,CH,CT,CL,L,N,M,AK,AH,AT,AL,K,KP,LJ,AP,NC)
C----- SUBROUTINE TO FCRM K,H,T,L,BETA, ARRAYS.
C----- DIMENSION CK(L,N),CH(L,N),CT(L,N), AK(KP),CL(L,N),
C----- CAH(LJ,KP),AT(LJ,KP),AL(LJ,KP),M(LJ),BB(L,N),AB(LJ,KP)
C----- DIMENSION AKX(300),AD(300),CKJ(25),CKJ1(25),CKJ2(25),
C----- CKJ(25),CTJ(25),CLJ(25),CKJ3(25),CBJ(25),ADS(25)
C----- I1 = 0
C----- PLACE ALL THE K VALUES INTO A 1-D ARRAY.
C----- C0 10 J=i,LJ
C----- MJ = M(J)
C----- PLACE ALL K'S WITH SAME VELOCITY RATIO INTO 1-D ARRAY AND SORT
C----- IN INCREASING ORDER.
C----- C0 3 I=1,MJ
C----- 3 CKJ(I) = CK(J,I)
C----- CALL SORTXY(CKJ,ADS,MJ)
C----- CONSTRUCT ARRAY OF DIFFERENCES BETWEEN SUCCEEDING K VALUES.
C----- ADS(1) = C.0

```

```

ADS(MJ) = 0.0
MJM1 = MJ-1
CO 4 I=2,MJM1
4 ADS(I) = CKJ(I) - CKJ(I-1)
C PLACE SMALLER ARRAYS INTO LARGER 1-D ARRAYS OF K VALUES.
C
C CO 5 I=1,MJ
I1 = I1 + 1
AD(I1) = ADS(I)
5 AKX(I1) = CKJ(I)
10 CONTINUE
C SURT LARGE ARRAYS SO THAT K IS IN INCREASING ORDER
C
C CALL SORTXY(AKX,AD,K)
C
C REDUCE THE NUMBER OF NON-ZERO ELEMENTS IN THE ARRAYBY REQUIRING
C ONLY THAT AN ELEMENT K EXISTS IN THE CLOSED INTERVAL BETWEEN
C SUCCEECING K'S WHERE THE VELGCITY RATIO IS HELD CONSTANT.
C
C J = 2
AK(1) = AKX(1)
CO 20 I = 2,K
IF(AC(I).LT.1.E-6) GO TO 15
AKXM = AKX(I) - AD(I)
IF(AKXM.EQ.AK(J-1)) GO TO 15
IF(AKXM.GT.AK(J-1)) GO TO 13
GO TO 20
13 AK(J) = AKX(I-1)
GO TO 19
15 AK(J) = AKX(I)
19 J = J + 1
20 CONTINUE
C ENLARGE NO. OF NON-ZERO ELEMENTS TO INCLUDE SOME LARGER
C VALUES OF K.
C XINCW = (AK(J-1)-AK(J-2))/100.
RI = 1.0
JP1 = J+1
CO 39 I = J,KP
AK(I) = AK(J-1)+RI*XINCW
RI=RI + 1.0
39 CONTINUE
C FORM 2-C ARRAYS.
C
C 36 CO 70 J = 1,LJ
PJ=M(J)
37 DO 40 I=1,MJ
CKJ(I)= CK(J,I)
CKJ1(I) = CKJ(I)
CKJ2(I) = CKJ(I)
CKJ3(I) = CKJ(I)
CHJ(I) = CH(J,I)
CTJ(I) = CT(J,I)
CBJ(I) = BB(J,I)
40 CLJ(I) = CL(J,I)
CALL SORTXY(CKJ,CHJ,MJ)
CALL SORTXY(CKJ1,CTJ,MJ)
CALL SORTXY(CKJ2,CLJ,MJ)
CALL SORTXY(CKJ3,CBJ,MJ)
ASSIGN 46 TJ KGT
45 CO 60 I = 1,KP
GO TO KGT,(46,60)
46 IP6 = I + 6
IF(IP6.GT.KP) GO TO 51
IF(AK(IP6).LT.CKJ(1)) GO TO 60
IF(I.LT.7) GO TO 52
51 IF(AK(I-6).GE.CKJ(MJ)) ASSIGN 60 TO KGT
52 AK I = AK(I)
53 CALL CISCOT(AK,I,AK,I,CKJ,CHJ,CKJ,CHJ, NC,MJ,O,AHI)
CALL CISCOT(AK,I,AK,I,CKJ,CTJ,CTJ, NC,MJ,O,ATI)
CALL CISCOT(AK,I,AK,I,CKJ,CLJ,CLJ, NC,MJ,O,ALI)
CALL CISCOT(AK,I,AK,I,CKJ,CBJ,CBJ, NC,MJ,O,ABI)
AH(J,I) = AHI
AT(J,I) = ATI
AL(J,I) = ALI
AB(J,I) = ABI
60 CONTINUE
70 CONTINUE

```

```

101 FORMAT(1H0,(10F12.5))
100 FORMAT(8F10.5)
102 FORMAT(1H1,(14F9.3))
105 FORMAT(1H0,(10I10))
100 RETURN
ENC
C **** SUBROUTINE DISCOT (XA,ZA,TABX,TABY,TABZ,NC,NY,NZ,ANS) **** CISCOT
C----- SUBROUTINE FOR LAGRANGIAN INTERPOLATION AND EXTRAPOLATION. CISCOT
C----- *** DOCUMENT DATE 08-01-68 SUBROUTINE REVISED 08-01-68 **** CISCOT
C THE DIMENSIONS IN THIS SUBROUTINE ARE ONLY DUMMY DIMENSIONS. CISCOT
C CIMENSION TABX(2),TABY(2),TABZ(2),NPX(8),NPY(8),YY(8) CISCOT
C CIMENSION TABX(2),TABY(2),TABZ(2),NPX(8),NPY(8),YY(8) CISCOT
C CALL UNS (NC,IA,ICX,IDX,IMS) CISCOT
C IF (NZ-1) .LE. 5,10 CISCOT
5 CALL DISSER (XA,TABX(1),1,NY,IDX,NN) CISCOT
NN=ICX+1 CISCOT
CALL LAGRAN (XA,TABX(NN),TABY(NN),NNN,ANS) CISCOT
GOTO 70 CISCOT
10 ZARG=ZA CISCOT
IP1X=ICX+1 CISCOT
IP1Z=ICZ+1 CISCOT
IF (IA) .EQ. 15,25,15 CISCOT
15 IF (ZARG-TABZ(NZ)) .EQ. 25,25,20 CISCOT
ZARG=TABZ(NZ) CISCOT
25 CALL CISSER (ZARG,TARZ(1),1,NZ,IDX,NPZ) CISCOT
NX=NY/NZ CISCOT
NPZL=NPZ+10Z CISCOT
I=1 CISCOT
IF (IMS) .EQ. 30,20,40 CISCOT
30 CALL CISSER (XA,TABX(1),1,NX,IDX,NPX(1)) CISCOT
CO 35 JJ=NPZ,NPZL CISCOT
NPY(I)=(JJ-1)*NX+NPX(1) CISCOT
NPX(I)=NPX(1) CISCOT
35 I=I+1 CISCOT
GOTO 50 CISCOT
40 CO 45 JJ=NPZ,NPZL CISCOT
IS=(JJ-1)*NX+1 CISCOT
CALL CISSER (XA,TABX(1),IS,NX,IDX,NPX(I)) CISCOT
NPY(I)=NPX(I) CISCOT
45 I=I+1 CISCOT
50 CO 55 LL=1,IP1Z CISCOT
NLOC=NPX(LL) CISCOT
NLOCY=NPY(LL) CISCOT
55 CALL LAGRAN(XA,TABX(NLOC),TABY(NLOCY),IP1X,YY(LL)) CISCOT
CALL LAGRAN (ZARG,TABZ(NPZ),YY(1),IP1Z,ANS) CISCOT
70 RETURN CISCOT
ENC CISCOT
C **** SUBROUTINE UNS (IC,IA,IDX,IDZ,IMS) UNS
IF (IC) .EQ. 5,5,10 UNS
5 IMS=1 UNS
NC=-IC UNS
GOTO 15 UNS
10 IMS=0 UNS
NC=IC UNS
15 IF (NC-10C) .EQ. 20,25,25 UNS
20 IA=0 UNS
GOTO 30 UNS
25 IA=1 UNS
NC=NC-10C UNS
30 IDX=NC/10 UNS
IDZ=NC-ICX*10 UNS
RETURN UNS
ENC UNS
C **** SUBROUTINE DISSER (XA,TAB,I,NX,IDX,NPX) CISSER
C----- CIMENSION TAB(2) CISSER
C----- CIMENSION TAB(2) CISSER
NPT=IC+1 CISSER
NPE=NPT/2 CISSER
NPU=NPT-NPB CISSER
IF (NX-NPT) .EQ. 10,5,10 CISSER
5 NPY=I CISSER
RETURN CISSER
10 NLOW=I+NPE CISSER
NUPP=I+NX-(NPU+1) CISSER
CO 15 II=NLOW,NUPP CISSER
NLOC=II CISSER
IF (TAB(II)-XA) .EQ. 15,20,20 CISSER

```

```

15 CONTINUE
NPX=NUPP-NPB+1
RETURN
20 NL=NLOC-NPB
NU=NL+1D
CO 25 JJ=NL,NU
NDIS=JJ
IF (TAB(JJ)-TAB(JJ+1)) 25,30,25
25 CONTINUE
NPX=NL
RETURN
30 IF (TAB(NDIS)-XA) 40,35,35
35 NPX=NCIS-ID
RETURN
40 NPX=NCIS+1
RETURN
ENC
C ****
* SUBROUTINE LAGRAN (XA,X,Y,N,ANS)
CIMENSION X(2),Y(2)
SUM=0.0
CO 3 I=1,N
PROC=Y(I)

CO 2 J=1,N
A=X(I)-X(J)
IF (A)
1 B=(XA-X(J))/A
PRCC=PROD*B

2 CONTINUE
3 SUM=SUM+PROD
ANS=SUM
RETURN
ENC
C ****
* SUBROUTINE NSIMEQ(JACOBI,P,QD,A,NMAX,IR,JC,N,M,L,ITMAX,S1,CS,SF,
1 EPS1,EPS2,EPS3,Q,XOLD,XNEW,X,ERR1,ERR2)
C----- THIS SUBROUTINE COMPUTES A ROOT OF THE SET OF SIMULTANEOUS
C----- NONLINEAR ALGEBRAIC EQUATIONS USING THE NEWTON-RAPHSON METHOD OR
C----- THE PARAMETER PERTURBATION METHOD.
C----- DIMENSION P(NMAX,M),QD(NMAX,M),A(NMAX,M),IR(N),JC(N),C(NMAX,M),XOLNSIMEQ
1 C(N),XNEW(N),X(N)
C----- NSIMEQ

```

## C PROGRAM INITIALIZATION.

```

C
IERR1=0
IERR2=0
IF (L.EQ.1) S=SI
C----- TRANSFER THE OLD ROOT TO THE XNEW ARRAY. IF L = 0, TRANSFER THE
C----- P PARAMETERS TO THE Q ARRAY. IF L = 1, COMPUTE A NEW SET OF
C----- PARAMETERS AND TRANSFER THEM TO THE Q ARRAY.
C----- 1 DO 2 I=1,N
XNEW(I)=XOLD(I)
DO 2 J=1,M
IF (L.EQ.1) GO TO 12
Q(I,J)=P(I,J)
GO TO 2
12 Q(I,J)=QC(I,J)+(P(I,J)-QC(I,J))*S/SF
2 CONTINUE
DO 5 ITER=1,ITMAX
C----- CALL SUBROUTINE JACGBI TO COMPUTE THE COEFFICIENTS OF THE JACOBIAN
C----- MATRIX AND STORE THEM IN THE A ARRAY.
C----- CALL JACGBI (Q,NMAX,XNEW,N,M,A)
C----- CALL SUBROUTINE LSIMEQ TO COMPUTE THE SOLUTION OF A SET OF
C----- SIMULTANEOUS LINEAR ALGEBRAIC EQUATIONS USING THE GAUSS-JORDAN
C----- REDUCTION SCHEME WITH THE MAXIMUM PIVOT CRITERION. THE CONTENTS
C----- OF THE X ARRAY ARE THE CHANGES WHICH MUST BE MADE IN THE
C----- XNEW ARRAY.
C----- CALL LSIMEQ (A,NMAX,IR,JC,N,EPS1,X,IERR1)
C----- TEST TO DETERMINE IF THE JACOBIAN MATRIX IS SINGULAR OR
C----- ILLCONDITIONED.
C----- IF (IERR1.LT.0) GO TO 11
C----- TEST TO DETERMINE IF ALL THE CHANGES IN THE XNEW ARRAY ARE
C----- LESS THAN EPS2.
C----- DO 3 I=1,N
IF (.NOT.ABS(X(I)).LT.EPS2) GO TO 4
3 CONTINUE
GO TO 6
C----- CONVERGENCE HAS NOT BEEN ACHIEVED. UPDATE THE XNEW ARRAY AND
C----- REPEAT THE ITERATION.
C----- 4 DO 5 I=1,N
5 XNEW(I)=XNEW(I)+X(I)
C----- MAXIMUM NUMBER OF ITERATIONS HAS BEEN EXCEEDED. IF THE PARAMETER
C----- PERTURBATION METHOD IS BEING USED, HALVE THE STEP SIZE AND
C----- DETERMINE IF IT IS LESS THAN EPS2.
C----- IF (L.EQ.0) GO TO 10
S=S-DS
DS=0.5*DS
IF (DS.LT.EPS2) GO TO 10
GO TO 8
C----- CONVERGENCE HAS BEEN ACHIEVED. IF THE PARAMETER PERTURBATION IS
C----- BEING USED, TEST TO DETERMINE IF THE STEPPING PROCESS IS
C----- COMPLETE. IF IT IS OR IF THE NEWTON RAPHSON METHOD WAS USED,
C----- RETURN WITH THE SOLUTION IN THE XNEW ARRAY.
C----- 6 IF (L.EQ.0) GO TO 9
IF (.NOT.S.LT.SF) GO TO 9
C----- TRANSFER THE NEW ROOT TO THE XOLD ARRAY, INCREASE THE STEP SIZE BY
C----- ITS CURRENT VALUE AND RETURN TO COMPUTE NEW Q PARAMETERS.
C----- DO 7 I=1,N
7 XOLD(I)=XNEW(I)
8 S=S+DS
GO TO 1
C----- RETURN...SUCCESSFUL SOLUTION.
C----- 9 IERR2=-1
RETURN

```

```

C----- ERROR RETURN... IF THE NEWTON RAPHSON METHOD HAS BEEN USED, THE NSIMEQ
C----- MAXIMUM NUMBER OF ITERATIONS HAS BEEN EXCEEDED. IF THE PARAMETER NSIMEQ
C----- PERTURBATION METHOD HAS BEEN USED, THE STEP SIZE IF LESS THAN EPS2 NSIMEQ
C----- NSIMEQ
C----- 10 IERR2=-1 NSIMEQ
C----- 11 RETURN NSIMEQ
C----- ENC NSIMEQ
C----- ****
C----- **** SUBROUTINE LSIMEQ (A,NMAX,IR,JC,N,EP51,X,IERR1) NSIMEQ
C----- ****
C----- THIS SUBROUTINE COMPUTES THE SOLUTION OF A SET OF SIMULTANEOUS LSIMEQ
C----- LINEAR ALGEBRAIC EQUATIONS USING THE GAUSS-JORDAN REDUCTION LSIMEQ
C----- SCHEME WITH THE MAXIMUM PIVOT CRITERION. LSIMEQ
C----- ****
C----- DIMENSION A(NMAX,6),IR(N),JC(N),X(N) LSIMEQ
C----- ****
C----- BEGIN THE ELIMINATION PROCEDURE. LSIMEQ
C----- ****
C----- NP1=N+1 LSIMEQ
C----- CO 7 K=1,N LSIMEQ
C----- KM1=K-1 LSIMEQ
C----- ****
C----- BEGIN THE SEARCH FOR THE MAXIMUM PIVOT ELEMENT. LSIMEQ
C----- ****
C----- BIGA=0.0 LSIMEQ
C----- CO 3 I=1,N LSIMEQ
C----- CO 3 J=1,N LSIMEQ
C----- IF (KM1.EQ.0) GO TO 2 LSIMEQ
C----- ****
C----- CHECK ROW AND COLUMN PIVOT SUBSCRIPTS ALREADY USED. LSIMEQ
C----- ****
C----- CO 1 II=1,KM1 LSIMEQ
C----- IF (I.EQ.IR(II)) GO TO 3 LSIMEQ
C----- CO 1 JJ=1,KM1 LSIMEQ
C----- IF (J.EQ.JC(JJ)) GO TO 3 LSIMEQ
C----- 1 CONTINUE LSIMEQ
C----- 2 IF (.NOT.ABS(A(I,J)).GT.BIGA) GO TO 3 LSIMEQ
C----- BIGA=ABS(A(I,J)) LSIMEQ
C----- IR(K)=I LSIMEQ
C----- JC(K)=J LSIMEQ
C----- 3 CONTINUE LSIMEQ
C----- ****
C----- CHECK TO SEE IF THE MAXIMUM PIVOT ELEMENT IS GREATER THAN EP51. LSIMEQ
C----- ****
C----- IF (.NOT.BIGA.LT.EP51) GO TO 4 LSIMEQ
C----- IERR1=-1 LSIMEQ
C----- RETURN LSIMEQ
C----- ****
C----- NORMALIZE THE PIVOT ELEMENT. LSIMEQ
C----- ****
C----- 4 IRK=IR(K) LSIMEQ
C----- JCK=JC(K) LSIMEQ
C----- BIGA=A(IRK,JCK) LSIMEQ
C----- CO 5 J=1,NP1 LSIMEQ
C----- 5 A(IRK,J)=A(IRK,J)/BIGA LSIMEQ
C----- ****
C----- ELIMINATE THE NON ZERO ELEMENTS IN THE JC(K) TH COLUMN. LSIMEQ
C----- ****
C----- CO 7 I=1,N LSIMEQ
C----- IF (I.EQ.IRK) GO TO 7 LSIMEQ
C----- AJCK=A(I,JCK) LSIMEQ
C----- CO 6 J=1,NP1 LSIMEQ
C----- 6 A(I,J)=A(I,J)-AJCK*A(IRK,J) LSIMEQ
C----- 7 CONTINUE LSIMEQ
C----- ****
C----- REORDER THE SOLUTION AND TRANSFER IT TO THE X ARRAY. LSIMEQ
C----- ****
C----- CO 8 I=1,N LSIMEQ
C----- IR1=IR(I) LSIMEQ
C----- JC1=JC(I) LSIMEQ
C----- 8 X(JC1)=A(IR1,NP1) LSIMEQ
C----- ****
C----- SUCCESSFUL RETURN. LSIMEQ
C----- ****
C----- IERR1=+1 LSIMEQ
C----- RETURN LSIMEQ
C----- ENC LSIMEQ
C----- ****
C----- SUBROUTINE DVCINT(X,FX,XT,FT,NP,ND) LSIMEQ
C----- ****
C----- DIMENSION XT(NP),FT(NP),T(16) LSIMEQ
C----- N=NC LSIMEQ

```

```

31 N1=(N-1)/2          CVCINT 4
N2=N/2                CVCINT 5
N3=NP-N2+1            CVCINT 6
IF(NP-N)3C,41,41      CVCINT 7
41 N4=N1+2            CVCINT 8
IF(XT(1)-XT(2))22,80,60 CVCINT 9
22 CONTINUE           CVDINT10
IF(X-2.*XT(1)+XT(2))20,20,21 CVCINT11
21 IF(X-2.*XT(NP)+XT(NP-1))1441,441,20 CVCINT12
441 IF(NP.LT.10)GO TO 42 CVCINT13
N5=NP-N              CVCINT14
443 N5=N5/2            CVCINT15
N6=N4+N5              CVDINT16
IF(XT(N6).LT.X)N4=N6  CVCINT17
IF(N5.GT.1)GC TO 443  CVCINT18
42 IF(X-XT(N4))45,43,43 CVOINT19
43 IF(N4-N3)44,45,44  CVCINT20
44 N4=N4+1            CVCINT21
GOTO 42              CVCINT22
45 N4=N4-1            CVCINT23
N5=N4-N1              CVCINT24
L046 I=1 N             CVCINT25
T(I)=FT(N5)           CVCINT26
46 N5=N5+1            CVCINT27
L=(N+1)/2             CVCINT28
TR=T(L)               CVCINT29
N6=N4                 CVCINT30
N7=N4+1               CVCINT31
JU=1                  CVCINT32
N2=N-1                CVCINT33
UN=1.0                CVCINT34
L012 J=1,N2            CVCINT35
N5=N4-N1              CVCINT36
N3=N-J                CVCINT37
L09 I=1,N3            CVCINT38
N8=N5+J               CVCINT39
T(I)=(T(I+1)-T(I))/(XT(N8)-XT(N5)) CVCINT40
9 N5=N5+1            CVCINT41
GOTO(10,11) JU        CVCINT42
10 UN=UN*(X-XT(N6))  CVCINT43
JU=2                  CVCINT44
N6=N6-1               CVCINT45
GOTO 12              CVCINT46
11 UN=UN*(X-XT(N7))  CVCINT47
JU=1                  CVCINT48
N7=N7+1               CVCINT49
L=L-1                CVCINT50
12 TR=TR+UN*T(L)     CVCINT51
FX=TR                 CVCINT52
RETURN               CVCINT53
20 WRITE(6,50) X,XT(1),XT(NP) CVCINT54
STCP
50 FORMAT(23H ARG. NOT IN TABLE X= ,E14.7,9H XT(1)= , CVCINT55
1 E14.7,1CH XT(NP)= ,E14.7,2X,6HDVDINT) CVCINT56
30 WRITE(6,51) NP,ND  CVCINT57
51 FORMAT(22H TABLE TOO SMALL NP= ,I5,6H ND= ,I5,2X,6HDVDINT) CVCINT58
STOP
60 IF(X-2.*XT(1)+XT(2))61,20,20 CVCINT59
61 IF(X-2.*XT(NP)+XT(NP-1))20,721,721 CVCINT60
721 IF(NP.LT.10)GO TO 72 CVCINT61
N5=NP-N              CVCINT62
723 N5=N5/2            CVCINT63
N6=N4+N5              CVCINT64
IF(XT(N6).GT.X)N4=N6  CVCINT65
IF(N5.GT.1)GC TO 723  CVCINT66
72 IF(X-XT(N4))73,73,45 CVCINT67
73 IF(N4-N3)74,45,74  CVCINT68
74 N4=N4+1            CVCINT69
GOTO 72              CVCINT70
80 WRITE(6,52) XT(1)  CVCINT71
STOP
52 FORMAT(23H CONSTANT TABLE XT(1)= ,E14.7,2X,6HDVDINT) CVCINT72
ENC
C ****
SUBROUTINE SCRTXY(X,Y,N)
DIMENSION X(N),Y(N)
M=A
1 M=M/2
IF(M.EQ.0)RETURN
K=A-M+1
J=1
2 I=J

```

```

*** 1
SORTXY 2
SORTXY 3
SORTXY 4
SORTXY 5
SORTXY 6
SORTXY 7
SORTXY 8

```

```

3 L=I+M
4 IF(X(I).GT.X(L))GOTO 5
5 J=J+1
6 IF(J-K)2,1,1
7 T=X(L)
8 X(L)=X(I)
9 X(I)=T
10 T=Y(L)
11 Y(L)=Y(I)
12 Y(I)=T
C INTERCHANGE THE I-TH AND L-TH ELEMENTS OF ADDITIONAL VECTORS.
13 I=I-M
14 IF(I)4,4,3
15 END
C ****
16 FUNCTION TDINT(X,Y,XT,NX,YT,NY,FT,NXMAX,NPX,NPY)
17 CIMENSION XT(NX),YT(NY),FT(NXMAX,NY),F(16),G(16)
18 NX1=NX
19 NY1=NY
20 NPX1=NPX
21 NPY1=NPY
22 X1=X
23 Y1=Y
24 IF(NPX1.GT.NX1.OR.NPY1.GT.NY1)GOTO 14
25 A=Z.*XT(1)-XT(2)
26 B=Z.*XT(NX1)-XT(NX1-1)
27 C=Z.*YT(1)-YT(2)
28 D=Z.*YT(NY1)-YT(NY1-1)
29 IF(XT(1).GT.XT(2))GOTO 7
30 IF(X1.LT.A.OR.X1.GT.B)GOTC 20
31 CO 1 I=1,NX1
32 IF(X1.LE.XT(I))GOTO 2
33 CONTINUE
34 I=I-NPX1/2
35 IF(I.LT.1)I=1
36 IF(I.GT.NX1-NPX1+1)I=NX1-NPX1+1
37 IF(YT(1).GT.YT(2))GOTO 9
38 IF(Y1.LT.C.OR.Y1.GT.D)GOTC 21
39 CO 2 J=1,NY1
40 IF(Y1.LE.YT(J))GOTO 4
41 CONTINUE
42 J=J-NPY1/2
43 IF(J.LT.1)J=1
44 IF(J.GT.NY1-NPY1+1)J=NY1-NPY1+1
45 IF(NPX1.LT.NPY1)GOTO 11
46 CO 6 K=1,NPY1
47 J1=J+K-1
48 CO 5 L=1,NPX1
49 I1=I+L-1
50 G(L)=FT(I1,J1)
51 CALL COINTP(X1,F(K),XT,I,G,1,NPX1,NPX1,1,1)
52 CALL COINTP(Y1,TDINT,YT,J,F,1,NPY1,NPY1,1,1)
53 RETURN
54 IF(X1.GT.A.OR.X1.LT.B)GOTC 20
55 CO 8 I=1,NX1
56 IF(X1.GE.XT(I))GOTG 2
57 CONTINUE
58 GOTJ 2
59 IF(Y1.GT.C.OR.Y1.LT.D)GOTC 21
60 CO 10 J=1,NY1
61 IF(Y1.GE.YT(J))GOTO 4
62 CONTINUE
63 GOTO 4
64 CO 13 L=1,NPX1
65 I1=I+L-1
66 CO 12 K=1,NPY1
67 J1=J+K-1
68 G(K)=FT(I1,J1)
69 CALL CCINTP(Y1,F(L),YT,J,G,1,NPY1,NPY1,1,1)
70 CALL CCINTP(X1,TDINT,XT,I,F,1,NPX1,NPX1,1,1)
71 RETURN
72 WRITE(6,22)X1,XT(1),XT(NX1)
73 STOP
74 WRITE(6,23)Y1,YT(1),YT(NY1)
75 STOP
76 FORMAT(30H ERRCR TDINT X CUT OF TABLE X=,E15.7,7H XT(1)=,E15.7,8H
77 1XT(NX)=,E15.7)
78 FORMAT(30H ERROR TDINT Y CUT OF TABLE Y=,E15.7,7H YT(1)=,E15.7,8H
79 1YT(NY)=,E15.7)
80 WRITE(6,15)NX1,NPX1,NY1,NPY1
81 STOP
82 FORMAT(32H ERROR TDINT TABLE TCG SMALL NX=,I5,5H NPX=,I5,4H NY=,I5TCINT 67

```

1,5+ NPY=,151

TCINT 68

END

TCINT 69

C \*\*\*\*\* SUPROUTINE DCINTP(XX,FX,XT,NX,FT,NF,NPS,ND,IXI,IFI)  
CIMENSION XT(NPS),FT(NPS),I(16),S(16)

\*\*\*\*\*

CCINTP 1

CCINTP 2

CCINTP 3

CCINTP 4

CCINTP 5

CCINTP 6

CCINTP 7

CCINTP 8

CCINTP 9

CCINTP10

CCINTP11

CCINTP12

CCINTP13

CCINTP14

CCINTP15

CCINTP16

CCINTP17

CCINTP18

CCINTP19

CCINTP20

CCINTP21

CCINTP22

CCINTP23

CCINTP24

CCINTP25

CCINTP26

CCINTP27

CCINTP28

CCINTP29

CCINTP30

CCINTP31

CCINTP32

CCINTP33

CCINTP34

CCINTP35

CCINTP36

CCINTP37

CCINTP38

CCINTP39

CCINTP40

CCINTP41

CCINTP42

CCINTP43

CCINTP44

CCINTP45

CCINTP46

CCINTP47

CCINTP48

CCINTP49

CCINTP50

CCINTP51

CCINTP52

CCINTP53

CCINTP54

CCINTP55

CCINTP56

CCINTP57

CCINTP58

CCINTP59

CCINTP60

CCINTP61

CCINTP62

CCINTP63

CCINTP64

CCINTP65

CCINTP66

CCINTP67

CCINTP68

CCINTP69

CCINTP70

CCINTP71

CCINTP72

CCINTP73

CCINTP74

CCINTP75

CCINTP76

CCINTP77

CCINTP78

CCINTP79

X=XX

CCINTP 1

NSX=NX

CCINTP 2

NSF=NF

CCINTP 3

NP=NPS

CCINTP 4

N=ND

CCINTP 5

IX=IXI

CCINTP 6

IY=IFI

CCINTP 7

N1=(N-1)/2

CCINTP 8

N2=N/2

CCINTP 9

N3=NP-N2+1

CCINTP 10

IF(NP-N1)30,41,41

CCINTP11

41 N4=N1+2

CCINTP12

N44=(N4-1)\*IX+NSX

CCINTP13

N20=NSX+IX

CCINTP14

N22=(NP-1)\*IX+NSX

CCINTP15

N21=N22-IX

CCINTP16

IF(XT(NSX)-XT(N20))22,80,60

CCINTP17

22 IF(X-2.\*XT(NSX)+XT(N20))20,21

CCINTP18

21 IF(NP.LT.10)GOTO 42

CCINTP21

N5=NP-N

CCINTP22

443 N5=N5/2

CCINTP23

N6=N4+NSX

CCINTP24

IF(IXT(N66).GE.X)GOTO 444

CCINTP25

N4=N6

CCINTP26

N44=N66

CCINTP27

IF(N5.GT.2)GOTO 443

CCINTP28

42 IF(X-XT(N44))45,43,43

CCINTP29

43 IF(N4-N3)44,45,44

CCINTP30

44 N4=N4+1

CCINTP31

N44=N44+IX

CCINTP32

GOTO 42

CCINTP33

45 N4=N4-1

CCINTP34

N5=N4-N1

CCINTP35

N20=(N5-1)\*IY+NSF

CCINTP36

N21=(N5-1)\*IX+NSX

CCINTP37

CO 46 I=1,N

CCINTP40

T(I)=FT(N20)

CCINTP41

S(I)=XT(N21)

CCINTP42

N20=N20+IY

CCINTP43

46 N21=N21+IX

CCINTP44

L=(N+1)/2

CCINTP45

TR=T(L)

CCINTP46

N4=N1+1

CCINTP47

N6=N4

CCINTP48

N7=N4+1

CCINTP49

JU=1

CCINTP50

N2=N-1

CCINTP51

UN=1.0

CCINTP52

IF(N.EQ.1)GOTO 13

CCINTP53

CO 12 J=1,N2

CCINTP54

N5=N4-N1

CCINTP55

N3=N-J

CCINTP56

CO 9 I=1,N3

CCINTP57

N8=N5+J

CCINTP58

T(I)=(T(I+1)-T(I))/(S(N8)-S(N5))

CCINTP59

9 N5=N5+1

CCINTP60

GOTO(10,11),JU

CCINTP61

10 UN=UN\*(X-S(N6))

CCINTP62

JU=2

CCINTP63

N6=N6-1

CCINTP64

GOTO 12

CCINTP65

11 UN=UN\*(X-S(N7))

CCINTP66

JU=1

CCINTP67

N7=N7+1

CCINTP68

L=L-1

CCINTP69

12 TR=TR+UN\*T(L)

CCINTP70

13 FX=TR

CCINTP71

RETURN

CCINTP72

20 WRITE(6,50)X,XT(NSX),XT(N22)

CCINTP73

STOP

CCINTP74

50 FORMAT(23H ARG. NOT IN TABLE X=E14.7,9H XT(1)= ,

E14.7,10H XT(NPS)=,E14.7,2X,6HDDINTP)

CCINTP75

30 WRITE(6,51)NP,NC

CCINTP76

51 FORMAT(22H TABLE TOO SMALL NPS= ,15,6H ND= ,15,2X,6HDDINTP)

CCINTP77

STOP

CCINTP78

```

60 IF(X-2.*XT(NSX)+XT(N2C))>1.61,20,2C
61 IF(X-2.*XT(N22)+XT(N21))>20,721,721
721 IF(NP.LT.10)GOTO 72
    N5=NP-N
723 N5=N5/2
    N6=N4+N5
    N66=(N6-1)*IX+NSX
    IF(XT(N66).LE.X)GOTO 724
    N4=N6
    N44=N66
724 IF(N5.GT.2)GOTO 723
72 IF(X-XT(N44))>73,73,45
73 IF(N4-N3)>74,45,74
74 N4=N4+1
    N44=N44+IX
    GOTO 72
80 WRITE(6,52)XT(NSX)
STOP
52 FORMAT(23H CCNSTANT TABLE XT(1)= ,E14.7,2X,6HDDINTP)
ENC
C ****
C **** SUBROUTINE KUTMER(DNXT,DPST,DMAX,N,Y,YP,DERIV,ER,ME,W,ITYP,PS,
1PV,PRIN,TC,NTC,NTS,TERM)
CIMENSION Y(50),YP(50),W(100),TC(25)
CIMENSION Q(50),Q1(50),Q2(50),FA(25),FB(25)
ITTC=0
INCD=0
IF(ITYP.GT.1)GOTO 7C
ERM=5.*ER
ER1=.1*ERM
CPST=CNXT
I=1
ER2=ER1
IF(ER2.EQ.0.)ER2=.000001*PS
10 CALL CERIV(Y,YP)
GOTO (20,90,IIC,130,150,7C,250),I
20 IF(ITYP.EQ.1)REURN
25 CALL TERM(Y,YP,TC,PV)
GOTC (30,270),I
30 CALL PRIN(Y,YP)
GOTC (40,360,25C),I
40 DO 50 I=1,NTC
    IF(TC(I).GT.C.)GOTO 41
    FB(I)=1.
    FA(I)=0.
    GOTC 50
41 FA(I)=1.
    FB(I)=0.
50 CONTINUE
FC=0.
PV2=AINT(PV/PS+SIGN(ER2,DNXT))
PV1=PV2+PS
IF(ABS(PV2-PV).LT.ER2)PV2=PV2-PS
K=0
70 F6=CNXT/6.
F3=F6+H6
F8=.125*CNXT
F2=.5*CNXT
DO 80 I=1,N
    C(I)=Y(I)
    C1(I)=YP(I)
80 Y(I)=C(I)+H3*Q1(I)
    I=2
    GOTC 10
90 DO 100 I=1,N
    Y(I)=Q(I)+H6*(Q1(I)+YP(I))
    I=3
    GOTC 10
110 DO 120 I=1,N
    C2(I)=3.*YP(I)
120 Y(I)=Q(I)+H8*(Q2(I)+Q1(I))
    I=4
    GOTC 10
130 DO 140 I=1,N
    T1=C1(I)-Q2(I)
    C2(I)=4.*YP(I)
140 Y(I)=Q(I)+H2*(T1+Q2(I))
    I=5
    GOTC 10
150 ERMAX=0.
    DO 190 I=1,N

```

```

T1=G(I)+H6*(G1(I)+Q2(I)+YP(I))
T2=CAFS(T1-Y(I))
Y(I)=T2
IF(RM,EC,0.)GOTO 190
GOT(I)170,160,180),ME
.70 IF(ABS(T1).GE.1.)T2=T2/ABS(T1)
.70 IF(T2.GT.ERMAX)ERMAX=T2
GOTO 190
.80 IF(T1.EQ.0.)GOTO 170
T1=T2/CAFS(T1)
J=I+1
T2=W(J-1)*T2
T1=W(J)*T1
IF(T2.GT.T1)T2=T1
GOTO 170
160 CONTINUE
DPST=CNXT
IF(FRM,EL,C.)GOTO 240
IF(ITTC,EC,1)GOTO 240
IF(ERMAX,EO,C.)GOTO 210
T1=ER1/ERMAX
IF(T1.GE.-1..AND.INDO.GT.0)GOTO 192
IF(ABS(T1-1.).LT..5)GOTO 195
CNXT=DPST+T1*.2
.91 E 20
.92 INCD=INDC-1
.93 E 220
C1 ENXT=DPST+(1.+2*([I-1.])
.94 IF(ABS(CNXT).LT.EMAX)GOTO 220
.95 IF(INDC.GT.0)GOTO 192
CNXT=DMAX
IF(DPST.LT.C.)ENXT=-DMAX
.96 IF(ERMAX.LT.ERM)GOTO 240
.97 EO 230 I=1,N
.98 Y(I)=G(I)
.99 INDC=3
I=6
GOTO 10
140 I=7
.101 I=8
.102 IF(ITYP.GT.1)RETURN
TPV=PV
.103 EO 260 I=1,NTC
.104 -1(I)=TC(I)
I=2
.105 COT(I) 25
.106 EO 300 I=1,NTC
IF(FA(I).EQ.FB(I))GOTO 370
IF(TC(I).GT.C.OC) GC TC 280
FB(I)=1
IF(ABS(JI(I)).GE.ER2.OR.K.GT.1)GOTC 290
FA(I)=0;
.107 COT(I) 290
.108 FA(I)=1
IF(ABS(QI(I)).GE.ER2.OR.K.GT.1)GOTC 290
FB(I)=0;
.109 IF(FA(I).EQ.FB(I))GOTO 370
.110 C0 CONTINUE
K=K+1
IF(ABS(PV-PV1).LT.ER2)GOTC 350
IF(ABS(PV-PV2).LT.ER2)GOTC 350
.111 IF(FC.NE.0.)GOTO 340
.112 IF(PV.GT.PV1)GOTO 330
IF(PV.GT.PV2)GOTO 70
PV2-PV2
.113 FC=1.
.114 SH=ENXT
.115 ENXT=DPST*(PV2-PV)/(PV-TPV)
.116 ITTC=1
.117 GOTO 70
.118 PV2=PVI
.119 GOTO 310
.120 IF(FC.GT.4.)GOTC 350
FC=FC+1.
.121 COT(I) 320
.122 I=2
.123 GOTO 30
.124 PV1=PVI+PS
.125 PV2=PVI-PS
ITTC=0
IF(FC.EQ.0.)GOTC 305
FC=0.

```

|   |          |
|---|----------|
| CNXT=SH                                   | KUTME141 |
| GOTO 305                                  | KUTME142 |
| 370 IF(ABS(TC(1))<ER2)GOTO 360            | KUTME143 |
| CNXT=CPST+TC(1)/(Q1(1)-TC(1))             | KUTME144 |
| ITTC=1                                    | KUTME145 |
| GOTO 70                                   | KUTME146 |
| 380 NTS=1                                 | KUTME147 |
| I=2                                       | KUTME148 |
| GOTO 30                                   | KUTME149 |
| 390 RETURN                                | KUTME150 |
| ENC                                       | KUTME151 |
| 0.15 1.66 -1.43 .159 .349 .302 -.385 0.04 |          |
| 20.0                                      |          |
| 0.40 1.76 -1.4 .159 .349 .302 -.385 0.04  |          |
| 0.25 1.66 -1.4 .159 .349 .302 -.385 0.04  |          |
| 0.2 1.66 -1.45 .159 .349 .302 -.385 0.04  |          |

## LIST OF SYMBOLS

|             |   |
|-------------|---|
| a           | radius of circular cylinder in physical plane   |
| $c_f$       | skin friction coefficient, $(\partial u / \partial y)_w / (\rho u_0^2 / 2)$                 |
| d           | diameter of rotating cylinder in physical plane   |
| h           | coordinate scaling function of x, $\eta = y/h(x)$   |
| i           | unit imaginary value  |
| k           | nondimensionalized outer velocity at the separation point on the upper part of the cylinder |
| m           | angle used in $\bar{z}$ plane, see Figure 2   |
| $m_s$       | angle of m corresponding to separation  |
| p           | local pressure  |
| q           | inviscid velocity along cylinder surface in $\zeta$ plane                                   |
| $\bar{q}$   | dimensioned inviscid velocity   |
| r, $\phi$   | polar coordinates in $\zeta$ plane  |
| r, $\sigma$ | polar coordinates in $\bar{z}$ plane  |
| u           | nondimensionalized local velocity in direction tangential to cylinder                       |
| $u_c$       | nondimensionalized circulation velocity on circle in $\zeta$ plane                          |
| $u_e$       | inviscid velocity along cylinder surface in z plane   |
| $u_w$       | peripheral velocity of cylinder wall  |
| $u_0$       | free-stream velocity  |
| $\hat{u}_e$ | dimensioned form of $u_e$   |
| $\alpha$    | dimensioned boundary-layer velocity in direction tangential to cylinder                     |
| v           | boundary-layer velocity in direction normal to cylinder                                     |
| $\hat{v}$   | dimensioned local velocity in direction normal to cylinder                                  |

LIST OF SYMBOLS (Continued)

|               |   |
|---------------|---|
| $w(\zeta)$    | complex inviscid velocity in $\zeta$ plane  |
| $x$           | nondimensionalized coordinate along surface of cylinder - $\bar{x}/a$                               |
| $\bar{x}$     | distance along cylinder from X axis   |
| $y$           | nondimensionalized coordinate normal to surface - origin at surface of cylinder in physical plane   |
| $\bar{y}$     | dimensioned value of $y$  |
| $z$           | complex coordinates in physical plane $z = \bar{x} + i \bar{y}$                                     |
| $\tilde{z}$   | complex coordinate rotated by angle $\alpha$ to the $z$ plane,<br>$\tilde{z} = \bar{x} + i \bar{y}$ |
| $c_D$         | the drag coefficient on the cylinder  |
| $c_L$         | the lift coefficient on the cylinder  |
| $E_c$         | value of the convergence criterion  |
| $h_1$         | asymptotic breadth of wake  |
| $M(\zeta)$    | conformal mapping function, maps from $\zeta$ plane to $\tilde{z}$ plane                            |
| $N(\zeta)$    | function relating the fluid velocities on the untransformed and transformed circles                 |
| $Q_1$         | nondimensionalized strength of single source on upper part of cylinder                              |
| $Q_2$         | nondimensionalized strength of single source on lower part of cylinder                              |
| $\tilde{Q}_1$ | dimensioned value of $Q_1$  |
| $Q_2$         | dimensioned value of $Q_2$  |
| $R$           | radius of circle in $\zeta$ plane, $R = \csc \theta$  |
| $S_1$         | upper separation point  |
| $S_2$         | lower separation point  |

LIST OF SYMBOLS (Continued)

|                    |   |
|--------------------|---|
| $V_0$              | magnitude of free-stream velocity in $\zeta$ plane  |
| $W(\bar{z})$       | complex velocity in $\bar{z}$ plane   |
| $\alpha$           | polar angle of upper separation point in $\bar{\zeta}$ plane  |
| $\gamma$           | angle of upper source from real axis in $\zeta$ plane   |
| $\delta$           | angle of lower source from real axis in $\zeta$ plane   |
| $\epsilon$         | angle that $\bar{\zeta}$ system needs to be turned to coincide with $\zeta$ system  |
| $\tilde{\epsilon}$ | angle that $\bar{z}$ system needs to be turned to coincide with $z$ system after a translation of $\bar{z}$ coordinates so that the origins of the two systems coincide |
| $\zeta$            | primary untransformed complex plane   |
| $\bar{\zeta}$      | untransformed complex plane rotated by an angle of $-\epsilon$ to the $\zeta$ plane   |
| $\mu$              | viscosity   |
| $\nu$              | kinematic viscosity   |
| $\xi_1$            | real coordinate for $\zeta$ plane   |
| $\bar{\xi}_1$      | real coordinate for $\bar{\zeta}$ plane   |
| $\rho$             | mass per unit volume  |
| $\sigma$           | polar angle in $\zeta$ plane  |
| $\tau$             | surface shear stress  |
| $\dot{\sigma}$     | polar angle in $\zeta$ plane  |
| $X(\zeta)$         | complex-potential flow field  |
| $\psi_1$           | imaginary coordinate for $\zeta$ plane  |
| $\bar{\psi}_1$     | imaginary coordinate for $\bar{\zeta}$ plane  |
| $\Gamma$           | circulation strength  |
| $\Phi$             | flow potential  |

## LIST OF SYMBOLS (Continued)

$\Delta\theta$  angular increment from separation points

### SUBSCRIPTS

e boundary-layer edge conditions

f final conditions, also stands for fixed wall conditions

i initial conditions

s boundary-layer separation conditions

w wall conditions

1 upper side conditions

2 lower side conditions

### SUPERSCRIPTS

some dimensioned quantities

- transformed quantities with a few exceptions